

THE ROLE OF ETS FAMILY TRANSCRIPTION FACTOR ELK-1 IN CANCER STEM  
CELLS



by  
Melis Savaşan Söğüt

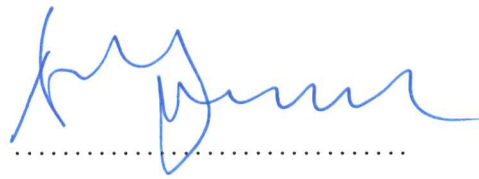
Submitted to Graduate School of Natural and Applied Sciences  
in Partial Fulfillment of the Requirements  
for the Degree of Doctor of Philosophy in  
Biotechnology

Yeditepe University  
2019

THE ROLE OF ETS FAMILY TRANSCRIPTION FACTOR ELK-1 IN CANCER STEM  
CELLS

APPROVED BY:

Prof. Dr. Bayram Yılmaz  
(Thesis Supervisor)  
(Yeditepe University)



Prof. Dr. Işıl Kurnaz  
(Thesis Co-Supervisor)  
(Gebze Technical University)

Prof. Dr. Ece Genç  
(Yeditepe University)



Assoc. Prof. Dr. Nagehan Ersoy Tunalı  
(Medeniyet University)



Assist. Prof. Dr. Güleğül Duman  
(Yeditepe University)



Assist. Prof. Dr. Neşe Altuncu  
(Medipol University)



DATE OF APPROVAL: ...../...../2019



*To my son, my Little Prince, Deha ...*

## ACKNOWLEDGEMENTS

I would like to express my great gratitude to Prof. Dr. Isil KURNAZ, my co-supervisor, for her supervision, advice, and guidance starting from the very early stages of my graduate studies. She is my idol. I am thankful to my supervisor Prof. Dr. Bayram YILMAZ for being there with his continuous positive support when we really needed it. I want to thank my dissertation committee members for spending their precious time for me and their guidance.

I thank my fellow labmates Merve USTUN, Ekin SONMEZ, Dogukan METINER, Yigit Koray BABAL, Busra Nur CICEK, Betul ERTURAL, Esranur YIGIT, Bayram KAS, and all AxanLab members for their help, friendship and for all the fun we have had each day. They helped me keep my motivation flying high when I thought the struggle would never end. Now that we are resilient to life challenges Dr. Oya ARI UYAR and Dr. Basak KANDEMIR. Thank you for the goodwill you have shown me over these years. I hope, we will keep doing great things.

My dearest Deha SOGUT, my precious, shared his childhood with the studies of this thesis and spent some time in the laboratory, too. My love, Ibrahim SOGUT, starting from the very beginning of our relation, always supported my career in any situation. Now it is time to live those missed times.

My beloved mother, Guler SAVASAN, and my dear father, Necmi SAVASAN, have always been with me, supporting me at any time and any situation. I know by heart that the limit is the sky for what they can do for me. They made so many sacrifices in their life to support me through each situation, yet I do not know how I can manage to put them back. All I can offer is a huge hug and a big thank you. Moreover, Volkan SAVASAN, Elcin SAVASAN, and my beloved nephews, Kuzey and Kaan. You are far away for too long. I miss you, and I love you all.

I want to thank The Scientific and Technical Council of Turkey (TUBITAK) BIDEB 2211-A National PhD Scholarship Programme for funding my PhD education. This study was partially supported by TUBITAK under the research grant no: 115Z804.

*“Fais de ta vie un rêve, et d'un rêve, une réalité.” Saint-Exupéry*



## ABSTRACT

### THE ROLE OF ETS FAMILY TRANSCRIPTION FACTOR ELK-1 IN CANCER STEM CELLS

According to the cancer stem cell theory, tumors have a subpopulation of cells that have the capacity for self-renewal and differentiation. These group of cells, namely cancer stem cells (CSCs), share some properties of normal stem cells. The dysregulation of specific signaling pathways and changes in downstream gene expression can cause failure in the regulation of stemness properties of stem cells, eventually causing tumorigenesis. There exists a complex interplay at both transcriptional and translational levels in the ultimate decision a stem cell or in this case a brain tumor-initiating cell (BTIC) to either keep itself as a stem cell (self-renewal) or become a specific cell through differentiation. The ETS family of transcription factors is one of the largest well-conserved transcription factor families. Elk-1, a TCF subfamily member, regulates many critical processes within the cell including apoptosis, tumorigenesis, and proliferation within the body. Elk-1 regulates neuronal survival and is neuroprotective; however, its survival-related transcriptional targets in neurons have not entirely identified yet. Together with the results of a former microarray conducted in the AxanLab, this led to the hypothesis that Elk-1 transcription factor may also be functional in regulating stemness genes and supporting their proliferation/self-renewal/survival in BTICs. In this study, CD133, a CSC marker, was used for the isolation of BTICs through positive selection. To find out the role of Elk-1, CD133+ BTICs were isolated, characterized, the effect of Elk-1 expression on the expression of various genes including the leading group of stemness genes, self-renewal, and proliferation in both normoxia and hypoxia were evaluated. The putative role of Elk-1 on the activity of selected promoters, namely *SOX2*, *NANOG*, and *POU5F1*, were assessed and the potential Elk-1 occupancy on several promoters were checked. Elk-1 roles in the regulation of the stemness gene promoters. The control over BTICs is not direct, but a rather complex mechanism is present. Finding out the role of Elk-1 from which the CSCs evade the regulations and the possible ways to overcome the progression of cancer can be the key for anti-cancer therapies.

## ÖZET

### ETS AİLESİ TRANSKRİPSİYON FAKTÖRÜ ELK-1'İN KANSER KÖK HÜCRELERİNDEKİ ROLÜNÜN İNCELENMESİ

Kanser kök hücre teorisine göre, tümörlerin kendini yenileme ve farklılaşma kapasitesine sahip hücrelerin bir alt popülasyonu, kanser kök hücreleri (KHK), normal kök hücrelerin bazı özelliklerini paylaşır. Spesifik sinyal yollarında ve akış aşağı gen anlatımlarındaki bozulmalar, kök hücrelerin düzenlenmesinde bozukluğa ve sonuçta tümör oluşumuna neden olabilir. Kök hücrenin kendini yenileme ya da farklılaşma kararını vermesinde transkripsiyonel ve translasyonel seviyelerdeki karmaşık etkileşim rol oynar. ETS transkripsiyon faktörleri ailesi, evrimsel olarak korunmuş en büyük transkripsiyon faktörü ailelerinden biridir. ETS'nin üçlü kompleks faktörü (TCF) alt ailesinin bir üyesi olan Elk-1, apoptoz, tümör genез ve proliferasyon da dahil olmak üzere hücre içindeki birçok önemli işlemde sorumludur. Elk-1 nöronal sağkalımı düzenler ve nöroprotektiftir, ancak nöronlardaki sağkalımla ilgili transkripsiyon hedefleri henüz tam olarak tanımlanmamıştır. AxanLab'da daha önce yapılan bir mikrodizinin sonuçları da göz önüne alındığında, Elk-1 transkripsiyon faktörünün, köklülük genlerinin düzenlenmesinde ve beyin tümörü başlatıcı hücrelerde (BTBH) çoğalma/kendini yenileme/hayatta kalmada işlevsel olabileceği hipotezini açığa çıkarmıştır. Bu çalışmada BTBH'lerin pozitif seçim yoluyla izolasyonu için KHK markörü olarak CD133 kullanılmıştır. Elk-1'in bu bağlamdaki rolünü bulmak için, CD133+ BTBH'ler izole edilerek, karakterize edilmiş ve Elk-1 anlatımının hem kendini yenileme, hem de proliferasyon üzerindeki etkisi normoksik ve hipoksik koşullarda değerlendirilmiştir. Elk-1'in seçilen köklülük genlerinin, *SOX2*, *NANOG* ve *POU5F1*, promotörlerinin aktivitesi üzerindeki etkileri ve bunlar dahil bir grup seçili promotöre bağlanma kapasitesi kontrol edilmiştir. Elk-1 köklülük genlerinin promotörlerinin düzenlenmesinde rol alır. Bununla birlikte, BTBH'ler üzerindeki kontrolü doğrudan değildir ve oldukça karmaşık bir mekanizma mevcuttur. Elk-1'in, kanser kök hücrelerinin aktivitelerinin düzenlenmesindeki rolünün belirlenmesi ilerleyen dönemlerde başka çalışmalar ile desteklenerek kanser önleyici tedavilerin anahtarı olabilecektir.

## TABLE OF CONTENTS

ACKNOWLEDGEMENTS .....	iv
ABSTRACT.....	v
ÖZET .....	vi
LIST OF FIGURES .....	x
LIST OF TABLES .....	xv
LIST OF SYMBOLS/ABBREVIATIONS.....	xvii
1. INTRODUCTION .....	1
2. THEORETICAL BACKGROUND.....	2
2.1. THE ETS-DOMAIN TRANSCRIPTION FACTOR FAMILY .....	2
2.1.1. The Structure and Function of ETS Family Proteins.....	2
2.2. TERNARY COMPLEX FACTOR (TCF) SUBFAMILY.....	3
2.2.1. ELK-1 Transcription Factor.....	4
2.2.1.1. The Role of Elk-1 in Neuronal Context.....	5
2.3. STEM CELLS.....	7
2.3.1. Adult Neural Stem Cells (NSCs) .....	10
2.3.2. Cancer Stem Cell Theory and Brain Tumor-Initiating Cells.....	12
2.3.2.1. CSCs and Self-Renewal Pathways .....	14
2.3.2.2. Isolation and Identification of CSCs.....	16
2.3.2.3. Enrichment and Culture of CSCs.....	17
2.4. ELK-1 AND STEM CELLS .....	18
3. AIM OF THE STUDY .....	20
4. MATERIALS AND METHODS.....	21
4.1. CELL CULTURE .....	21
4.1.1. Monolayer Cultures .....	21
4.1.2. Tumorsphere Cultures and Brain Tumor-Initiating Cell Cultures.....	21
4.1.2.1. Poly-HEMA Coating .....	22
4.1.2.2. Initial Proliferation Medium (IPM) and N2 Medium Preparation.....	23
4.1.2.3. Culturing Spheroids and BTICs.....	23

4.2. ISOLATION OF BRAIN TUMOR INITIATING CELLS (BTICs).....	24
4.2.1.    CD133/1 (AC133)-PE Staining for Flow Cytometry .....	25
4.3. HANGING DROP METHOD .....	25
4.4. SELF-RENEWAL ASSAYS .....	27
4.4.1.    Soft Agar Assay .....	27
4.4.2.    Limiting Dilution Analysis (LDA) .....	28
4.5. TRANSIENT TRANSFECTION FOR ADHERENT CELLS .....	28
4.6. TRANSFECTION TRANSFECTION FOR BTICS .....	29
4.7. XTT CELL PROLIFERATION ANALYSIS.....	29
4.8. LUCIFERASE REPORTER ASSAY .....	30
4.8.1.    Preparation of Reporter Plasmid Constructs.....	30
4.8.2.    Site-directed Mutagenesis (SDM) .....	34
4.8.3. <i>Firefly-Renilla</i> Luciferase Assay .....	36
4.9. RNA INTERFERENCE .....	37
4.10. GENE EXPRESSION ANALYSIS .....	37
4.10.1.    Total RNA Extraction and cDNA Synthesis .....	37
4.10.2.    Primer Design for qPCR .....	39
4.10.3.    Gene Expression Analysis .....	42
4.11. WESTERN BLOTTING.....	42
4.11.1.    Preparation of Protein Samples and Buffers.....	43
4.11.2.    Immunoblotting and Imaging .....	44
4.12. CHROMATIN IMMUNOPRECIPITATION ASSAY (ChIP) .....	45
4.12.1.    Primer Design for ChIP .....	46
4.12.2.    Crosslinking and DNA Shearing .....	49
4.12.3.    Immunoprecipitation of DNA-Protein Complex .....	50
4.12.4.    Reverse Crosslink and Purification.....	51
4.12.5.    Quantification of ChIP .....	51
4.12.6.    ChIP Buffers .....	51
4.13. STATISTICAL ANALYSIS.....	52
5. RESULTS & DISCUSSION .....	53
5.1. ISOLATION AND CHARACTERIZATION OF CD133+ HUMAN BTICS.....	54
5.1.1.    Tumorsphere and CD133+ BTIC Formation Under Special Conditions ....	54

5.1.2.	Transfection of Tumorspheres and CD133+ BTICs.....	62
5.1.3.	Assessment of Self-renewal Capacity.....	64
5.1.3.1.	Limiting Dilution Analysis (LDA) .....	66
5.1.3.2.	Soft Agar Analysis.....	67
5.1.4.	Characterization of BTICs by CSC-related Gene Expression and Protein Levels.....	71
5.2.	THE MOLECULAR ANALYSIS OF POTENTIAL GENE TARGETS OF ELK-1 IN NORMOXIA AND HYPOXIA.....	75
5.2.1.	Verification of Hypoxia .....	75
5.2.2.	Gene Expression Levels of Elk-1 and Target Genes in Normoxia and Hypoxia.....	79
5.3.	THE EFFECT OF ELK-1 OVER-EXPRESSION OR SILENCING ON THE PROLIFERATION OF THE CD133+ BTICS AND CD133- SPHEROIDS.....	86
5.4.	THE REGULATION OF PLURIPOTENCY GENES BY ELK-1 .....	88
5.4.1.	Functional Assessment with Luciferase Reporter Assay.....	89
5.4.1.1.	The Analysis of the Target Promoter Activities in Hypoxia .....	101
5.4.2.	Analysis of Pluripotency Promoter Occupancies by Chromatin Immunoprecipitation (ChIP).....	104
5.5.	ROLE OF ELK-1 IN THE REGULATION OF EARLY NERVOUS SYSTEM DEVELOPMENT AND STEMNESS-RELATED GENES .....	110
5.6.	CSC-RELATED SIGNALING PATHWAYS IN THE PRESENCE/ABSENCE OF ELK-1 IN CD133+ BTICS AND CD133- SPHEROIDS.....	117
6.	CONCLUSION.....	120
	REFERENCES .....	124
	APPENDIX A.....	142

## LIST OF FIGURES

Figure 2.1. Comparison of TCF subfamily members .....	3
Figure 2.2. The domains and PTMs of Elk-1 .....	5
Figure 2.3. Schematic representation for stem cell division.....	8
Figure 3.1. Schematic representation of a small set of genes showing expression patterns with respect to Elk-1 in SH-SY5Y neuroblastoma cells.....	20
Figure 4.1. Schematic representation of the hanging drop method .....	26
Figure 4.2. Soft agar assay in summary.....	27
Figure 4.3. pGL3 Basic vector circle map .....	31
Figure 4.4. ChIP assay .....	45
Figure 4.5. Elk-1 binding sites on stemness promoters for ChIP primers .....	47
Figure 5.1. Hanging drop method to produce 3D spheres without changing the culture medium .....	55
Figure 5.2. Flow cytometric analysis of SKNBE(2) cells for CD133-PE staining .....	57
Figure 5.3. SKNBE(2)-derived cells with IPM on non-coated dishes.....	58
Figure 5.4. SKNBE(2)-derived cells with IPM on coated dishes .....	59
Figure 5.5. CD133 gene expression level comparison following isolation with MACS.....	59

Figure 5.6. First passage, day 4, poly-HEMA coated dish .....	60
Figure 5.7. Second passage, day 10, poly-HEMA coated dish.....	60
Figure 5.8. EGFP-N2 transfection of CD133+ BTICs with Lipofectamine2000.....	64
Figure 5.9. CD133+ BTICs and C133- cells after transfecting with Elk-1 series .....	65
Figure 5.10. The frequency of sphere formation in isolated CD133+ and CD133- cells in BTIC conditions.....	67
Figure 5.11. Colony numbers following soft agar assay .....	69
Figure 5.12. Colonies formed in LMP soft agar .....	69
Figure 5.13. Crystal violet-stained photos of soft agar assay groups, 4X. ....	70
Figure 5.14. Nestin expression in neuroblastoma and glioblastoma cells .....	71
Figure 5.15. Nestin expression in SKNBE(2) CD133+ BTICs .....	72
Figure 5.16. Stemness gene expression analysis of (a) SKNBE(2) passage 0, passage 1 and passage 2 cells; (b) SKNBE(2) CD133+ BTICs vs CD133- spheroids.....	73
Figure 5.17. Stemness gene expressions related to Elk-1 .....	74
Figure 5.18. Western blot analysis for the tumorspheres .....	75
Figure 5.19. Protein expression of HIF1 $\alpha$ in normoxia and hypoxia .....	76
Figure 5.20. VEGF expression in normoxic vs. hypoxic conditions in SKNBE(2) cell line .....	77

Figure 5.21. (a) <i>VEGF</i> promoter analysis for Elk-1 binding, (b) <i>VEGF</i> expression in normoxic vs. hypoxic conditions in Elk-1-transfected SKNBE(2) cells .....	78
Figure 5.22. Quantitative gene expression analysis of stemness genes following intervals of hypoxia treatment .....	80
Figure 5.23. Gene expression of CSC markers in SKNBE(2) monolayer cells and tumor cells at hypoxic conditions .....	82
Figure 5.24. Anti-SOX2 Western blot with Elk-1 over-expressed/repressed SKNBE(2) cells at normoxia and hypoxia.....	83
Figure 5.25. Stemness gene expressions in CD133+ BTICs and CD133- spheroids with Elk-1 over-expression at normoxic vs. hypoxic conditions.....	84
Figure 5.26. Stemness gene expressions in CD133+ BTICs and CD133- spheroids with Elk-1 repression at normoxic vs. hypoxic conditions.....	85
Figure 5.27. Evaluation of cell proliferation in CD133 + BTICs and CD133- spheroids at normoxia and hypoxia by XTT analysis.....	87
Figure 5.28. Luciferase assay for <i>NANOG</i> -Luc and <i>NANOGΔ</i> -Luc reporters in SKNBE(2) cells .....	90
Figure 5.29. Luciferase assay for <i>NANOG</i> -Luc and <i>NANOGΔ</i> -Luc reporters in SH-SY5Y cells .....	92
Figure 5.30. Luciferase assay for <i>NANOG</i> -Luc and <i>NANOGΔ</i> -Luc reporters in U87-MG cells .....	93
Figure 5.31. Luciferase assay for wild-type <i>POU5F1</i> -Luc and its deletion mutant reporters in SKNBE(2) cells .....	95



Figure 5.32. Luciferase assay for wild-type POU5F1-Luc and its deletion mutant reporters in SH-SY5Y cells.....	96
Figure 5.33. Luciferase assay for wild-type POU5F1-Luc and its deletion mutant reporters in U87MG cells.....	97
Figure 5.34. SOX2 promoter activity analysis with respect to ELK-1 over-expression and silencing.....	98
Figure 5.35. <i>SOX2</i> , <i>NANOG</i> and <i>POU5F1</i> promoter activity analysis with respect to ELK-1 over-expression and silencing in T98G cell line .....	99
Figure 5.36. <i>SOX2</i> , <i>NANOG</i> , and <i>POU5F1</i> promoter activity analysis with respect to ELK-1 over-expression and silencing in A172 cell line.....	100
Figure 5.37. HIF1 binding site on <i>SOX2</i> promoter.....	101
Figure 5.38. The promoter activities in normoxic vs. hypoxic conditions following transient transfection for Elk-1 over-expression vs. silencing .....	102
Figure 5.39. Luciferase assay results for NANOG vs. NANOG $\Delta$ in normoxic vs. hypoxic conditions in SK-N-B (2) cell line.....	103
Figure 5.40. Luciferase assay results for wild-type POU5F1 vs. mutants in normoxic vs. hypoxic conditions in SKNBE(2) cell line .....	103
Figure 5.41. ChIP for the identification of Elk-1 binding sites on the target pluripotency gene promoters pCMV-transfected vs. Elk-1 over-expressing SKNBE(2) cells .....	105
Figure 5.42. ChIP-qPCR results for the identification of Elk-1 binding sites on the target gene promoters pCMV-transfected vs. Elk-1 over-expressing SKNBE(2) cells.....	106

Figure 5.43. ChIP for the identification of Elk-1 binding sites on the target pluripotency gene promoters in pCMV-transfected vs. Elk-1 over-expressing T98G glioblastoma cells.....	108
Figure 5.44. ChIP-qPCR results for the identification of Elk-1 binding sites on the target gene promoters in T98G glioblastoma cells .....	109
Figure 5.45. Expression profiles after over-expression with Elk1-VP16.....	115
Figure 5.46. Expression profiles after silencing with siElk-1.....	116
Figure 5.47. Gene expression of signaling pathway members .....	118
Figure 5.48. The change in the expression of canonical WNT signaling pathway members with respect to increasing passage number in SKNBE(2) CD133+ BTICs .....	119

## LIST OF TABLES

Table 2.1. The debated origins of CSCs .....	13
Table 2.2. The comparison of properties of SCs and CSCs [78], [79] .....	14
Table 4.1. Poly-HEMA coating for various size of dishes .....	22
Table 4.2. Cloning primers for chosen <i>Homo sapiens</i> stemness gene promoters .....	31
Table 4.3. Gradient PCR ingredients .....	32
Table 4.4. PCR ingredients and cycling conditions for insert preparation .....	33
Table 4.5. Restriction enzyme digestion setup for cloning.....	33
Table 4.6. Ligation reaction setup for cloning.....	34
Table 4.7. SDM primers .....	35
Table 4.8. The setup and conditions for SDM PCR .....	35
Table 4.9. KLD reaction setup for SDM .....	36
Table 4.10. The setup and conditions for cDNA synthesis .....	38
Table 4.11. Designed qPCR primers .....	39
Table 4.12. qPCR setup and cycling conditions .....	42
Table 4.13. Western blot buffer recipes.....	44


Table 4.14. Dissimilarity rates for potential promoter binding sites of promoters.....	46
Table 4.15. The list of primers used in ChIP Assay .....	47
Table 4.16. ChIP washing steps.....	50
Table 4.17. ChIP buffer recipes .....	52
Table 5.1. Tumorsphere morphologies for various cell lines .....	61
Table 5.2. PEI transfection setup for each cell line after optimization.....	63
Table 5.3. Soft agar assay colony formation .....	68
Table 5.4. ETS transcription factor family binding site profiles for the selected pluripotency gene promoters.....	91
Table 5.5. The expression of selected potential Elk-1 target genes after Elk1-VP16 over-expression in neuroblastoma cell lines .....	110
Table 5.6. The expression of selected potential Elk-1 target genes after Elk1-VP16 over-expression in glioblastoma cell lines .....	111
Table 5.7. The expression of selected potential Elk-1 target genes after siElk-1 silencing in neuroblastoma cell lines.....	112
Table 5.8. The expression of selected potential Elk-1 target genes after siElk-1 silencing in glioblastoma cell lines .....	113
Table 5.9. The expression of pluripotency genes with (a) ELK-1 over-expression, (b) ELK-1 silencing .....	114

**LIST OF SYMBOLS/ABBREVIATIONS**

$\mu\text{l}$	Microliters
$\mu\text{M}$	Micromolar
A172	Human glioblastoma cell line
AD	Activation domain
APS	Ammoniumpersulphate
ATCC	American type culture collection
BSA	Bovine serum albumin
BTIC	Brain tumor initiating cell
CSC	Cancer stem cell
DMEM	Dulbecco's modified eagle medium
DMSO	Dimethylsulfoxide
DNA	Deoxyribonucleic acid
DTT	Dithiothreitol
E26	E-twenty-six
EDTA	Ethylenediaminetetraacetic acid
EGF	Epidermal growth factor
Elk-1	Ets-like transcription factor-1
ERK	Extracellular regulated kinase
ESC	Embryonic stem cell
EtOH	Ethanol
ETS	E-twenty six
FBS	Fetal bovine serum
FGF	Fibroblast growth factor
GFP	Green fluorescent protein
HCL	Hydrochloric acid
HLH	Helix-loop-helix domain
HRP	Horse-radish peroxidase
ID	Inhibitory domain
IEG	Immediate early gene

IP	Immunoprecipitation
iPSC	Induced pluripotent stem cell
JNK	c-Jun <i>N</i> terminal kinase
MAPK	Mitogen activated protein kinase
ml	Milliliters
mM	Milimolar
NaCl	Sodium chloride
NaOH	Sodium hydroxide
Ng	Nanogram
NP-40	Octyl phenoxypolyethoxyethanol
nM	Nanomolar
O/N	Overnight
PBS	Phosphate buffered saline
PCR	Polymerase chain reaction
PEI	Polyethylenimine
pH	Negative log of hydrogen ion concentration
PLB	Passive lysis buffer
PNT	Pointed domain
PTM	Post translational modification
PVDF	Polyvinylidene difluoride
RD	Repression domain
RPM	Rotation per minute
SAP	SRF accessory protein
SC	Stem cell
SDM	Site directed mutagenesis
SDS	Sodium dodecyl sulphate
SDS-PAGE	Sodium dodecyl sulfate polyacrylamide gel electrophoresis
SH-SY5Y	Human neuroblastoma cell line
SKNBE(2)	Human neuroblastoma cell line
SRE	Serum response element
SRF	Serum response factor
STRE	Stress responsive element
SUMO	Small ubiquitin-like modifier

T98G	Human glioblastoma cell line
TAD	Transactivation domains
TBS	Tris-buffered saline
TCF	Ternary complex factor
TEMED	N, N, N', N'-tetramethylethylenediamine
TF	Transcription factor
U87-MG	Human glioblastoma cell line
VEGF	Vascular endothelial growth factor
w-HTH	Winged-helix-turn-helix
WB	Western blot



## 1. INTRODUCTION

Brain tumors stem from brain parenchyma and the surrounding tissues. They may invade the brain tissue and develop resistance to chemotherapy aggressively. They generate a burden for both the individuals and the health care systems. They cause severe morbidity and mortality at any age. The average life expectancy of the diagnosed patients after diagnosis varies between 15 months to 5 years.

The presence of cancer stem cells (CSCs) is of main concern in cancer therapy. Cancer stem cell theory states that the CSCs are crucial for the tumor proliferation and survival just like the stem cells renewal and sustain the tissues within the body. In brain tumors, this cell group is called the Brain Tumor-Initiating Cells (BTICs) [1]. BTICs are regarded as the key contributors to the resistance, metastasis, and invasion in brain tumors, especially in glioblastoma (GBM). Unveiling the mechanism by which BTICs self-renew and proliferate within their microenvironment can be invaluable for ceasing the BTIC growth both *in vitro* and *in vivo* as well as developing therapeutics.

The ETS (**E**-twenty-six **T**ransformation **S**pecific) transcription factor family has diverse roles including survival, angiogenesis, differentiation, inflammation both in the developmental stage and in the adult organism. The ETS family members have a role in human carcinogenesis by altering the expression patterns, being in translocation breakpoints or causing deletion mutations [2].

This study deals with the potential role of Elk-1 in the moderation of CSCs. The putative target genes of Elk-1 and their interaction were explored *in vitro*. This study may pave the way for targeting the CSCs in the future.



## 2. THEORETICAL BACKGROUND

The sequencing of whole genomes led to the fact that the main reason behind the incredible diversity of animal and plant species is not only the number of genes. It is the more sophisticated regulation of gene expression that results in the development of complex organisms. Transcription factors are central players organizing the activation of genes. Their binding to *cis*-regulatory DNA sites on their partner genes either solely or with indirect interaction through other transcription factors results in highly specific response, positive or negative regulation of a gene. Together with other gene regulation mechanisms including chromatin modifications, signal transduction, and RNA splicing, eukaryotic gene expression is regulated.

### 2.1. THE ETS-DOMAIN TRANSCRIPTION FACTOR FAMILY

The ETS transcription factors are the members of an evolutionarily conserved transcription factor family. They are classified into 11 subfamilies with respect to the homology of the similarity of sequences at DNA-binding domain, conservation of other domains and the location of their ETS domain [3]. The family has 28 paralogous *ets* genes in humans, eight genes in *Drosophila melanogaster*, 27 genes in mouse, and ten genes in *Caenorhabditis elegans* [4].

#### 2.1.1. The Structure and Function of ETS Family Proteins

The presence of an ETS domain is necessary to characterize the ETS family. This is a well-conserved domain of 85 amino acids that interacts with a specific core sequence. The purine-rich DNA motifs together with 5'-GGA(A/T)-3' and bordering sequences forms the domain [5]. Three  $\alpha$ -helices and four-stranded antiparallel  $\beta$ -sheets together with a winged-helix-turn-helix (w-HTH) motif makes up the ETS domain [6]. The domain usually exists at C-terminus. In ERF and TCF subfamilies it resides at N-terminus.

Hydrogen bonding between the third  $\alpha$ -helix and the two guanines at the core is required for the direct interaction between the ETS domain and DNA binding. Thus, the sequences

neighboring the domain mark the location of interaction through additive hydrophobic and electrostatic interactions [7]. Thereby, the specificity of the interaction is determined.

The transactivation domains (TAD) of ETS transcription factors confer specificity and control over the target genes. They allow the regulation of target genes in different contexts. This allows a variation in expression between members of the subfamilies. Also, the number of the present TADs may lead to higher induction of target gene expression [8].

ETS transcription factors take part in various processes within the cell. Tumorigenesis, migration, inflammation, extracellular matrix remodeling, apoptosis, and vertebrate embryogenesis are some of them [9]. To carry out such functions successfully and totally correct, a tight control of activity is necessary. The required control for these transcription factors is carried through co-regulatory proteins, microRNAs and transcriptional control. Apart from transcriptional regulation, through phosphorylation, glycosylation, SUMOylation, ubiquitylation and acetylation, they role in the protein-protein interactions, localization and appropriate expression of ETS-related gene expressions [10].

## 2.2. TERNARY COMPLEX FACTOR (TCF) SUBFAMILY

Ternary complex factors (TCFs) are a well-known subfamily of ETS transcription factors. The first member was recognized in the context of *c-fos* proto-oncogene regulation through the complex formation between the *c-fos* serum response element (SRE) and serum response factor (SRF). This protein was first called p62; however, p62 was then found to be the previously named Elk-1 protein [11]. Sap-1 (Serum response factor accessory protein 1)/Elk-4 [12], Net/Erp/Sap-2/Elk-3 (New ETS) ([13]; [14]; [15]) and the splicing variant of Net, Net-b, were identified and grouped as members of TCF subfamily as shown in Figure 2.1.

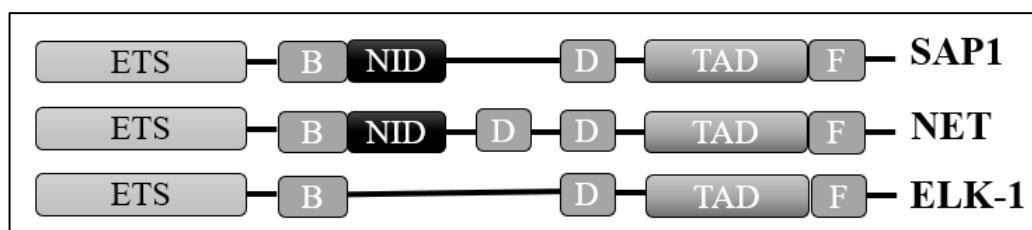


Figure 2.1. Comparison of TCF subfamily members [16]

TCFs have been involved in activating promoters of immediate early genes (IEGs). The complex executes cell-type-specific tight control over SRE-containing promoters. ELK-1 transcription factor, a well-known member of TCF subfamily, and its potential interactions were investigated in the context of BTICs within this thesis.

### **2.2.1. ELK-1 Transcription Factor**

Transactivation functions of TCFs and their binding to the DNA are regulated by MAPKs through phosphorylation. The major MAPK cascades are the extracellular signal-regulated kinase (ERK), the Jun N-terminal kinase/stress-activated protein kinase (JNK/SAPK) and the p38 kinase and they role in the regulation of Elk-1 [17]. These pathways can be activated through mitogens, growth factors, cytokines, and stress, respectively. Among the nine known potential phosphorylation sites at C-terminal, phosphorylation from the Serine383 and Serine389 are critical for the induction of genes through SRE [18].

Elk-1 phosphorylation by MAPK cascades is pivotal for its regulation. ELK-1 transcription factor is an eminent substrate of ERK, p38 kinase and JNK. When phosphorylated, the conformation of Elk-1 changes and the DNA-binding domain of Elk-1 is uncovered. The change in conformation increases the ternary complex formation (Elk-1/SRF/SRE) [17]. Apart from this, when Elk-1 is phosphorylated by MAPKs, as for negative feedback, it interacts with HDAC corepressor complex, thereby blocking the expression level of Elk-1 regulated genes [19].

The immediate early gene (IEG) response is regulated by Elk-1 [20]. It is expressed at the cerebellum, striatum, hippocampus, cortex and various regions within the brain [21]. It may be localized in either nuclear or extranuclear compartments, like soma and dendrites [22]. The expression of Elk-1 at different localizations affects its function.

The members of the TCF subfamily have four evolutionarily conserved domains (A-D). The domain structure for Elk-1 is in Figure 2.2 [23]. The presence of the ETS domain at the N-terminus discriminates the TCF subfamily. The A domain is made up of the ETS DBD along with a nuclear localization signal (NLS) [24]. This domain may take a role in the inhibition of Elk-1 by employing co-repressors and DNA binding inhibitors to the site. The B-box domain is the primary site interacting with SRF [25]. The C domain, also referred to as the

transactivation domain (TAD), has many motifs that are targets of mitogen-activated kinases (MAPKs). Following the activation of JNK or p38 kinases, the Elk-1 binds through the D domain [26]. At the C-terminus, the interface of Elk-1 and activated ERK is accomplished with DEF motif [23]. The R domain lowers the reaction of protein to mitogenic signals by reducing the basal transcription activity of Elk-1 [27].

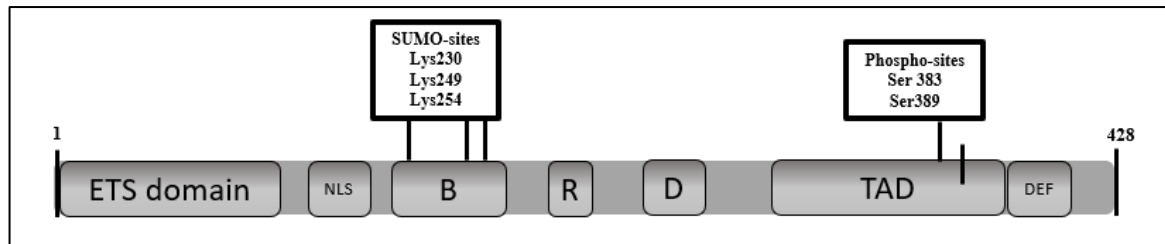


Figure 2.2. The domains and PTMs of Elk-1 [23]

Apart from mRNA expression levels; translational control, cellular localization and posttranslational modifications are crucial regulators for Elk-1 expression [28]. When there is no MAPK signaling, the activity of Elk-1 TAD is suppressed by corepressors recruited to the site by R motif and ETS domain [29]. The suppression of TAD maintains Elk-1 in the inactive basal state. Detailed analysis of R motif revealed that small ubiquitin-related modifier addition (SUMOylation) on lysines 230, 249 or 254 have role in the regulation of Elk-1 through repression [30]. There exists an antagonism between phosphorylation and SUMOylation. Both SUMO removal and ERK promotion for activation of Elk-1 are necessary to convert Elk-1 into the transcriptionally active state [31].

### 2.2.1.1. *The Role of Elk-1 in Neuronal Context*

Elk-1 is responsible for many crucial processes within the cell including apoptosis, tumorigenesis, and proliferation throughout the body. Studies on the function of Elk-1 in neurons reveal that it plays a role in neuronal outgrowth/axon regeneration as well as neuronal survival or apoptosis [22, 32, 33].

When expression and regulation of Elk-1 was assessed in the adult rat brain, Sgambato *et al.* came across to three main findings. According to the findings of Sgambato, Elk-1 mRNA was expressed in brain structures that are all neuronal. Secondly, despite being a nuclear

transcription factor that is supposed to be present around the nucleus, Elk-1 protein is not only nuclear, but it is also localized in the axon terminals, cell body (soma) and dendrites. Thirdly, Elk-1 phosphorylation can take place in various compartments within the cell [21]. Likewise, in their review, Besnard *et al.* underlined the diverse functions of Elk-1 in neurons that change depending on the location, either cytoplasm or nucleus [23].

It was previously shown by our laboratory that there exists a co-localization and interaction of Elk-1 with neuronal microtubules in both neuroblastoma cell lines and primary hippocampal cells in the unstimulated state. When the setup was stimulated with serum, Elk-1 was phosphorylated, and microtubule-anchored Elk-1 was translocated to the nucleus [34].

Barrett identified the extranuclear functions and localization of Elk-1 in primary rat hippocampal neurons. The interaction between Elk-1 and mitochondrial permeability transition pore (PTP) complex, a voltage-gated channel that allows molecules non-selectively to the inner membrane, was assessed [35]. The change in mitochondrial PTP proteins may result in various cellular processes including apoptosis, necrosis, membrane depolarization and release of stored soluble proteins [36]. Barrett and her colleagues revealed that Elk-1 is localized around mitochondrial membranes and found out that the level of Elk-1 raises with increasing DNA damage and apoptosis in neurons. When Elk-1 was over-expressed, the cell viability was decreased through siRNA-mediated knockdown, the cell viability increased, leading to the idea that either Elk-1 is directing the mitochondria to cell death or it triggers transcription of genes that take part in mitochondrial function [22].

Nevertheless, Vickers reported that when gene activity related to TCF regulation was blocked that led to cell growth arrest and cell death took place [37]. When cells were transfected with a construct of Elk-1 fused with *Drosophila* engrailed repressor domain (EN), Elk-EN, it led to growth arrest and apoptosis. That was in a ternary-complex-dependent manner. However, either constitutively active construct of Elk-1, where it is fused to the acidic activation domain of HSV VP16 transactivator, the Elk-VP16, or the wild-type Elk-1 was sufficient for promoting cell survival. Similarly, with another study of our laboratory, it was shown that when the dominant repressive Elk-EN construct was tested in PC12 rat pheochromocytoma cell line, it interfered with survival and increased caspase-dependent apoptosis. Over-expression of exogenous Elk-1 or Elk1-VP16 expression protected neurons from cobalt chloride-induced apoptosis [33]. In primary dorsal root ganglia (DRG) culture system, following axotomy (neuronal injury), phospho-Elk-1 levels

increased, leading to enhanced survival. In this study, *MCL-1* and a survival motor neuron protein *SMN1* were reported to be the target genes of Elk-1 in SH-SY5Y cells [33].

Furthermore, Demir and Kurnaz have shown that Elk-1 leads a role in repressing *egr-1* (*early growth response-1*) expression, commonly known as an intermediate-early gene in mitogenic stimulus yet a pro-apoptotic protein in neuroblastoma cells. When Elk-1 was over-expressed, the EGR-1 protein level was reduced. However, a SUMOylation mutant of Elk-1 restored the protein level of EGR-1. These results lead to the hypothesis that in SH-SY5Y cells, Elk-1 represses *egr-1* promoter through its R-domain, probably by changing the SUMOylation status, thereby preventing apoptosis and promoting cell survival [38]. Thus, there exists controversy about the role of Elk-1 in cell survival, and this controversy may be due to localization and/or phosphorylation of Elk-1.

Elk-1 is also involved in progression of neurodegenerative diseases. Synucleinopathies, Huntington Disease (HD), and Alzheimer's Disease (AD) are the examples for Elk-1-related disorders. At specific doses of amyloid- $\beta$  ( $A\beta$ ) peptides, BDNF-induced activation of Elk-1 is triggered in cortical neurons, leading to deregulation of SRE-controlled genes [39]. In a HD model, the hyperphosphorylation of ERK, CREB, Elk-1 was reported [40]. In Parkinson's Disease, the formation of aggregates made up of  $\alpha$ -Synuclein is observed. Iwata *et al.* showed that there exists an interaction between Elk-1 and  $\alpha$ -Synuclein through ERK, resulting in the attenuation of Elk-1 phosphorylation on Ser383 residue. This also led to the induction of *c-fos* [41].

According to recent literature, the fundamental mitogenic role of Elk-1 can be stated clearly. However, further analyses related to illuminating the survival-proliferation-apoptosis roles of Elk-1 in neurons is necessary.

### **2.3. STEM CELLS**

Stem cells are specialized cells that have the potential to turn into various cell types both in embryogenesis and adulthood. They play a role like an internal repair system with their unique regenerative abilities.

Stem cells have two characteristic properties: (1) they have the potential to retain self-renewal and (2) differentiate into different cell types when the conditions are appropriate.

Stem cells maintain these properties by going through either asymmetric or symmetric cell divisions. When symmetric cell division takes place, two stem cells or two differentiated daughter cells are produced as shown in Figure 2.3. Stem cells undergo symmetric division often for proliferation. In the case of asymmetric division, the process yields two cells with different cellular fates, a stem cell, and a more differentiated cell. Self-renewal often occurs via asymmetric divisions [42].

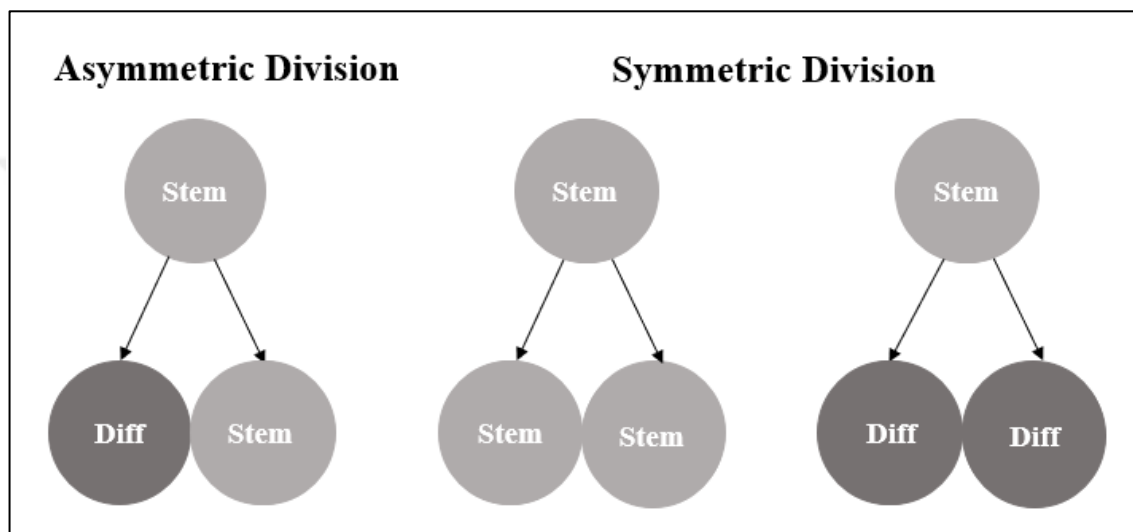


Figure 2.3. Schematic representation for stem cell division [42]

There exists a hierarchy in tissues based on differential potential (potency) of the cells. Stem cells are a reservoir of undifferentiated cell types. They can generate committed progenitors, which then produce terminally differentiated cells. While totipotent stem cells have the potential to differentiate into all embryonic cell types and construct an entire organism, the capacity of pluripotent stem cells is more restricted. Pluripotent cells cannot potentiate the development of the whole organism due to their inability to generate extraembryonic trophoblast cells. However, they are able to form the cells of any of the three germ layers (endoderm, mesoderm or ectoderm) [43].

According to the basis of their sources, they can be considered in two major groups: embryonic stem cells (ESCs) and adult stem cells (somatic stem cells). Pluripotent ESCs are derived from the inner cell mass (ICM) of blastocyst stage embryos. ESC cultures are usually accomplished by isolating the stem cells from embryos that are sparsely generated throughout *in vitro* fertilization (IVF) [44].

When ESCs do not take part in organogenesis during embryogenesis, they reside quiescently as adult stem cells during adulthood. Adult stem cells are present at various parts within the body including brain, teeth, heart, bone marrow, skeletal muscle, liver, testis and umbilical cord [44]. The main function of adult stem cells is to sustain tissue homeostasis by restoring damaged tissues in which they are located [45].

There are advantages and disadvantages for the potential use of both ESCs and adult stem cells. While ESCs, being pluripotent, they have the ability to differentiate into all cell types of all lineages within the body. The production and maintenance of ESCs with *in vitro* culture are relatively straightforward. However, issues including the probability of teratoma formation, the presence of animal pathogens, immunological response and ethics cause limitations for the use of ESCs. The isolation of adult stem cells from the tissues they reside in and expanding them in cell culture is quite challenging as they are rare. Studies on adult stem cells do not cause ethical problems; they are controversial. There are many sources for obtaining the adult stem cells, and they are immune-privileged. While all these properties make the adult stem cells advantageous over ESCs, their differentiation and self-renewal capacity, and the rarity among somatic cells cause limitations.

There are safety issues for the usage of these two kinds of stem cells for transplantation therapies. The tissues developed from ESCs may be rejected following the transplantation, or through uncontrolled proliferation, they may harbor the risk of tumor formation within the host. Apart from the molecular assessment of the ESCs, their genetic stability and potential chromosomal aberrations and polymorphisms also have to be considered. Apart from either ESCs or adult stem cells, another kind of stem cell was established due to the problems stated above: induced pluripotent stem cells (iPSCs) [46]. These cells are also pluripotent; they have the specific stem cell markers; they give rise to the cells of all three germ layers; they form different tissues in mouse embryos.

The therapeutic applications of pluripotent cells (both ESCs and iPSCs) have been investigated for specific diseases including ophthalmic diseases [47], neurological diseases, diabetes [48] and cardiac disease [49].

For the transplantation studies with adult cells, the cells are collected from the host's cells, cultured, differentiated to a specific cell type and reintroduced to the host. When these are considered, the adult stem cells are thought to be less likely to initiate immune rejection. In



each case, the exact control mechanisms have to be unveiled for the safety of therapeutic studies.

iPSCs are useful tools for both disease modeling and therapeutic studies. However, they also have drawbacks. For the induction of reprogramming on site, the factors have to be introduced to the cells via viral delivery. In addition to this, with recent studies it has been shown that the iPSCs maintain the epigenetic memory of the original cell type, moving them away from being true ESCs [50]. These are the limits for the usage of the method for treatment in humans.

### **2.3.1. Adult Neural Stem Cells (NSCs)**

For a long time, it was thought that neurogenesis was not taking place in the adult mammalian brain. However, starting with the autoradiography studies of Altman in the 1960s, research over mammalian brain advanced with electron microscopy and immunostaining techniques, which further led to defining the concept of genesis, mitosis, and differentiation of neurons [51, 52]. This led to an array of studies finally resulting in the breaking a dogma in neurobiology.

In 1992, Reynolds and Weiss first reported the presence of spheroid bodies cultured in a defined, serum-free medium supported with epidermal growth factor (EGF) [53]. The spheroid bodies were able to form the secondary spheres, and they were positive for Nestin expression. These spheroids were named as neurospheres later [53]. Morshead et al. stated that the cells that Reynold et al. could culture with EGF-supported medium were the EGF-responsive cells that were residing around the lateral ventricles in the subventricular zone [54].

In an adult mammalian brain, neurogenesis takes places within only two zone, the subventricular zone (SVZ) of the lateral ventricles and in the hippocampus the subgranular zone (SGZ) of the dentate gyrus [55]. Neuroblasts that are generated by the SVZ stem cells migrate through the rostral migratory stream (RMS) to their destination, olfactory bulb. There, they differentiate into olfactory interneurons and either join to the olfactory circuitry or function as oligodendrocyte progenitors [56, 57]. The SGZ stem cells can generate either new granule neurons or astrocytes. Unlike SVZ neuroblasts, these new granule neurons

migrate only a short distance up to the granule cell layer, join the functional circuitry of the dentate gyrus and receive glutamatergic inputs [58]. The characteristics of neurospheres isolated from SVZ and SGZ are different.

A fundamental mechanism is necessary for the dynamic regulation of adult NSCs through transcription factors. In a study comparing the transcriptome data for ESCs, it was shown that the transcription factors associated with the maintenance of ESC pluripotency were not expressed in MAPCs [59]. There was a unique molecular signature between each stem cell type.

SOX2, NANOG and POU5F1 transcription factors are the critical regulators of the properties of ESCs. POU5F1 (Oct4) is a member of POU-domain transcription factors and takes part in the pluripotency of ESCs by acting synergistically with SOX2 *in vitro*. They activate Oct-Sox enhancers together to regulate *nanog*, *sox2* and *pou5f1* itself [60, 61]. In mammalian development, POU5F1 has a critical role in the regulation of cell fate decisions [62]. It is important for the regulation of reprogramming and production of iPSCs. The over-expression of only POU5F1 is sufficient for the formation of iPSC cells while the other factors necessary for iPSC formation were expressed endogenously [63].

The cell fate of mouse embryonic stem cells (mES) has shown to be determined with POU5F1 expression. With low or no expression of POU5F1, the mES either sustain pluripotency or differentiate forming trophoblast [64]. With a high level of POU5F1, mES cells differentiate into endodermal and mesodermal lineages [65].

The dosage-dependent regulation is also shown for SOX2 [66]. SOX2 is involved in the inhibition of neuronal differentiation and self-renewal in ESCs [67]. Its endogenous expression levels are higher in adult NSCs of SVZ and SGZ than in ESCs [67]. With an array of experiments including the gain of function and loss of function mutations in transgenic animals the role of SOX2 in neurogenesis, proliferation and self-renewal/survival are shown. NANOG is a homeodomain-comprising protein that maintains pluripotency of ESCs by working with Stat3 to inhibit nuclear factor kappa B (NFκB) [68].

### 2.3.2. Cancer Stem Cell Theory and Brain Tumor-Initiating Cells

Normal adult stem cells form cells that can go an unlimited number of cell divisions and self-renew; these cells keep the indefinite capacity of the stem cells. They are also able to produce daughter cells that have limited capacity and once differentiated mature cells these cells are used for maintaining the homeostasis in adult tissues that are continuously in cellular turnover. The idea of CSC hypothesis stems from this heterogeneous pool of cells.

In the CSC model of tumors, a subpopulation of tumor cells that are capable of self-renewal and differentiation is known as CSCs. CSCs possess the ability to form tumors when transplanted to animal hosts. Altered gene expression and symmetric cell division with the tumor are two properties that distinguish the CSCs from other cells [69].

CSCs mostly have genetic mutations as well as epigenetic changes that lead to the misregulation of signaling pathways. Also, dysregulated self-renewal causes overpopulation of CSCs and eventually tumor growth. This may be because of an imbalance in symmetric cells division vs. asymmetric cell division [70]. The multilineage differentiation potential of CSCs may be impaired. It is stated that usually there exists a heterogeneous population within the tumor with partially differentiated types stemming from the cells of the tumor's origin. In addition to this, malignant tumors generally resemble normal adult stem cells and grouped as poorly differentiated cells [71].

The CSC theory makes the pavement for not only eradicating the cancer cells that are terminally differentiated and forming the bulk portion of the tumor tissues yet refocusing is necessary to the small subpopulation that supports tumor growth. There are various possibilities for the origins of CSCs that lead to tumor formation. First, the initiation of a tumor may be a result of an array of mutations that result in the transformation of a cell type, or that transformation may lead to the gain of stem cell properties later. The genetic and epigenetic instability of tumors may be the cause of heterogeneity within the tumor at different targets [72]. In this possibility, the cell is strengthened by stem-cell characteristics. Second, a normal adult stem cell may be converted into a CSC. This time, as the identity of the cell would be well-known, its differentiation and transport to other sites within the body will be easier. Thus, the conversion of a normal stem cell to a CSC to initiate cancer has a higher probability [73]. Third, the fusion of a "bad" body cell with a "good" stem cell within

the body, ultimately resulting in malignancy. The origin of cancer, whether it is caused by stem cells or cells that have stem cell-like properties, has been debated for a long time [74]. The possibilities for the formation of CSCs are summarized in Table 2.1.

In the 1980s, Goldie and Coldman proposed a mathematic model indicating that the probability of curing declines when the size of the tumor increases as tumor cells mutate to a resistant phenotype. The tumor cells are not genetically stable, so the treatment should be started immediately, and multiple drugs should be used in combination to be able to exert effects on a heterogeneous group of cancer cells [75]. The Goldie and Coldman hypothesis paved the way for tumor stem cell theory.

Table 2.1. The debated origins of CSCs

The fusion of circulating stem cells with residing cells
Normal SC to CSCs conversion
Transformation of early precursors to gain self-renewal properties
Dedifferentiation and gain of stem cell properties of somatic cells through a series of mutations and epigenetic instability

The idea that brain tumors stem from a subset of undifferentiated cells with NSC characteristics is mainly acknowledged [76]. Even there is still disagreement about scientific terminology, these cells accountable for the initiation of tumors and extra resistance to therapy in brain tumors are called brain tumor-initiating cells (BTICs).

CSCs and normal stem cells share some similarities, like the cell surface markers and signal transduction pathways related to stemness [72]. The point where they diverge is that the regulations are tight for the normal stem cells in both signaling pathways and mutations. However, due to the epigenetic changes and genetic mutations gained, the regulation of signaling pathways is not proper for the CSCs. This leads to unlimited self-renewal cycles and improper differentiation patterns, eventually causing cancer cell formation.

Like normal stem cells, CSCs also proliferate slowly, and they may be quiescent. They can have improved DNA repair mechanisms, multidrug resistance mechanisms and anti-apoptotic proteins that support the survival of CSCs. All these properties cause CSCs to have

resistance to chemotherapeutic agents, cause recurrence of tumors and distant metastases [77]. The similarities and differences between normal stem cells and CSCs are summarized in Table 2.2. These properties are making the base for studying and coping with cancer stem cells.

Table 2.2. The comparison of properties of SCs and CSCs [78], [79]

<b>Common properties of SCs and CSCs</b>	
Similar surface receptors (e.g. LIF-R, CXCR4, CD133)	
Extended life span due to increase telomerase activity	
Interaction with angiopoietic factors and stimulating angiogenesis	
The hierarchy between the cells (from progenitors to differentiated cells)	
Self-renewal	
Regulation of self-renewal through convergent signaling pathways	
<b>Comparison of SCs and CSCs</b>	
<b>Stem Cells</b>	<b>CSCs</b>
Limited self-renewal ability	Unlimited self-renewal ability
Capacity of organogenesis	Capacity of tumorigenesis
Tight regulation of self-renewal	Dysregulation of self-renewal
Proper karyotype	Improper karyotype
Quiescent cells present	Quiescent cells present
Identification through surface markers	Identification through surface markers

### **2.3.2.1. CSCs and Self-Renewal Pathways**

The dysregulation of specific signaling pathways and changes in downstream gene expression can cause failure in the regulation of stemness properties of stem cells, eventually causing tumorigenesis. The cascade of events leading to this failure is not elucidated yet for some of the signaling pathways [80]. The microenvironment and the role of specific pathways may differ according to the type of cancers. The over-expression of signaling pathways can cause resistance to cell therapies.

Wnt/ $\beta$ -Catenin has a prominent function in embryogenesis and stem cells of the embryo, the proliferation, and differentiation of adult stem cells and CSCs. Thus, the interruptions through the signal transduction of this pathway result in dysfunction and malignancy [81]. The presence of a high concentration of  $\beta$ -catenin in many of the CSC-related settings has been shown. In colon CSCs, high  $\beta$ -catenin concentration, together with supportive microenvironment is found to be related to metastasis and drug resistance [82].

Wnt signaling pathway drives epithelial-mesenchymal transition (EMT). Many of the human cancers stem from epithelial tissue. These cells are attached to a basement membrane, and they have well-organized layers. The high concentration of  $\beta$ -catenin results in the cell division arrest of tumors and the cells get mesenchymal characters [83]. The mesenchymal cells do not have apical-basolateral polarity. They do not shape regular layers like epithelial cells, but they form only focal adhesions. CSC initiation and EMT conversion are thought to be tightly controlled by mechanisms related to stemness, Wnt and Hedgehog signaling pathways.

Hedgehog signal transduction pathway is also another critical pathway that take part in proliferative niches of stem cell, regeneration, and carcinogenesis. It has been confirmed by the studies that both the presence and self-renewal capacity of CSCs are related to Hedgehog signaling [84]. Two models have been anticipated for the possible action of Hedgehog ligands on tumor initiation and growth. According to the first model, cancer cells themselves generate Hedgehog ligands and proper stromal environment [85] and as for the second, Hedgehog pathway in the stromal microenvironment prompts the growth of the tumors [86] In mouse models of chronic myeloid leukemia, Hedgehog signaling was shown to support the malignant clone through sustaining self-renewal capacity.

Notch signal transduction pathway is the key pathway for balancing cell proliferation and angiogenesis. It rfunctions in stem cell maintenance, differentiation, and angiogenesis. Studies show that the Notch pathway is activated in both cancer cells and CSCs, contributing to their malignant character through three different strategies [87]. Loss of contact inhibition and activation of Notch signaling leads to eventual oncogenic transformation and acquisition of EMT, cell motility and invasiveness, resulting in enhanced malignancy. The increased expression of the Notch signaling pathway promotes the CSC phenotype through supporting the self-renewal of CSCs, again causing malignant profile. Nevertheless, it has been

demonstrated that the blockage of Notch signaling enhances the sensitivity of the chemotherapy-resistant B-cell acute lymphoblastic leukemia [88].

Various strategies have been developed for the inhibition of oncogenic transformation and malignant character accumulated through the activation of these signaling pathways. In mouse models, it was shown that the Wnt signaling-targeted therapy resulted in a decrease in the CSCs in the bone marrow and eventually prolonged survival rate [89]. When mice were treated with cyclopamine, which is an inhibitor for a component of the pathway, the number of leukemic stem cells decreased and eventually survival rate prolonged [90]. Notch inhibitor therapy together with chemotherapy was effective in attenuating the chemoresistant CSCs of nude mice head and neck squamous cell carcinoma both *in vitro* and *in vivo* [87].

The interaction and crosstalk between different pathways for the control of stem cell self-renewal *in vivo* are clear, yet, there are still missing parts to find out for CSCs and stem cells.

#### **2.3.2.2. Isolation and Identification of CSCs**

To elucidate the role of CSCs, to follow their development, to design therapeutics it is crucial to isolate and identify the CSCs from a large number of cells. To understand the biology of the stem cells *in vitro*, the isolation method is crucial as it may alter the downstream processes. Various markers can be used to isolate stem cells from different contexts. Depending on the lineage and cell-cycle status, different methods have been used to isolate adult NSCs. Stem cell markers (e.g., surface markers), metabolic substrates, fluorescently-complexed molecules, dye efflux, and transgenic reporter mice are utilized [91].

To isolate/enrich NSCs, various methods can be used depending on the downstream applications. For immunopanning, culture dishes are incubated with specific antibodies at certain conditions to cause the electrostatic attachment of the antibody to the dish. The dishes are blocked with protein, and the single cell suspension is incubated within the plates to cause protein-antibody interactions. By using direct epitope binding or secondary antibodies, cells are positively selected and removed by either enzyme treatment or cell scrapers [92].

Fluorescence-activated cell sorting (FACS) is another valuable method for isolating NSCs. It involves separation of subpopulations of cells based on dye binding characteristics, light scattering properties and immunofluorescent labeling [92]. CSCs can be isolated with FACS

by employing various cell surface markers including C44, CD133, and CD24 depending on the type of the tumor. These markers can be used either alone or together with another marker or isolation method. For immunomagnetic selection or magnetic-activated cell sorting (MACS), the cells of interest are separated from the heterogeneous cell culture by using antibodies labeled with iron microbeads. This time, single cell suspensions are incubated with those antibodies to label the stem cells magnetically and then the mixture is exposed to magnetic field [92].

Assays based on the enzymatic activity of ALDH can be used for purification of CSCs from tumor tissues. This method, also known as Aldefluor assay, is also useful for the identification of the subtype of the cancers [93] Another method for purification is to use side population (SP) assay. It depends on the dye-exclusion of a particular subpopulation with distinct properties from the sorted cells [94].

Once the CSCs are isolated, they are characterized. The self-renewal of CSCs can be analyzed with sphere-forming assays (e.g., limiting dilution analysis or soft agar assay) *in vitro* or xenograft assay *in vivo*. Serial passages *in vitro* for clonogenic assays or serial transplantation *in vivo* for tumor-initiating ability are also used. High throughput screens can be used for drug screening on CSCs and eventually the development of cancer therapies. Also, computational modeling and *in silico* screening are useful for gathering both preliminary and expandable data.

### **2.3.2.3. Enrichment and Culture of CSCs**

Brain tumor-initiating cells (BTICs) from a series of tumors were identified by Singh *et al.* [95]. Those cells had the stem cell potential both *in vitro* and *in vivo*. It has been shown that by positive selection, CD133+ cells can be isolated, and these cells can form free-floating clusters (neurospheres), secondary spheres and differentiate into both neurons and astrocytes [96].

CD133 is a transmembrane glycoprotein with a unique structure. It has a cytoplasmic tail, five transmembrane domains, and an N-terminal extracellular domain. It shares approximately 60 percent homology with its mouse ortholog Prominin-1 [97]. Antibodies against Prominin-1/CD133 is useful for identifying and isolating neural stem and progenitor



cells from both human and murine tissues [98]. Prominin-1/CD133 is a marker that can be used alone or in combination with other specific markers to isolate stem cells from an array of tissues including kidney, prostate, skin, sarcoma, pancreas, bone marrow and brain [99].

The use of only surface markers for the isolation of CSCs is not sufficient for defining a population as a stem cell. The surface above markers are not exclusively expressed on CSCs; they may also be present on non-stem cells. In this thesis, CD133 is used to enrich BTICs for further assays related to stem-cell characterization.

NSCs can be cultured *in vitro* as either adherent monolayers on matrix or neurospheres. To keep the cells undifferentiated and preserve the multipotent properties, it is essential to support the media with mitogens such as basic fibroblast growth factor-2 (FGF-2) as well as epidermal growth factor (EGF) [100]. Each culture system has its own advantages and disadvantages. Neurosphere culture systems are valuable as they are believed to set up a niche for stem cells that simulate the *in vivo* conditions more than adherent cultures. This system enables the formation of three-dimensional interactions between the cells. These clusters may prevent the entrance of oxygen and mitogens to the center of the cluster, thereby causing variations.

Monolayer adherent cultures can be kept as pure stem cell cultures, and all the cells may have equal access to nutrients and metabolic exchange [101]. In their study, Tsai and McKay have shown that cell density is instructive for determining cell fate [102]. When multipotent cortical stem cells were kept at high density, they gave rise to neurons, oligodendrocytes, and astrocytes. When the density of cells was low, the differentiation pattern was different, and the stem cells generated mostly smooth muscle cells.

#### **2.4. ELK-1 AND STEM CELLS**

Within the context of COST TD901 action (TUBITAK 211T167 project), to examine the role of Elk-1 in neuroprotection under hypoxia, a microarray analysis with Elk1-VP16 over-expressed SH-SY5Y neuroblastoma cells has previously been performed by our laboratory (Ugur Dag, Eray Sahin, Basak Kandemir, unpublished data). In the light of these microarray results, when Elk1-VP16 regulated genes were examined, the pluripotency factors significant for stem cell regulation were also found to be potential Elk-1 targets: Pou5f1 (at

different probes, 3.7 fold increase), Sox2 (at different probes, 2.7 fold increase), Nanog (at different probes, 2.7 fold increase). In a short-term sabbatical study conducted in Canada through TUBITAK BIDEB support, Prof. Dr. Isil Kurnaz showed that CD133+ BTICs, as well as fetal human NSCs, exhibited higher expression levels of Elk-1 (unpublished data).

In a study performed by Jiang *et al.*, it was stated that Elk-1 plays a role in cerebral hypoxic preconditioning through enhanced neuron-specific phosphorylation [103]. Müller *et al.* revealed that at hypoxia, *c-fos* is triggered via the MAPK pathway through phosphorylation of Elk-1, thereby coupling tumor growth and metastasis to Elk-1 expression [104]. On human embryonic stem cells (hES), it was shown that HIF1 $\alpha$  (hypoxia-inducible factor 1-alpha) and HIF3 $\alpha$  (hypoxia-inducible factor 3-alpha) had negative control over each other and at 48 hours of hypoxia, HIF1 $\alpha$  inhibited LIF-STAT (leukemia inhibitory factor-signal transducers and activators of transcription signaling) and its self-renewal. Though at long-term hypoxia, HIF2 $\alpha$  (hypoxia-inducible factor 2-alpha) expression was induced owing to HIF3 $\alpha$ , and that led to Sox2, Nanog and POU5F1(Oct4) expression, thereby restarting the self-renewal and proliferation [105]. Furthermore, Aprelikova *et al.* demonstrated that many of the hypoxia-related genes had been regulated by HIF1 $\alpha$ , while a small subgroup that was responsive to HIF2 $\alpha$  was also co-regulated by Elk-1 [106].

Oxygen level within the developing brain and adult brain is lower than the traditional cell culture conditions (20 percent). Known as “physiologic hypoxic condition,” this situation causes various changes both through development and differentiation, as reviewed by Mannello *et al.* [107], also affecting the NSC proliferation.

Silencing of Elk-1 by RNAi in *C. elegans* model is cause mitotic errors [108]. The amount of Elk-1 is higher in the XaXa ESCs that have high pluripotency, but the difference between the cells decrease in low oxygen amounts. In their study, Goke *et al.* evaluated genome-wide kinase-chromatin interactions and ERK signaling has been shown to have a regulatory role in human ESCs [109]. In human ESCs, Elk-1 is essential, and its co-localization with Erk2 plays a role in pluripotency.

### 3. AIM OF THE STUDY

The microarray analysis of human neuroblastoma cell line SH-SY5Y showed that Elk-1 takes a role in the regulation of stemness genes *sox2*, *nanog* and *pou5f1* among with many others (unpublished data). In addition to this, Elk-1 regulates neuronal survival and is neuroprotective; however, its survival-related transcriptional targets in neurons have not entirely identified yet. This led to the hypothesis that Elk-1 transcription factor may also be functional in regulating stemness genes and supporting their proliferation/self-renewal/survival in brain tumor-initiating CSCs. This thesis aims to understand the leading role of Elk-1 in BTICs and unveil its putative target genes based on microarray results, wet-lab, and bioinformatics tools.

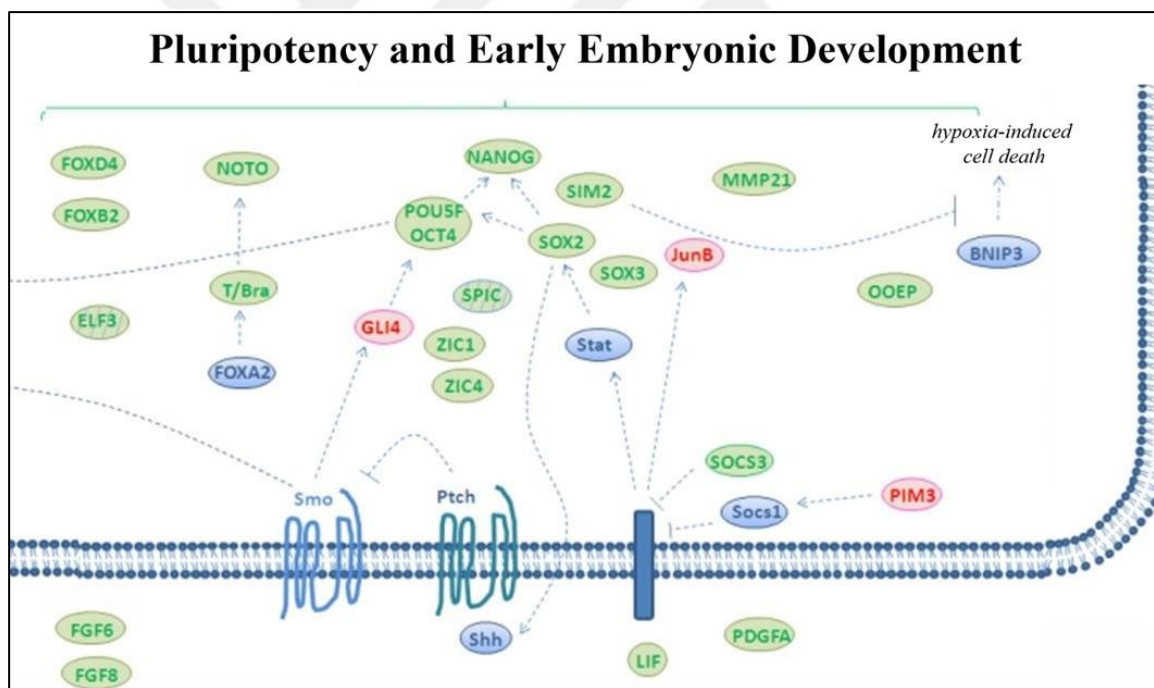


Figure 3.1. Schematic representation of a small set of genes showing increased (green) or decreased (red) expression with respect to Elk1-VP16 over-expressed SH-SY5Y neuroblastoma cells (based on unpublished microarray results by our group)

## 4. MATERIALS AND METHODS

### 4.1. CELL CULTURE

In this thesis, three types of *in vitro* culture systems were used. Monolayer (2D), tumorsphere culture (3D), and BTIC culture (3D) following CD133+ cell enrichment setups were used depending on the related experimental procedures and they were compared to each other.

#### 4.1.1. Monolayer Cultures

SKNBE(2) (ATCC® CRL-2271) and SH-SY5Y (ATCC® CRL-2266) human neuroblastoma cell lines as well as A172 (ATCC® CRL-1620), U-87 MG (ATCC® HTB-14), and T98G (ATCC® CRL-1690) human glioblastoma cell lines were used at different parts of this thesis. U87-MG, A172, and T98G cell lines were generous gifts of Assist. Prof. Tugba Bagci Onder from Koc University.

For for monolayer culture of all the stated cell lines, High Glucose (4.5 g/L) DMEM medium (Gibco, #41966029) was used as a basal medium and supplemented with one percent penicillin-streptomycin solution (Gibco, #15140122) and 10 percent fetal bovine serum (FBS) (Life Technologies, #10500064). This medium was called *complete DMEM medium* in the following sections. Cells were grown in 37°C and 5 percent CO<sub>2</sub> incubator with either normoxia (21 percent oxygen) or hypoxia (one percent oxygen).

#### 4.1.2. Tumorsphere Cultures and Brain Tumor-Initiating Cell Cultures

To form tumorsphere cultures from monolayer cells and support BTICs after conducting CD133+ isolation; initial proliferation media (IPM), N2 media and coated culture plates were necessary.

#### 4.1.2.1. Poly-HEMA Coating

Plates were prepared by coating with Poly-HEMA (Poly (2-hydroxyethyl methacrylate) solution. To prepare Poly-HEMA solution, 38 ml absolute ethanol was mixed with two ml double distilled water into a 50 ml falcon. Following the addition of 1.2 grams of poly-HEMA (Sigma, #P3932) powder into the mixture, it was placed in a shaker at 37 °C with a vigorous shake for four-five hours until no powder could be seen with the naked eye. This poly-HEMA solution was filtered to sterilize and kept at 4 °C up to six months.

There were critical steps for the preparation of poly-HEMA solution. It would not dissolve if first the poly-HEMA powder was weighed or the ethanol was not diluted with water. Also, the low attachment property of the material was lost when the solution was kept for more than six months, or the coated-plates were kept for more than three months.

Table 4.1. Poly-HEMA coating for various size of dishes [110]

	Volume per dish/per well
3.5 cm dish	500 $\mu$ l
6 cm dish	1.3 ml
10 cm dish	3.2 ml
12-well plate	200 $\mu$ l
24-well plate	100 $\mu$ l
96-well plate	25 $\mu$ l

The stated amounts of poly-HEMA solution (Table 4.1) was poured to the dishes to cover their surfaces. They were kept under the biosafety cabinet with their covers open for drying. However, the cabinet should not be open to prevent over-drying and the formation of unwanted coating style on the dishes. The following day, the dishes were UV-sterilized and stored at RT in a cool and dry place for three months.

The dishes could be coated two or three times to have homogenous coating depending on the ongoing experiment. In addition, the presence of remaining ethanol on the dishes could lead to cell death so the time of incubation in the cabinet was critical.

#### ***4.1.2.2. Initial Proliferation Medium (IPM) and N2 Medium Preparation***

Initial proliferation medium is necessary for culturing tumorspheres and isolated BTICs up to three passages. IPM is made up of Neurobasal Medium (Gibco, #21103049), 1X B27, 1X GlutaMAX, one percent penicillin-streptomycin solution (Gibco, #15140122), 20 ng/ml FGF-2 (#13256029) and 20 ng/ml EGF (#SRP3027).

N2 medium is necessary for culturing spheroids and isolated BTICs over three passages. N2 medium is made up of Neurobasal Medium (Gibco, #21103049), 1X N2 (Gibco, #17502048), 1X GlutaMAX (Gibco, 35050061), one percent penicillin-streptomycin solution (Gibco, #15140122), 20 ng/ml FGF-2 (#13256029) and 20 ng/ml EGF (#SRP3027).

#### ***4.1.2.3. Culturing Spheroids and BTICs***

Tumorspheres and CD133+/- BTICs were grown and maintained in complete initial proliferation medium (IPM) for 7-10 days in an incubator at 37°C and five percent CO<sub>2</sub>, replacing the medium with freshly prepared IPM every three-four days until their size reaches 200 microns, or they start dying from the center.

When they reached the limitations, the cells were separated with passaging. For passaging the cells, the suspension cells were collected from the dishes to a falcon and spinned down at 300xg for 10 minutes. Following the centrifugation, the medium was aspirated, and one ml StemPro Accutase Cell Dissociation Reagent (Gibco, #A1110501) was added onto the cells and cells were incubated 37°C for five minutes. They were triturated for about 40 times until the spheroids become single cell suspension. Onto this single cell suspension, five ml of PBS with antibiotics was added. Cells were counted at this stage if necessary or to continue cells were spinned down at 300xg for five minutes.

For cryopreservation, tumorspheres or BTICs were collected with their media and were spinned down at 150xg for five minutes. The cells were mixed with freezing media (IPM without growth factors and 10 percent DMSO) and placed to a freezing container at -80 °C O/N.

For thawing the vials, they were placed in a beaker with 70 percent ethanol in 37°C water bath. They were transferred to fresh IPM without growth factors and spun down at 150xg for five minutes. The recovery of the freeze-thawed cells was not efficient. Freshly isolated cells were preferred for the experiments.

#### **4.2. ISOLATION OF BRAIN TUMOR INITIATING CELLS (BTICs)**

SKNBE(2) neuroblastoma cells were grown on about 20x T150 flasks as monolayer cells with complete High Glucose DMEM media, as described previously. The cells were grown to 80 percent confluency, and on the day of isolation, the media was taken away and cells were washed with five ml PBS/flask and three ml of StemPro Accutase/flask was added onto the cells. The cells were resuspended with MACS Buffer (two percent bovine serum albumin (BSA), two mM EDTA and phosphate-buffered saline (PBS) pH 7.2).

Accutase is a natural enzyme mixture with proteolytic and collagenic enzyme activity. It has a similar effect with trypsin and collagenase, but less harmful to cell surface receptors because it is a less toxic and more sensitive enzyme.

For the experiments, CD133/1 (AC133)-PE, human (clone: AC133) (Miltenyl Biotec, #130-098-826) was chosen as a marker for multipotent progenitor cells. This epitope is expressed on various adult stem cells as well as ES and iPS cell-derived cells.

To prevent the clogging of the columns at the ongoing isolation procedure, cells were passed through the first 70-micron cell strainer several times until they can pass freely through it. Then, they were passed through 30-micron filter several times, cell aggregates were removed, and the single cell suspension was prepared. Cells could be counted at this stage of the procedure. The viable cell number was determined by staining the cells with 0.4 percent Trypan Blue Solution (Gibco, #15250061). To continue, cells were spun down at 300xg for 10 minutes, and the supernatant was removed. Cells were resuspended in 60  $\mu$ l MACS buffer/ $10^7$  cells and 20  $\mu$ l FcR Blocking Agent/ $10^7$  cells, and 20  $\mu$ l CD133 Microbeads/ $10^7$  cells were added (Miltenyl Biotec, #130-100-857). The cells were kept at 4°C for 30 minutes at a constant, slow rotation (12 rpm). Following incubation, two ml buffer/ $10^7$  cells were added to wash the cells, and then they were spun down at 300xg for 10 minutes again.

MACS MS column (Miltenyl Biotec, #130-042-201) was placed on the MACS Mini Separation stand. The cells prepared in the previous step were loaded onto that column, and with gravity effect, the suspended cells flow through the column for positive selection. That is, the cells labeled for CD133 (CD133+) were kept in the column while marker-free cells (CD133-) would not bind and washed away with the buffer.

The column was washed three times with 500  $\mu$ l of the buffer to wash column-retaining CD133+ cells, the flowing liquid was collected again, and the resulting cells were combined to assemble CD133- cells. For elution of CD133+ cells, the column was separated from the magnetic stand and allowed to stand in the non-magnetic field for about two minutes and flushed out with one ml MACS buffer with the supplied plunger.

Cells were counted with Trypan Blue, spun down for five minutes at 150xg and resuspended in complete IPM and cultured for 7-10 days in an incubator at 37°C and five percent CO<sub>2</sub>, replacing the medium with freshly prepared IPM every three-four days.

#### **4.2.1. CD133/1 (AC133)-PE Staining for Flow Cytometry**

To test the fractions for the presence of CD133 marker, the unsorted, CD133+, and CD133- fractions were checked with flow cytometry. For this, cells were grouped as unsorted (stained-unstained), CD133+ (stained-unstained) and CD133- (stained-unstained) and they were stained with CD133-PE antibody. For staining, 10  $\mu$ l of CD133/1 (AC133)-PE, human (clone: AC133) (Miltenyl Biotec, #130-098-826) was added to up to  $2 \times 10^6$  cells/group, and they were incubated for 15 minutes in the refrigerator in the dark. Following the incubation, two ml MACS buffer was added, and cells were spun down at 300xg for 10 minutes. The obtained fractions resuspended in 200  $\mu$ l MACS buffer were analyzed via flow cytometry.

#### **4.3. HANGING DROP METHOD**

To mimic the spheroid formation with changing culture conditions and low attachment plates, hanging drop method was used as shown in Figure 4.1. For this, cells were grown as monolayers and seeded for transfection on day zero. On day one, they were transfected with DNA and PEI transiently as done routinely in our laboratory and incubated for 24 hours. The



following day, they were trypsinized, counted and suspended in complete high glucose DMEM medium at a concentration of  $5 \times 10^4$  cells/ml. Twenty microliters of cells were placed inside the cover of a 100 mm sterile culture dish and seven ml of PBS was added inside the lower part of the dish to prevent the drops from drying. The drops were incubated at 37°C, five percent CO<sub>2</sub> incubator for 48 hours to allow for spheroid formation. At the end of 48 hours, pictures were taken with a stereomicroscope (Leica LED3000 SLI), and cells were collected by washing with PBS to be used for the following experiments.

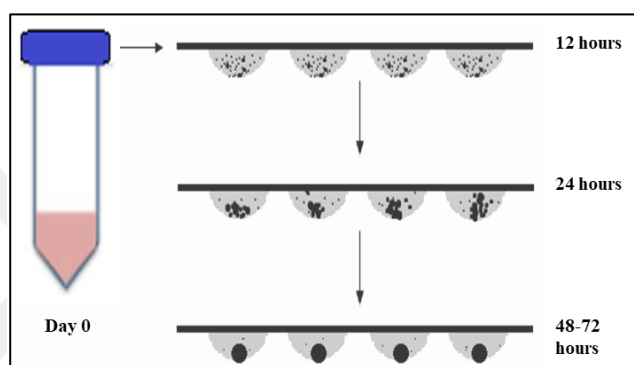


Figure 4.1. Schematic representation of the hanging drop method (based on experimental procedure)

The hanging-drop method was also used to check whether Elk-1 transfection was effective in the formation of these drops or not. With this purpose, SKNBE(2) cells were first seeded as  $25 \times 10^4$  cells/well of a 6-well plate before the day of transfection. The following day, cells were transfected with PEI (Polyethylenimine, linear, MW 25000, Polysciences) transfection reagent at a ratio of 1:3 and incubated O/N at 37°C incubator. The overall incubation time necessary for SKNBE(2) cells to express Elk-1 protein following transformation was 48 hours.

For this part of hanging-drop experiments, the transfected cells were dissociated and collected from the dish and counted to prepare the suspension necessary for the preparation of drops. This time, the drops were prepared with neuroblastoma cells transfected with pcDNA3.1 (+) and Elk1-VP16 plasmids as  $5 \times 10^4$  cells/ml in 20 microliters and incubated 24 hours after transfection. Once the drops were prepared on 100 mm culture dishes, they were again incubated for 24 hours to complete the total 48 hours of incubation time necessary for Elk-1 expression.

## 4.4. SELF-RENEWAL ASSAYS

### 4.4.1. Soft Agar Assay

The 3D growth conditions of *in vivo* environment were mimicked with both the media and the semisolid matrix, in this case, low melting point (LMP) agar. Soft agar assay is summarized in Figure 4.2.

At the end of 14 days, colonies were counted under a 10X magnification or stereo microscope. For staining, crystal violet was dissolved in PBS with two percent ethanol at a final concentration of 0.04 percent, filtered with 0.45  $\mu\text{m}$  filter and dishes were stained with 50  $\mu\text{l}$  of this solution for one hour at RT. The dishes were checked every ten minutes to prevent the staining of background. Then, the staining solution was taken away carefully, and the wells were washed with water three times for 30 minutes. At the last wash, water was kept in the wells O/N to remove the background. The dishes were ready for counting then.

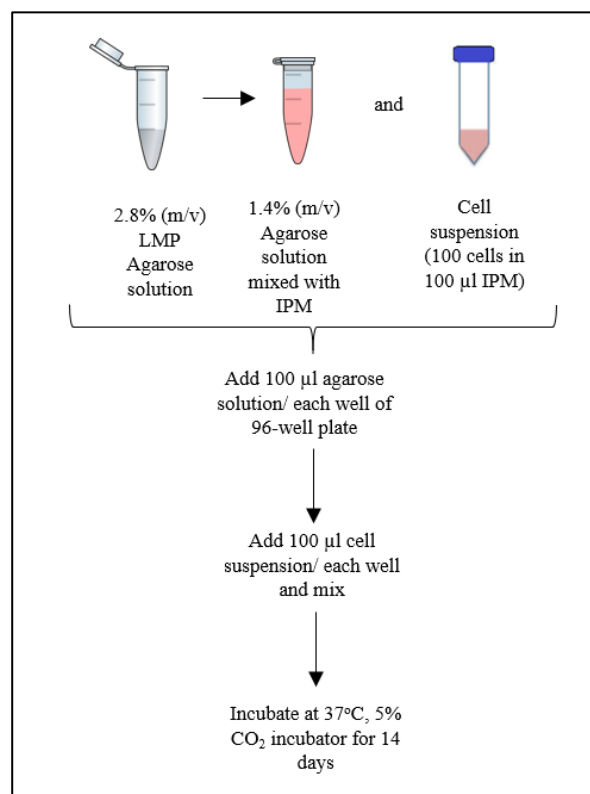


Figure 4.2. Soft agar assay in summary (based on experimental procedure)

#### **4.4.2. Limiting Dilution Analysis (LDA)**

Limiting dilution analysis (LDA) has been extensively used to find out differences within multiple groups for a particular trait. In our case, LDA was used for determining the cancer cell initiating frequency of CD133+ and CD133- SKNBE(2) cells; in other words, to evaluate the self-renewing capacity of BTICs. For LDA, following the BTIC isolation procedure, cells were counted so that 10000 cells/50  $\mu$ l complete IPM would be present in the first tube. Through serial dilution by factor two up to 1 cell/50  $\mu$ l, cells were seeded on poly-HEMA coated 96-well plates. For each condition/cell number, samples were seeded in quintuplet. 25  $\mu$ l culture media was added to each well every three-four days and cells were examined for the presence/absence of spheres and quantified on day 10.

#### **4.5. TRANSIENT TRANSFECTION FOR ADHERENT CELLS**

In the thesis, nucleic acids were introduced into the cells through liposome-mediated transient transfection. Linear polyethyleneimine, which is a polycation with high ionic charge density, PEI (MW 25000 kDa, Polysciences), was used for the formation of liposome complexes over the nucleic acids. Cell density and PEI ratio were determined for each cell line.

One day before transfection, single cell suspensions of adherent cell cultures were prepared and seeded at  $0.3-0.6 \times 10^6$  cells/cm<sup>2</sup> density in complete DMEM medium, and they were incubated in 37°C, five percent CO<sub>2</sub> incubator at transfection the flasks would be 85-90 percent confluent. At day one, for the formation of the carrier liposome complex, the desired plasmid and PEI were mixed at the determined ratio for each cell line in serum-free DMEM and incubated at RT for 20 minutes. At the end of the period, complete DMEM medium with 10 percent FBS was added to the mixture at half the volume of the mix. Two hours later, complete DMEM medium was added to the wells/dishes and the cells were incubated for 48 hours in 37°C, five percent CO<sub>2</sub> incubator for the transgene expression.

#### **4.6. TRANSFECTION TRANSFECTION FOR BTICS**

The suspension cells were collected from the dishes to a falcon and spun down at 300xg for 10 minutes. Following the centrifugation, the medium was aspirated, and one ml StemPro Accutase Cell Dissociation Reagent (Gibco, #A1110501) was put onto the cells and cells were incubated 37°C for five minutes. Cells were triturated for about 40 times until the spheroids become single cell suspension. Onto this single cell suspension, five ml of PBS with antibiotics was added and spun down at 300xg for five minutes. The cells were resuspended in complete IPM at the proper volume. Cell density and Lipofectamine 2000 (Thermo Fischer Scientific) ratio were determined.

Cells were seeded at  $0.3-0.6 \times 10^6$  cells/cm<sup>2</sup> density in complete IPM without antibiotics on the day of transfection. Following the cell seeding, Lipofectamine 2000 and the nucleic acids were diluted in neurobasal medium without antibiotics, incubated at RT for five minutes, then the diluted Lipofectamine 2000 was gently combined with the dilute nucleic acids, and the mixture was incubated at RT for 20 minutes to form liposome. Then, the mixture was added directly onto wells containing cells, and the cells were incubated for 24-72 hours in 37°C, five percent CO<sub>2</sub> incubator for the transgene expression.

#### **4.7. XTT CELL PROLIFERATION ANALYSIS**

Tetrazolium salt XTT is generally used in cell proliferation, cytotoxicity and apoptosis assays. The dehydrogenase enzyme in cells with metabolic activity reduces XTT, a yellow tetrazolium salt, into a colored formazan dye. This transformation can only take place in living cells, so the produced formazan amount is directly proportional to the number of live cells in the sample.

XTT Cell Proliferation Assay (Intron) was used as per the manufacturer's instructions to determine the change in the proliferation of cells after transfection of SKNBE(2) cells with Elk-1 series plasmids and hypoxia treatment. SKNBE(2) cells were cultured, and one day before the experiments  $15 \times 10^3$  cells were seeded in 96-well cell culture plates in six replicates per group. As the "Blank" group, only the proper medium was placed into the wells. The following day, five ml of XTT was dissolved in water bath, XTT agent and the

activation agent were mixed at 50:1 ratio to obtain the XTT assay mix. The seeding medium on the cells was replaced with fresh 100  $\mu$ L medium per each well, and 50  $\mu$ L of XTT assay mix was added onto the cells gently. Cells were incubated for two, three and four hours, and absorbances at 450 nm and 660 nm were measured at Thermo Scientific-MultiSkan Spectrum. OD650 from OD450 and only medium readings for analysis were subtracted, and the cell proliferation was calculated as percent by reference to non-transfected cells.

#### **4.8. LUCIFERASE REPORTER ASSAY**

Dual-Glo® Luciferase Assay System (E2940, Promega) was used for luciferase analysis. In this test, the interaction at the expression level between the promoter of interest and the transcription factor can be demonstrated. *Firefly* luciferase gene is located at the downstream of the promoter of interest. *Renilla* luciferase reporter gene is used to eliminate the differences due to the transfection-related efficiency problems and/or cell death related to transfection. The results are indicated as *Firefly/Renilla* ratio and shown as relative luciferase activity.

##### **4.8.1. Preparation of Reporter Plasmid Constructs**

To identify the putative Elk-1 binding sites in selected stemness gene promoters (*SOX2*, *NANOG*, *POU5F1*), the Cold Spring Harbor Laboratory - TRED, Swiss Institute of Bioinformatics - EPD and Alggen-Promo algorithmic analysis program were used. The promoter binding regions for transcription factors can be analyzed by Promo 3.0 tool and the results are displayed as “dissimilarity rate.” The dissimilarity matrix expresses the similarity pair to pair between Elk-1 DNA binding sequence and the putative sequences at analyzed genes. There exists an indirect relationship between the dissimilarity rate and the possibility of interaction between Elk-1 and the promoter of interest. The binding ability of Elk-1 to the predicted sites on the promoters could be confirmed by luciferase and chromatin immunoprecipitation assays, thereby verifying the microarray results.

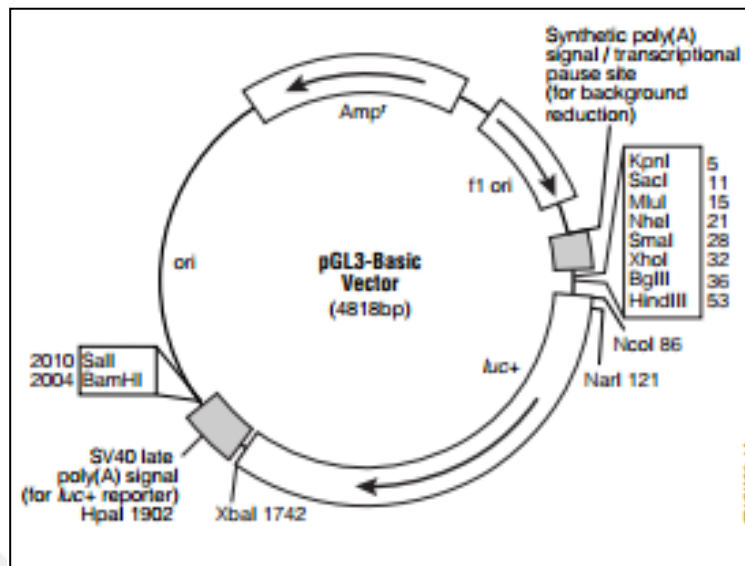


Figure 4.3. pGL3 Basic vector circle map [111]

pGL3 Basic Vector (Promega) does not have a promoter and enhancer sequences. It was chosen for assessing the possible promoter and Elk-1 interaction with luciferase assay. For this purpose, various genes both known for taking a role in maintaining stem cell characteristics and have significant expression changes in the microarray were chosen.

Table 4.2. Cloning primers for chosen *Homo sapiens* stemness gene promoters

Promoter	Forward Primer	RE	Reverse Primer	RE	Product (bp)
<i>POU5F1</i>	AGACggtaccAGGGCTG TTGGCTTTGGACA	<i>KpnI</i>	CTGTagatctAGCCATTTAA GAATTCCAGAGTAGG	<i>BglIII</i>	993
<i>SOX2</i>	CTGTggtaccGGGGAGTG ATTATGGGAAGAA	<i>KpnI</i>	CTGTagatctCACTAGACTG TCTTCATTCAACCGTAGC	<i>BglIII</i>	993
<i>NANOG</i>	CTGTggtaccTTTCTGCC TAAACTAGCCA	<i>KpnI</i>	CTGTagatctAGGTGAAGA TTCTTTACAGTCG	<i>BglIII</i>	988

These genes, namely, *SOX2* (mean fold change 2.75), *POU5F1* (mean fold change 3.68), *NANOG* (mean fold change 2.65), all have at least one Elk-1 binding site as according to ALGGEN Promo Analysis of their promoters. Primers were designed and listed in Table 4.2

for cloning *SOX2*, *NANOG* and *POU5F1* promoters into pGL3 Basic Vector (Promega) (Figure 4.3). Restriction sites and putative flanking docking sites for the restriction enzymes were added to the primers.

Gradient PCR with five different annealing temperatures was performed to detect the optimum annealing temperature of the primers. The PCR reactions were prepared with *i-Taq* DNA Polymerase (Intron, #25024) kit using the genomic DNA isolated from the SH-SY5Y cell line as a template. The PCR mixes and are given in Table 4.3.

Table 4.3. Gradient PCR ingredients

<b>Ingredient</b>	<b>Amount</b>
10x PCR Buffer (w/ 20 mM MgCl <sub>2</sub> )	2 μL
dNTP Mix (2.5 mM/each)	2 μL
Forward-Reverse Primer	10 pmoles
Template DNA	Variable (up to 1 μg)
<i>i-Taq</i> DNA Polymerase (5 U/μL)	1 U
Water	To 20 μL

The promoter regions for specified stemness genes were amplified with PCR to prepare inserts for the clonings. For the preparation of the insert, *Pfu* DNA Polymerase (Thermo Scientific, #EP0571) was used. *Pfu* is a DNA polymerase with proof-reading activity. The PCR mixes and cycling conditions are given in Table 4.4.

Following the preparation of inserts, both inserts and the vectors (in this case pGL3 Basic) were cut with proper restriction enzymes sequences of which were added while primer preparation according to the setup shown in Table 4.5.

The digestion mix was incubated at 37°C for 30 minutes, and it was purified by PureLink PCR Purification Kit (Invitrogen, # K3100-01) to obtain restriction site-digested cohesive ends of insert and vector. The concentrations and purities of the obtained products were determined by NanoDrop 2000 (Thermo Fisher).

Table 4.4. PCR ingredients and cycling conditions for insert preparation

<b>Ingredient</b>		<b>Amount</b>	
10x PCR Buffer (w/ MgSO <sub>4</sub> )		2 $\mu$ L	
dNTP Mix (2 mM/each)		2 $\mu$ L	
Forward Reverse Primer		0.1-1.0 $\mu$ M	
Template DNA		Variable (up to 1 $\mu$ g)	
<i>Pfu</i> DNA Polymerase (2.5 U/ $\mu$ L)		1.25-2.50 U	
Nuclease-free water		To 50 $\mu$ L	
<b>PCR Cycle</b>		<b>Temperature</b>	<b>Time</b>
Initial Denaturation		95°C	2 min
Denaturation	30 Cycles	95°C	20 sec
Annealing		Variable	20 sec
Extension		72°C	90 sec
Final Extension		72 °C	10 min

Table 4.5. Restriction enzyme digestion setup for cloning

<b>Component</b>	<b>Amount</b>	
	<b>Insert</b>	<b>Vector</b>
<b>10X FastDigest Buffer</b>	2 $\mu$ L	2 $\mu$ L
<b>DNA</b>	Up to 400 ng	Up to 1 $\mu$ g
<b>Restriction Enzyme-1</b>	1 $\mu$ L	1 $\mu$ L
<b>Restriction Enzyme-2</b>	1 $\mu$ L	1 $\mu$ L
<b>Nuclease-free water</b>	Up to 20 $\mu$ L	Up to 20 $\mu$ L

The ligation reaction was prepared at 1:3, 1:5 and 1:10 vector: insert ratios per 100 ng vector and T4 Ligase enzyme (NEB, #M0202S) as shown in Table 4.6. The mix was incubated at RT for 15 minutes, and ligase was inactivated by heating at 65°C for 10 minutes.



Table 4.6. Ligation reaction setup for cloning

Component	Amount
10X T4 DNA Ligase Buffer	2 $\mu$ L
Vector DNA (pGL3)	0.1 $\mu$ g
Insert DNA (promoter)	Variable (1:3, 1:5 and 1:10)
T4 DNA Ligase Enzyme	1 $\mu$ L
Nuclease-free water	Up to 20 $\mu$ L

10  $\mu$ L ligation product was transformed to 100  $\mu$ L chemically-competent *E. coli* cells with heat shock, cells were incubated at 37°C for one hour to allow ampicillin resistance expression and were spread on Amp<sup>+</sup> LB agar plates. The plates were incubated O/N at 37°C.

The presence and/or orientation of the promoter DNA sequence was confirmed by restriction analysis following colony PCR. The plasmids passing the primary verification step were sent to sequencing to confirm cloning. Luciferase constructs of many promoters were prepared, including human *SRF*, *LIF*, *DRD3* and mouse *sox2*, *nanog*, *pou5f1*, *srf* gene promoters. However, in this thesis study, only human *SOX2-luc*, *NANOG-luc*, and *POU5F1-luc* plasmids were used for further experiments.

#### 4.8.2. Site-directed Mutagenesis (SDM)

Intentional deletion mutations were made on cloned promoter sequences with site-directed mutagenesis. The promoter sequences were analyzed with Promo 3.0. Potential Elk-1 binding sites on stemness promoters were chosen according to the dissimilarity rate displayed as a result. SDM primers were designed using the NEB Base Changer (<http://nebasechanger.neb.com/>) website, and Q5® Site-Directed Mutagenesis Kit Protocol (NEB, #E0554) was followed for the mutations. The primer pairs designed flanking the region to be deleted and eventually forming deletion mutants from the cloned promoter sequences are given in Table 4.7.

Table 4.7. SDM primers

Primer	Site	Oligo	Length	T <sub>m</sub> (°C)	T <sub>a</sub> (°C)
<i>NANOG-etsA1</i>	Fwd	TACTAACATGAGTGTGGATC	20	59	58
	Rev	AGGAGGAAAAAATTTAAGAGG	21	57	
<i>POU5F1- etsA1</i>	Fwd	CCTTTCCCCCTGTCTCTG	18	64	65
	Rev	CAGGGAAAGGGACCGAGG	18	68	
<i>POU5F1- etsA2</i>	Fwd	GAATTGGGAACACAAAGG	18	57	57
	Rev	TGAATGAAGAACTTAATCCC	20	56	
<i>POU5F1- etsA3</i>	Fwd	GTGAAGTTCAATGATGCTCTTG	22	61	62
	Rev	AACCAGTTGCCCAAACCT	18	64	
<i>SOX2- etsA1</i>	Fwd	TTGAAATCACCCCTCCCC	18	64	65
	Rev	ATCCCACGGCACTGTATG	18	65	
<i>SOX2- etsA2</i>	Fwd	GTGTCTTTCCCCAGCCCC	18	69	68
	Rev	GGCGCTCAAAGTGCAGG	18	67	

Table 4.8. The setup and conditions for SDM PCR

Ingredient		Amount	
2X Master Mix		12.5 $\mu$ L	
Forward & Reverse Primer		10 $\mu$ M	
Template DNA		1 $\mu$ L (up to 25 ng/ $\mu$ L)	
PCR Cycle		Temperature	Time
Initial Denaturation		98°C	30 sec
Denaturation	25 Cycles	98°C	10 sec
Annealing		Variable	30 sec
Extension		72°C	30 sec/kb
Final Extension		72 °C	2 min

At the first step, the sequence was exponentially amplified using the SDM primers and proper annealing temperatures. The setup and conditions for the SDM PCR are shown in Table 4.8.

As for the second step, the PCR product was treated with kinase, ligase and *DpnI* restriction enzyme (KLD). The setup for KLD treatment is given in Table 4.9.

Five  $\mu\text{l}$  of the KLD mix was mixed 50  $\mu\text{l}$  chemically competent *E. coli* cells with heat shock, cells were incubated at 37°C for one hour to allow ampicillin resistance expression and were spread on Amp+ LB agar plates. The plates were incubated O/N at 37°C.

Table 4.9. KLD reaction setup for SDM

Component	Amount
2X KLD Reaction Buffer	5 $\mu\text{l}$
10X KLD Enzyme Mix	1 $\mu\text{l}$
PCR Product	1 $\mu\text{l}$
Nuclease-free Water	3 $\mu\text{l}$

#### 4.8.3. Firefly-*Renilla* Luciferase Assay

For each cell line, the necessary optimization experiments were performed, and cell numbers and DNA: PEI ratios were determined for co-transfections. For 24-well cell culture plates for luciferase analysis; for SKNBE(2), T98G and A172 cells  $80 \times 10^4$  cells/well and for SH-SY5Y and U87-MG cells  $60 \times 10^4$  cells/well were seeded with triplicates for each transfection group. The following day, *SOX2-luc*, *NANOG-luc*, *POU5F1-luc* or one of the deletion mutant of these plasmids, one of the Elk-1 series plasmids (pcDNA3.1, Elk1-VP16, Elk1-EN, siElk1 or scrRNA), *Renilla-luc* plasmid (pRL-TK (Promega, #E2241) and the proper ratio of PEI mixture was prepared. After transfection, the cells were incubated for 42 hours in a normoxic medium and subjected to one percent hypoxia for the last six hours for the normoxia-hypoxia experiments. At the end of hypoxia treatment, luciferase analysis was performed with Thermo Luminoskan Ascent device by using Dual-Glo Luciferase kit

(Promega) with some modifications. For luciferase analysis of monolayer cell lines, 48 hours of incubation was necessary before performing luciferase analysis.

On the day of the luciferase assay, the medium on the cells was aspirated, and the wells were washed with PBS. Cells were lysed with 100  $\mu$ l of 5X Passive Lysis Buffer (PLB) (Promega, #E1941) diluted to 1X. 75  $\mu$ l of the cells were transferred to luminometer compatible white-bottomed 96-well plates. To measure the *Firefly* luciferase activity, 75  $\mu$ l of Dual-Glo® Luciferase Reagent was added onto the lysed cells. For at least 15 minutes, the plates were incubated at RT, and the luminescence for *Firefly* luciferase activity was measured.

To measure the *Renilla* luciferase activity, 75  $\mu$ l of Dual-Glo® Stop&Glo Luciferase Reagent was added onto the wells. They were incubated at RT for the equal time that was done for *Firefly* luciferase, and the luminescence for *Renilla* luciferase activity was measured. *Firefly*/*Renilla* ratios were calculated, normalizations were done, and the results were graphed as Relative Luciferase Activity.

#### **4.9. RNA INTERFERENCE**

The shElk-1 plasmid prepared by Dr. Özlem DEMİR (former AxanLab member) containing the siElk-1 sequence cloned into the psiSTRIKE hMGFP vector has been used for silencing Elk-1 expression through RNA interference in AxanLab [38]. For transient silencing of Elk-1, the transfections have to be carried out two consecutive days. The silencing of Elk-1 expression was confirmed with either qPCR on RNA level or with Western blot on the protein level.

#### **4.10. GENE EXPRESSION ANALYSIS**

##### **4.10.1. Total RNA Extraction and cDNA Synthesis**

To measure the gene expression in mRNA level, quantitative PCR reaction was used. Three main steps were necessary to be able to set up a qPCR reaction. First, cells were transfected with proper plasmid constructs. In this study, either monolayer cell lines or tumorspheres were transfected transiently with Elk-1 series of plasmids, in other words, Elk-1/pcDNA3.1,

Elk-1/pCMV6Flag, Elk1-VP16, Elk1-EN, siElk-1 and their control plasmids pcDNA3.1, pCMV-6Flag, and scrRNA. Secondly, total RNA was extracted, and thirdly cDNA was synthesized from mRNA to be used in qPCR reactions. The transfection procedure was explained in detail in sections 4.5 and 4.6 in this thesis. PureLink RNA Mini Kit (Life Technologies Ambion, #12183-018) and PicoPure RNA Isolation Kit (Arcturus, #KIT0202) were used for RNA isolation throughout the experiments.

In summary, adherent cells grown in cell culture plates (usually  $1.5 \times 10^6$  cells/10 cm culture dish) were washed with cold PBS; then the resuspended cells were spinned down at 300xg for 5 minutes at 4°C. 0.3-0.6 ml of lysis solution with beta-mercaptoethanol was put onto the cells, and they were mechanically burst and homogenized by triturating through insulin syringe for 15 times. The cells were spinned down at 2000xg for five minutes at 4°C, followed by addition of 70 percent ethanol equal to the volume of the present cell lysate. The lysates were transferred to the filter cartridges and were spinned down at 12000xg for 30 seconds. Total RNA isolation was completed with centrifugation at 12000xg for one minute. The concentrations of RNA samples obtained were determined with NanoDrop2000, and the samples were stored at -80°C in the presence of RNase inhibitors or used for further experiments.

Table 4.10. The setup and conditions for cDNA synthesis

<b>Component</b>	<b>Amount</b>	
5X Reaction Mix	4 $\mu$ L	
Total RNA	Variable (up to 1 $\mu$ g)	
iScript Reverse Transcriptase	1 $\mu$ L	
<b>PCR Cycle</b>	<b>Temperature</b>	<b>Time</b>
Priming	25°C	5 min
Reverse Transcription	46°C	20 min
Reverse Transcriptase Inactivation	95°C	1 min

Following total RNA isolation, cDNA synthesis was performed using modified *MMLV*-derived reversible transcriptase using the iScript cDNA Synthesis Kit (BioRad, #1708891). For this purpose, a maximum of one  $\mu$ g total RNA sample was diluted to a maximum volume

of 15  $\mu$ L. The RNA sample was denatured at 70°C for five minutes and spun down briefly. After the addition of the 5X reaction buffer and iScript reversible transcriptase, the mix was ready for the cycling. The setup and conditions for cDNA synthesis are shown in Table 4.10. Prepared cDNA samples were either used immediately for qPCR and/or stored at -20°C for a maximum of one month.

RNA isolation, cDNA synthesis, and qPCR studies were performed with monolayer, tumorsphere and BTIC samples to compare with the microarray results of SH-SY5Y neuroblastoma cells. For this purpose, qPCR primers of potential target genes were designed.

#### 4.10.2. Primer Design for qPCR

PrimerQuest software was used for the qPCR primer design. The mRNA sequences of the target genes were obtained from the NCBI Gene database, the exon regions of the respective genes were determined, and the primers were designed to be at the exon-exon boundary (if possible).

Potential primer pairs were evaluated for GC content, melting temperatures ( $T_m$ ) and the hairpin formation and appropriate primers were determined. The NCBI BLAST database was used to check the specificity of the designed primers. The designed primers are shown in Table 4.11.

Table 4.11. Designed qPCR primers

Gene	Site	Sequence (5'- 3')
<i>GAPDH</i>	<b>Frw</b>	CAT CTT CCA GGA GCG AGA TCC
	<b>Rev</b>	AAA TGA GCC CCA GCC TTC TCC
<i>ACTB</i>	<b>Frw</b>	ACG AAA CTA CCT TCA ACT CC
	<b>Rev</b>	GAT CTT GAT CTT CAT TGT GCT GG
<i>VEGFA</i>	<b>Frw</b>	AGG AGT ACC CTG ATG AGA TCG
	<b>Rev</b>	GAG GTT TGA TCC GCA TAA TCT GC
<i>ELK1</i>	<b>Frw</b>	GCT TCC TAC GCA TAC ATT GAC C
	<b>Rev</b>	ACT GGA TGG AAA CTG GAA GG
<i>SOX2</i>	<b>Frw</b>	GGG AAA TGG GAG GGG TGC AAA AGA GG

	<b>Rev</b>	TTG CGT GAG TGT GGA TGG GAT TGG TG
<i>POU5F1</i>	<b>Frw</b>	AAG GAT GTG GTC CGA GTG TGG
	<b>Rev</b>	CCT GAG AAA GGA GAC CCA GCA G
<i>NANOG</i>	<b>Frw</b>	TTC AGA GAC AGA AAT ACC TCA GCC
	<b>Rev</b>	CCT TCT GCG TCA CAC CAT TGC
<i>HIF1A</i>	<b>Frw</b>	CGT TCC TTC GAT CAG TTG TC
	<b>Rev</b>	TCA GTG GTG GCA GTG GTA GT
<i>WNT3A</i>	<b>Frw</b>	GACAAAGCTACCAGGGAGTC
	<b>Rev</b>	CTGCTGCAGCCACAGAT
<i>IRAK3</i>	<b>Frw</b>	ACATACTAGAGTTGGCTGCATATT
	<b>Rev</b>	TGTCACCTACACACTGCAATC
<i>MEF2B</i>	<b>Frw</b>	CAACCGCCTCTTCCAGTATG
	<b>Rev</b>	TCAGCGTCTCGAGGATGT
<i>TCF7L1</i>	<b>Frw</b>	TGAGCGTGAAATCACCAGTC
	<b>Rev</b>	TGGCCCTCATCTCCTTCATA
<i>RHO</i>	<b>Frw</b>	CATGATGAACAAGCAGTTCCG
	<b>Rev</b>	AGAGTCCTAGGCAGGTCTTAG
<i>HES7</i>	<b>Frw</b>	CGGGATCGAGCTGAGAATAG
	<b>Rev</b>	GTTCCGGAGGTTCTGGTC
<i>NOTO</i>	<b>Frw</b>	GCTGGAAGAGTTGGAGAAAGT
	<b>Rev</b>	ACTCTCACCTGGTTCTCTGTA
<i>SIX3</i>	<b>Frw</b>	CAGCAAGAAACGCGAACTG
	<b>Rev</b>	GTGCTGGAGCCTGTTCTT
<i>CREB3</i>	<b>Frw</b>	ACCTGCATCTTGGTCCTACTA
	<b>Rev</b>	GGACAACACTCCATGCTCAG
<i>LIFR</i>	<b>Frw</b>	GCTCTGGACAAGTTAAATCCATAC
	<b>Rev</b>	CCCTTTGAAGGACTGGCT
<i>FRZB</i>	<b>Frw</b>	AAGTTAAGCGCTGGGATATGA
	<b>Rev</b>	GGGATTTAGTTGCGTGCTTG
<i>GLUT3</i>	<b>Frw</b>	AGCTCTCTGGGATCAATGCTGTGT
	<b>Rev</b>	ATGGTGGCATAGATGGGCTCTTGA
<i>RXRβ</i>	<b>Frw</b>	GATGTGAAGCCACCAGTCTTAG
	<b>Rev</b>	GTAGTGTGTTGCCTGAGCTTCT
<i>NODAL</i>	<b>Frw</b>	TACATCCAGAGTCTGCTGAAAC

	<b>Rev</b>	CTAGGAGCACTCTGCCATTATC
<i>PAX6</i>	<b>Frw</b>	GTGAATGGGCGGAGTTATGA
	<b>Rev</b>	ATGAGTCCTGTTGAAGTGGTG
<i>GSK3B</i>	<b>Frw</b>	CCGAGGAGAACCCAATGTTT
	<b>Rev</b>	GCCAGCAGACCATACATCTATAC
<i>FGF11</i>	<b>Frw</b>	CAAAGGCATCGTCACCAAAC
	<b>Rev</b>	GATCAGGTTGAAGTGGGTGAA
<i>FRIT1</i>	<b>Frw</b>	GTGCAGGAAACCGAGTAGAA
	<b>Rev</b>	GCGCCTTTAGAGTGAGTGAA
<i>GLI4</i>	<b>Frw</b>	CTCGGAAGGTCCCAGGT
	<b>Rev</b>	CCCGGTGATGAGAGACTGA
<i>SALL2</i>	<b>Frw</b>	AGCTCGGAGGTGATGCTA
	<b>Rev</b>	CCATTACAGGAGGGTCAGTAGA
<i>LGR5</i>	<b>Frw</b>	ACTAAGAACACTGACTCTGAATGG
	<b>Rev</b>	GACGGTTTGAGGAAGAGATGAG
<i>MAP3K14</i>	<b>Frw</b>	GAAAGTGGGAGATCCTGAATGA
	<b>Rev</b>	CGGACTGGCTGTACTGTTT
<i>AXIN2</i>	<b>Frw</b>	GGACAGCAGTGTAGATGGAAT
	<b>Rev</b>	GTTCTCGGGAAATGAGGTAGAG
<i>EPO</i>	<b>Frw</b>	AATATCACGACGGGCTGTG
	<b>Rev</b>	TGGGAAGAGTTGACCAACAG
<i>CTNNB1</i>	<b>Frw</b>	AGGTGCTATCTGTCTGCTCTA
	<b>Rev</b>	CCTTCCATCCCTCCTGTTTAG
<i>GLI1</i>	<b>Frw</b>	CGTGAGCCTGAATCTGTGTATG
	<b>Rev</b>	GCTCGCTGTTGATGTGGTG
<i>DLK1</i>	<b>Frw</b>	CACCTATGGGGCTGAATGCT
	<b>Rev</b>	GTCACGCACTGGTCACAAAG
<i>NOTCH1</i>	<b>Frw</b>	CCAGAGTGGACAGGTCAGTA
	<b>Rev</b>	TGACACACACGCAGTTGTAG
<i>JAG1</i>	<b>Frw</b>	CGTGACCTGTGATGACTACTAC
	<b>Rev</b>	CGGCAAATAGCTCTGTTACATTC



### 4.10.3. Gene Expression Analysis

All the qPCR experiments were performed using SSOAdvanced Universal SYBR Green Supermix (Biorad, #1725274) and Applied Bioscience StepOne Plus Real-Time PCR System (Thermo Fisher Scientific). The setup and cycling conditions are shown in Table 4.12.

Table 4.12. qPCR setup and cycling conditions

Component		Amount	
SSOAdvanced Universal SYBR Green Supermix (2X)		5 $\mu$ L	
Forward / Reverse Primer		300 nM	
cDNA		1-10 ng	
Nuclease-free water		Variable (Up to 9 $\mu$ L)	
Step		Temperature	Time
<b>DNA Denaturation</b>	40 Cycles	95°C	30 sec
<b>Denaturation</b>		95°C	5 sec
<b>Annealing / Elongation</b>		60°C	1 min
<b>Melting Curve</b>		65°C-95°C	0.5°C / 3 sec

The differences between the expression of target genes were normalized by the expressions of  *$\beta$ -actin* and *gapdh* genes. Each setup was prepared in triplicate and analyzed by the  $\Delta\Delta C_T$  method. The fold changes in target gene expressions were calculated based on the mean of the reference gene expression. The mean and standard deviation values were calculated for each group, and the differences in the gene expression levels were determined according to the control group.

### 4.11. WESTERN BLOTTING

To be able to identify the differences at the protein level between experimental groups and conditions, Western blotting was done. For this, BTICs, tumorspheres or monolayer cells were either transfected with Elk-1 series of plasmids or directly cultivated, and protein

samples were prepared. Then, protein concentrations were determined, and the samples were run on SDS-PAGE, immunoblotted and images were taken.

#### **4.11.1. Preparation of Protein Samples and Buffers**

For monolayer cells; first, the medium of the cells was aspirated on ice and cells were washed with ice-cold PBS two times. Then, 0.5-1 ml RIPA Buffer (50mM Tris-HCl, pH 7.4, 1 percent NP-40, 0.5 percent Na-deoxycholate, 0.1 percent SDS, two mM EDTA and 150 mM NaCl) supplemented with proteinase and phosphatase inhibitors were added onto the cells and were incubated at 4°C for 30 minutes for lysis. The lysate was collected and spinned down at 4°C 25000xg for 20 minutes; the supernatant was stored at -20°C.

For tumorspheres and BTICs; cells were collected with their culture medium in a falcon and spinned down at 4°C 250xg for 5 minutes. The cells were washed with ice-cold PBS two times. 0.2-0.5 ml RIPA Buffer supplemented with proteinase and phosphatase inhibitors was added onto the cells, cells were transferred to a tube and were incubated at 4°C for 30 minutes for lysis. The tubes were spinned down at 4°C 25000xg for 20 minutes.

BCA (Bicinchoninic acid) Assay was used for the determination of unknown protein concentrations.  $\text{Cu}^{2+}$  is reduced to  $\text{Cu}^{1+}$  when cysteine, cystine, tryptophan, and tyrosine residues are present in the sample and each  $\text{Cu}^{1+}$  ion complexes with two BCA molecules, leading to a purple product that absorbs light at 562 nm wavelength. The deeper the color of the solution would mean that the solution contains more protein. However, for determination of the protein concentration, the presence of proteins with known concentrations are necessary. A standard curve is plotted with the proteins of known concentrations, and an equation of the curve is obtained. The concentrations of the unknown proteins can be calculated with that equation.

The number of reactions necessary for both standards and the unknown samples were determined and BCA working solution was prepared by mixing 50 volumes of BCA Reagent A with one volume of BCA Reagent B. 25  $\mu\text{l}$  sample, either standards or unknowns, were dispensed to a 96-well plate and 200  $\mu\text{l}$  BCA working solution was added onto the samples. The plate was incubated at 37°C for 30 minutes, and the absorbance at 562 nm was measured for each sample. The concentrations of unknown samples were calculated as  $\mu\text{g/ml}$ .

The components of the buffers used throughout the Western blotting are given in Table 4.13.

Table 4.13. Western blot buffer recipes

<b>RIPA Buffer</b>	<b>4X SDS Loading Dye</b>	<b>10 X Tank Buffer</b>	<b>Transfer Buffer</b>
50mM Tris-HCl, pH 7.4	200 mM Tris-Cl, pH 6.8	3 g Tris base	25 mM Tris base
1 percent NP-40	0.4 percent Bromophenol blue	1 g SDS	192 mM Glycine
0.1 percent SDS	8 percent SDS	14.4 g glycine	20 percent (v/v) Methanol
0.5 percent Na- deoxycholate	40 percent glycerol	In 100 ml dH <sub>2</sub> O	10 ml 10 percent SDS solution
150 mM NaCl	400 mM DTT	pH 8.3	1 L transfer buffer
2 mM EDTA			
<b>10X TBS Buffer</b>	<b>TBS-T Buffer</b>		<b>10 percent APS</b>
500 mM Tris-HCl, pH 7.4	100 mL 10X TBS		0.1g APS
1.5 M NaCl	900 ml dH <sub>2</sub> O		In 1 ml dH <sub>2</sub> O
	1 ml Tween-20		

#### 4.11.2. Immunoblotting and Imaging

For the transfer step, the PVDF membrane first activated in methanol for 5 minutes. The transfer cast was assembled, and wet-transfer was carried out for 1-1.5 hours (depending on the size of the protein of interest) at 100V. After transfer, the gel was checked with Coomassie Brilliant Blue stain for the remaining proteins and the membrane was quick-checked with Ponceau S. Once the success of the transfer was confirmed, the membranes were blocked with either three percent bovine serum albumin (BSA) or five percent non-fat dry milk prepared with TBS-T for one hour on shaker at RT. Then, membranes were incubated with the primary antibodies of interest (anti-Nestin (Sigma, #N5413) (1:1000), anti-Sox2 (CST, #D9B8N) (1:1000), anti-Elk-1 (SantaCruz, #sc-365876) (1:1000)) O/N at 4°C. The membranes were washed with TBS-T for 3x15 minutes and were incubated for 1.5

hours at RT with HRP-conjugated secondary antibodies prepared in TBS-T solution with 1:5000 dilution. The washing step was repeated two times with TBS-T and once with TBS solution for 10 minutes each. Eventually, the membranes were incubated with ECL substrate Crescendo Western HRP Substrate (Millipore) and analyzed at Bio-Rad Chemi-Doc system.

#### 4.12. CHROMATIN IMMUNOPRECIPITATION ASSAY (ChIP)

Identification of TF binding sites within the chromatin environment is one of the various uses of chromatin immunoprecipitation (ChIP) assay. With this assay, the protein-DNA interaction in their native environment can be identified, and components of signal transduction pathways can be figured out.

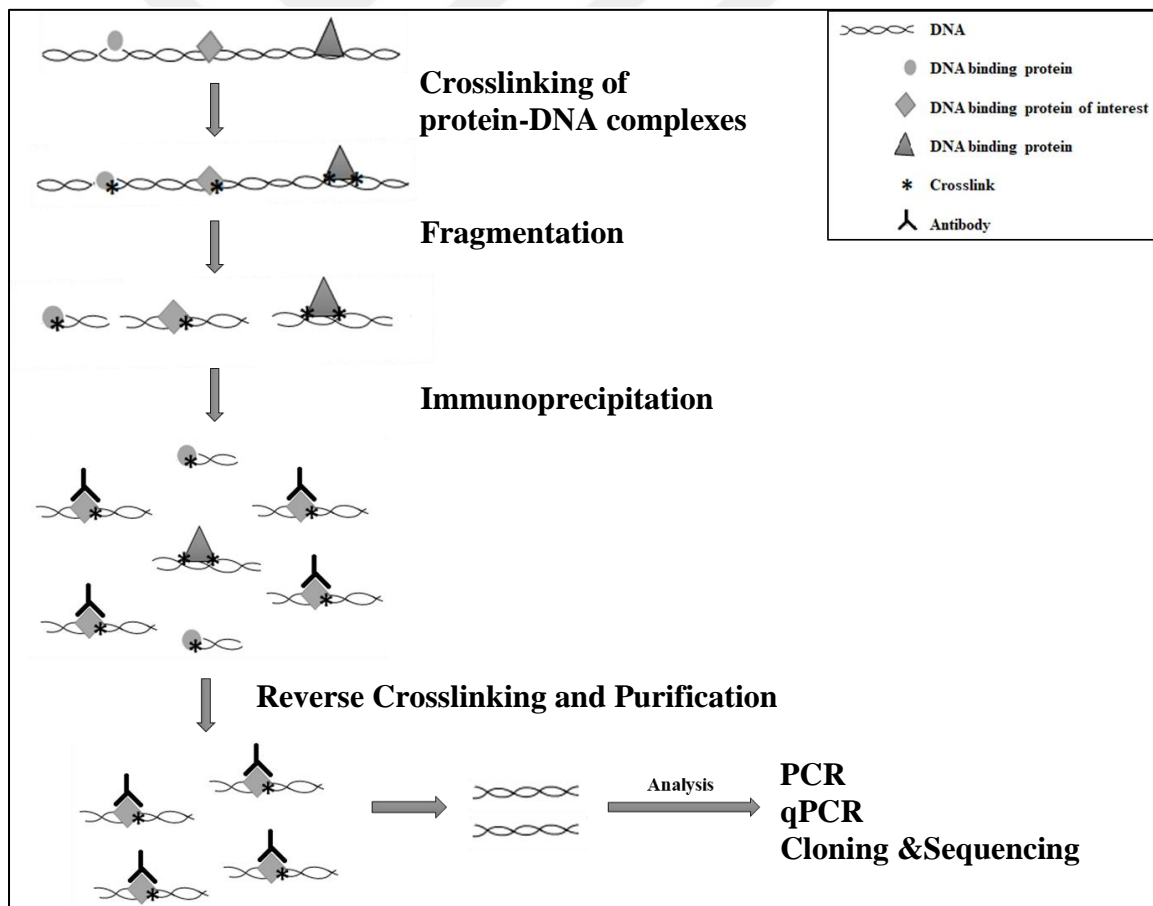


Figure 4.4. Schematic representation of ChIP assay (based on experimental procedure)

ChIP assay consists of multiple steps that require optimization at every single stage in order to obtain optimum results. To begin with, proteins and interacting DNA are crosslinked with formaldehyde; the chromatin is sheared with either sonication mechanically or micrococcal nuclease enzymatically. The nucleoprotein complex is enriched by immunoprecipitation and through the reversal of the crosslinking, DNA and the interacting protein is separated. In the end, the interacting DNA fragment is purified and quantified with ChIP-qPCR. The steps of ChIP assay are shown in Figure 4.4.

#### 4.12.1. Primer Design for ChIP

Apart from the basic elements such as  $T_m$ , hairpin formation, self- and hetero-dimer formation; the amplicon size, neighboring *cis* elements and transcription start sites (TSS) were also considered for the primer design of ChIP qPCR. The promoter sequences were retrieved and analyzed with Promo 3.0 for binding by a selected TF as shown in Table 4.14.

Table 4.14. Dissimilarity rates for potential promoter binding sites of specific promoters

	<b>Dissimilarity Rates for Promoter Binding Sites</b>		
	<b>0-1%</b>	<b>1-5%</b>	<b>5-10%</b>
<b>SRF</b>	-	2	1
<b>MCL1</b>	2	-	3
<b>KLF4</b>	1	-	1
<b>LIF</b>	-	2	1
<b>SOX2 (TRED)</b>	-	1	1
<b>NANOG (TRED)</b>	-	1	-
<b>POU5F1 (TRED)</b>	-	1	2
<b>SOX2 (EPD)</b>	1	2	3
<b>NANOG (EPD)</b>	-	1	1
<b>POU5F1 (EPD)</b>	1	2	1
<b>GLUT3</b>	-	1	2
<b>CD133</b>	-	-	1
<b>SIM2</b>	-	1	1
<b>ELF3</b>	-	1	1

The amplicon size was different from the other assays. It was arranged between 75-150 bp, trying to keep the size as much as small due to the fragmentation step. CpG islands were checked for the potential binding sites of Elk-1, and the position of Elk-1 to those sequences was considered for primer design.

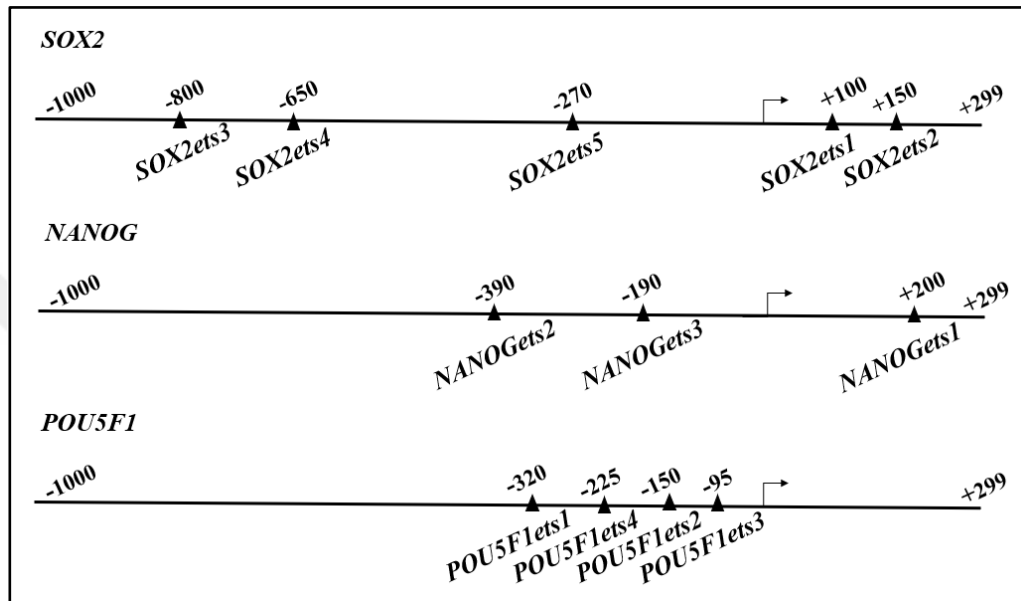


Figure 4.5. Elk-1 binding sites on stemness promoters for ChIP primers following promoter analysis

Figure 4.5 shows the sites for *ets* binding on the promoters of the stemness genes of interest. As two databases, namely TRED and EPD, were used at different times throughout the thesis and their results were combined, the numbering is not in line.

Table 4.15. The list of primers used in ChIP Assay

Name	Primer	Sequence	Product Size
ChIP_MCL1	Frw	GCCGCCCTAAAACCGTGATA	99
	Rev	CGCCTGGCTGAGAAAACCTG	
ChIP_SRF	Frw	TGACAGCAACGAGTTCCGGTA	130
	Rev	CCCCCATATAAAGAGATACAATGTT	
ChIP_SOX2_ETS1	Frw	TGGGAGGGAGTTTGTGACT	97
	Rev	AAAGTGCAGGCGATGGG	

ChIP_SOX2_ETS2	Frw Rev	GTGGGATGCCAGGAAGTT GTCGTGCGGCTTTCAAATG	102
ChIP_SOX2_ETS3	Frw Rev	AGACAGTCTAGTGGGAGATGTG CGGACCATAAGGCAGACTCTA	138
ChIP_SOX2_ETS4	Frw Rev	CTTATGGTCCGAGCAGGATTT TCCCGACTAGAAGTTAGGAGAC	103
ChIP_SOX2_ETS5	Frw Rev	CGCACCTTAGCTGCTTCC GTCACACCACACGCCTTT	143
ChIP_NANOG_ETS1	Frw Rev	CTGGAGGTCCTATTTCTCTAACATC ATGCTTCAAAGCAAGGCAAG	155
ChIP_NANOG_ETS2	Frw Rev	GCAGAGGAGAATGAGTCAAAGA CCCAAACCCAACATTCAAGAAA	131
ChIP_NANOG_ETS3	Frw Rev	CTTAGTCCAGCCTGTTCCAAA AGTGAAAGACCAAAGGGAAGG	136
ChIP_POU5F1_ETS1	Frw Rev	CTTCACTGCACTGTACTCCTC CACCTCAGTTTGAATGCATGG	101
ChIP_POU5F1_ETS2	Frw Rev	GGAGTTTGTGCCAGGGTT CCCTCCAACCAGTTGCC	105
ChIP_POU5F1_ETS3	Frw Rev	GTTGGAGGGAAGGTGAAGTT TACTGTGTCCCAAGCTTCTTTAT	93
ChIP_POU5F1_ETS4	Frw Rev	CATCATCTCTGCTGGGATTACC CTGACTCTAGTTGACGTGTTGG	143
ChIP_KLF4	Frw Rev	CATAGCAACGATGGAAGGGA TCTCTCTGGTCGGGAAACT	149
ChIP_LIF1	Frw Rev	CTTCCATTCATAATTTCTATGATGCAC CCTGATTTATATACTGGAGCCTGTG	111
ChIP_SIM2	Frw Rev	TCTTGGACCTGCAACACC TCTCGGGAAGGTCACCA	138
ChIP_ELF3	Frw Rev	CAGAGGGTGCGGGATGA GCCTTTAGACTGGGCTCCT	135
ChIP_GLUT3	Frw Rev	CCACCCTTTGCGGAGATTAT TCCTTCTCAGCAGCAAGTTT	115
ChIP_CD133	Frw Rev	TCTACAGGAAATGGATGCTGTC GGATCTGCCTCAGTCACTTAAA	131

Primers were designed for the chosen potential Elk-1 transcription factor binding sites as shown in Table 4.15. the primers were prepared. UCSC *in silico* PCR tool was used to verify the amplicon. The sites that had lower dissimilarity rate would have more possibility for the interaction with the transcription factor of interest.

#### 4.12.2. Crosslinking and DNA Shearing

Cells were seeded in  $2 \times 10^6$  cells/dish and three dishes per experimental group on day zero. On day one, cells were transfected with transient transfection with pcDNA3.1 and Elk1-VP16 plasmids and incubated 48 hours at 37°C, five percent CO<sub>2</sub> incubator. On day three, cells were treated with one percent formaldehyde at RT for 20 minutes cells, and the nucleoprotein complex formation (cross-linking) was achieved. Glycine was added to the dishes with a final concentration of 0.125 M and incubated for five minutes at RT on a shaker for quenching formaldehyde. From that point on, all manipulations to the cells were carried out on the ice.

The dishes were washed three times with cold PBS on ice and then spun down at 400xg for five minutes at 4°C with 1X protease inhibitor cocktail (PIC) (Roche, 4693159001) added to cold PBS. The supernatant was aspirated, and lysis buffer with 1X PIC was added onto the cells with a volume of at least 10 times the pellet obtained. The suspension was incubated on ice for 10 minutes and passed through insulin needle 20 times.

At this stage, one volume of the sample was mixed with an equal volume of 0.4 percent Trypan Blue Dye and the cell nuclei were checked under the microscope. The pellet obtained after centrifugation at 450xg for five minutes contained cell nuclei. The volume of the sonication buffer to be used to dissolve the pellet was adjusted to  $2-3 \times 10^6$  nuclei/ml and sonicated in the Biorupter UCD-200 Sonicator (Diagenode). The setup for sonication was optimized to be 20 cycles with 30 sec on and 30 sec off for both SKNBE(2) and T98G cell lines by running five  $\mu$ L of sheared sample on two percent agarose gel.

Once the chromatin was sheared, the fragmentation would lead to ladder-like bands concentrated at the proper size. Following the sonication, cell lysates were spun down at 22000xg for 20 minutes at 4°C to remove insoluble materials. If necessary, the sonicated DNA could be snap frozen in liquid nitrogen and kept -80°C for about a month.



To continue, the supernatant was diluted five-fold with dilution buffer. The resulting supernatant was pre-cleared for 4 hours with slow rotation with protein A/G mixture beads. After incubation, the samples were precipitated at 150xg for 5 minutes at 4°C, 11 percent of the total supernatant was removed as total input control and kept in -20°C until the elution step. The rest of the supernatant was divided into two fractions of negative control (IgG-mock) and immunoprecipitation (IP) per group.

#### 4.12.3. Immunoprecipitation of DNA-Protein Complex

60 µL ANTI-FLAG® M2 Affinity Gel (Sigma, #A2220) resin per group was washed and equilibrated with five volumes of dilution buffer and spun down three times at 400xg for one minute each at 4°C. The negative control and IP fractions separated from the dilution in the previous step were mixed with Protein G-Plus agarose beads and anti-Flag M2 resin, respectively. The tubes were incubated at 4°C O/N with slow rotation.

The following day, the mix was spun down at 4°C and 600xg for five minutes, and the pellet was collected. The washing steps are shown in Table 4.16. Following each of the washing steps, the beads were spun down at 4°C and 600xg for five minutes. Depending on the results gather from the qPCR the duration and the repetition times of washing steps were optimized.

Table 4.16. ChIP washing steps

	<b>Duration</b>	<b>Times</b>
Low Salt Buffer	5 minutes	2
High Salt Buffer	30 minutes	2
LiCl Buffer	30 minutes	1
TE Buffer	5 minutes	1

At the elution step, the inputs that were collected and frozen a day before were thawed and added as the third fraction of each group. After the last wash, 250 µL fresh elution buffer,

pre-heated at 65°C, was added onto the beads and they were incubated on a shaker for 15 minutes. The tubes were vortexed with five-minute intervals. The mix was spun down at 4°C and 18000xg for five minutes. The supernatant was collected for each fraction of each group, and the elution step was repeated with another 250 µL elution buffer. The supernatants from each elution were combined in a tube.

#### **4.12.4. Reverse Crosslink and Purification**

After elution of the crosslinked DNA-protein complex, 10 µL of RnaseA (10 mg/ml) (Intron, #BR003) and 25 µL of 5 M NaCl was added onto the elutes and incubated for at least five hours or O/N at 65°C. Using MEGAquick-spin™ Plus Total Fragment DNA Purification Kit (Intron, #17290) the DNA was cleaned up. The resulting fractions were used for qPCR analysis.

#### **4.12.5. Quantification of ChIP**

SSOAdvanced Universal SYBR Green Supermix (Biorad, #1725274) and Applied Biosciences StepOne Plus Real-Time System were used for qPCR analysis with DNA isolated from ChIP. 10 µl PCR reaction was prepared by mixing 2X SSOAdvanced Universal SYBR Green Supermix, 300 nM forward and reverse primers each and 1 µl template. In the analysis phase, qPCR signals obtained from the ChIP samples were normalized by the signals obtained from the input, and the mock samples and the results are presented as fold change.

#### **4.12.6. ChIP Buffers**

The components of the buffers used throughout the ChIP experiments are given in Table 4.17. The underlined reagents have to be added to the solution just before the use of the buffer. The buffers were either filtered or autoclaved for sterilization. They were kept up to six months.

Table 4.17. ChIP buffer recipes

<b>Lysis Buffer</b>	<b>Sonication Buffer</b>	<b>Low Salt Buffer</b>	<b>High Salt Buffer</b>
25 mM HEPES, pH 7.8	50 mM HEPES, pH 7.9	0.1 percent SDS	0.1 percent SDS
1.5 mM MgCl <sub>2</sub>	140 mM NaCl	1 percent Triton X- 100	1 percent Triton X-100
10 mM KCl	1 mM EDTA	2 mM EDTA	2 mM EDTA
0.1 percent NP-40	1 percent Triton X-100	20 mM Tris-Cl, pH 8.0	20 mM Tris-Cl, pH 8.0
1mM DTT	0.1 percent Na-deoxycholate	150 mM NaCl	500 mM NaCl
<u>0.5 mM</u> <u>PMSF</u>	0.1 percent SDS	<u>1 mM PMSF</u>	<u>1 mM PMSF</u>
<u>PIC</u>	<u>0.5 mM PMSF</u>		
	<u>PIC</u>		
<b>LiCl Buffer</b>	<b>TE Buffer</b>	<b>Elution Buffer</b>	<b>Dilution Buffer</b>
0.25 M LiCl	10 mM Tris-Cl, pH 8.0	50 mM Tris-Cl, pH 8.0	0.01 percent SDS
1 percent NP-40	1 mM EDTA	10 mM EDTA	1 percent Triton X-100
1 percent Na- deoxycholate	<u>1 mM PMSF</u>	1 percent SDS	167 mM NaCl
1 mM EDTA			20 mM Tris-Cl, pH 8.0
10 mM Tris-Cl, pH 8.0			1.1 mM EDTA
<u>1 mM PMSF</u>			

#### 4.13. STATISTICAL ANALYSIS

For statistical analysis, one-way ANOVA or two-way ANOVA with Tukey post hoc test or Student's t-test was used depending on the context. The graphs were drawn in Prism 6 GraphPad software. P value under 0.05 was considered significant.

## 5. RESULTS & DISCUSSION

The CSC hypothesis states that a subgroup of healthy adult stem cells gains the potential of cancer cells and prolonged lifespan due to continued proliferation. This increased lifespan makes the pave for the accumulation of carcinogenic traits, which in turn making them unresponsive to regulatory networks and treatments. Finding out the mechanisms that take place in the oncogenic transformation, the points from which the CSCs evade the rules and possible ways to overcome the progression of cancer can be the key for anti-cancer therapies.

There exists a complex interplay at both transcriptional and translational levels in the ultimate decision a stem cell or in this case a brain tumor-initiating cell makes to either keep itself as stem cell (self-renewal) or become a specific cell through differentiation. Signal transduction pathways, regulatory networks, and post-translational modifications work together for the final faith. Gene expression is regulated in multiple levels strictly. In eukaryotes, with the binding of TFs to DNA and synthesis of various genes in response to an array of stimuli lead to transcription and gene expression.

CSCs stated as the subset of adult stem cells, can be isolated from the leading group of cells through various methods as stated early in this thesis. In this case, marker isolation was preferred.

In this study, CD133, a speculative CSC marker that takes role in metastasis, tumorigenesis, and resistance to chemotherapy, was used for the isolation of possible BTICs. The suspected functions of CD133 on apoptosis inhibition [112], increasing angiogenesis through increasing the gene expression of VEGF-A and various signaling pathways like Wnt signaling pathway leads to the idea that CD133 may be the main point to concentrate, “*the Achilles’ heel*” for CSCs.

In the beginning, the optimum conditions for the isolation and growth of brain tumor-initiating cells (BTICs) were determined, and the isolated CD133+ BTICs were characterized according to the critical properties of CSCs. The studies were carried *in vitro* with well-known continuous brain tumor cancer cell lines.

## 5.1. ISOLATION AND CHARACTERIZATION OF CD133+ HUMAN BTICS

### 5.1.1. Tumorsphere and CD133+ BTIC Formation Under Special Conditions

A tumorsphere is a compact and rounded formation originated from the proliferation of one cancer stem/progenitor cell. They seem to be blended, and single cells cannot be distinguished. Cells are grown in a serum-free medium supplemented with growth factors and other nutrients, and non-adherent substratum to support the cancer stem/progenitor cell population since only cancer stem/progenitor cells can persist and propagate in this situation.

By forming spheres, the tumorspheres minimize environmental stimulation, thereby, keeping themselves in an undifferentiated state. The time necessary for the formation of tumorspheres, their size and the number of tumorspheres formed at a certain length of time can be useful for characterization of the tumor stem/progenitor cells within a population of cells, either *in vitro* or *in vivo*.

In some studies, the use of cell lines as the source of CSCs is not recommended. The main reason is that cells grown in the serum-containing medium are considered to be different cells from the primary tumor cells from which they are genetically and biologically derived. However, cancer cell lines are advantageous over tumor tissues in terms of the studies presented in this thesis. Working with homogeneous cells without the presence of other contaminating cells and obtaining more cells from these subsets than primary tissues is possible. Nestin and CD133 can be used as markers for both NSCs and CSCs [113]. Therefore, the cell lines that have been used are essential tools to examine the biology of CSCs.

Standard methods can be used either alone or together with other means for the generation of spheroids including hanging-drop method, non-adherent substratum methods, spinner flask suspension culture supplemented with media composition and lately the microfluidic techniques. Once the cell-substrate interactions overcome the cell-cell interactions, spheroids can form naturally.

Hanging drop method relies on the formation of suspension droplets on the lid of the culture dish due to gravity and surface tension. It is a cheap and straightforward method when the other practices are taken into consideration, and it enables the formation of defined-size

spheroids. However, there are an array of disadvantages for developing spheroid cultures *in vitro* such as spheroid size constrictions, handling difficulties, long-term culture problems, and low-throughput. Regardless of these difficulties, the hanging-drop method was used at the very beginning of these experiments.

For the preparation of hanging-drops with the help of gravity,  $5 \times 10^3$ - $10 \times 10^3$  SKNBE(2) cells per 20 microliters of complete DMEM High Glucose medium was prepared ( $5 \times 10^4$  cells/ml), and the drops were placed to the inside of the cover of a 100 mm sterile culture dish. The lower part of the dish was humidified. Even 24 hours was enough to see the cells to form a sphere-like structure for SKNBE(2) cells.

At the third day of drop formation, ten microliters of medium were replaced with fresh medium to support the proliferation. Otherwise, due to the energy consumption of the cells, the color of the media would turn into yellow – meaning the pH of the medium was acidic – and would affect the spheroid formation by increasing the environmental stress. Figure 5.1 shows the representative images taken with a stereotaxic microscope (upright) (LEICA LED3000 SLI) (LEICA LED3000 SLI) for the formation of spheroids with the hanging-drop method.

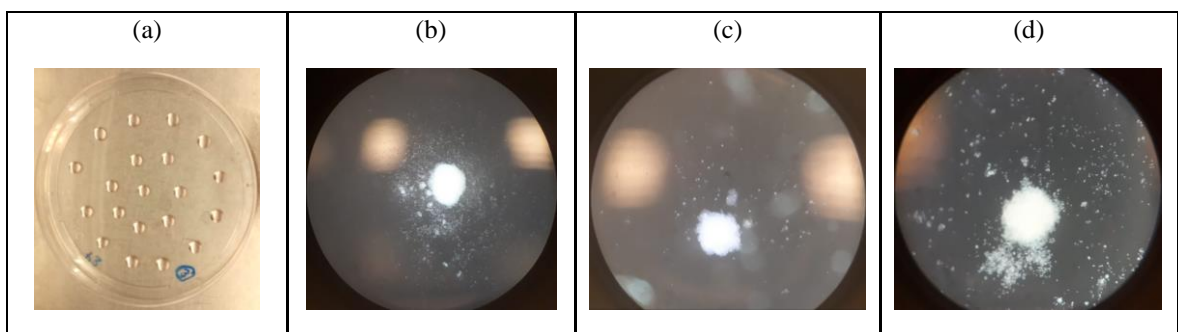


Figure 5.1. Hanging drop method to produce 3D spheres without changing the culture medium (a) set-up on culture dishes, (b) non-transfected SKNBE(2) cells, (c) pcDNA3.1-transfected SKNBE(2) cells, (d) Elk1VP16-transfected SKNBE(2) cells.

Due to the extra steps necessary for the drop formation of transfected cells and the low number of drops per dishes, the hanging-drop method was not used for the following experiments. A rather expensive but straightforward approach, growth factor-supplied medium together with poly-HEMA coated dishes was preferred for tumorsphere formation

at the ongoing experiments. With this technique, many of the disadvantages of the hanging drop method were overcome. However, this technique also had its limitations: spheroid size uniformity is a critical criterion for having reproducible results as it affects transport through the cells and eventually cell behavior.

A specific portion of the tumor cell population has the capacity for tumor initiation and self-renewal. The subpopulation of brain tumor cells that express CD133 epitopes, AC133 and AC141, have been shown to have increased tumor initiation capacity in xenograft models [114]. Since then, these two epitopes have been used for the enrichment of CSCs, but the specificity of each epitope at specific contexts is different [114]. For *in vitro* studies conducted through brain tumor cell lines CD133/1 (AC133) epitope is shown to be more useful in literature [115].

In this thesis, CD133/1 (AC133)-PE, human (clone: AC133) (Miltenyl Biotec, #130-098-826) was used as a marker for the enrichment of multipotent progenitor cells. Kelly *et al.* reported that the percentage of CD133+ BTICs isolated from T98G human glioblastoma cell line was only 0.3 percent and U87-MG human glioblastoma cell line was 0.2 percent of the total population [116], whereas Platet *et al.* reported no CD133 expression for U87-MG (ATCC HTB-14) and U138-MG (ATCC HTB-16) glioblastoma cell lines that are cultured for a long time at normoxia (20 percent oxygen).

This means CD133+ cell isolation would lead to a small number of cells when cell culture is considered. As the reports in literature do not converge on a specific statement, to detect the presence of CD133+ BTICs in T98G and U87-MG cell lines, isolation procedure was carried out for both T98G and U87-MG cell lines for up to  $5 \times 10^8$  cells for each cell line. However, the resulting isolated number of BTICs were not enough for the ongoing experiments (results not shown). Therefore, T98G human glioblastoma cell line was used for tumorsphere experiments without BTIC enrichment with CD133.

Mahller *et al.* stated that when various human neuroblastoma cell lines (LA-N-5, IMR-32, SKNBE (2), CHP-134, SH-SY5Y, SK-N-SH, CHLA-20, CHLA-79) were assessed for CD34, CD133 and Nestin expressions and the ability to form clonal spheres, only four of these cell lines had the capability to form tumorspheres [117]. SKNBE(2) (ATCC, CRL-2271) was one of those human neuroblastoma cell lines with 2.6 percent CD133+ BTICs that was commercially available at the beginning of the thesis, and for the CD133+ BTIC

isolation experiments this cell line was used. When five million SKNBE(2) cells were stained with CD133-PE before enrichment with CD133 microbeads (Miltenyl Biotec, #130-100-857) and analyzed with flow cytometer, as seen in Figure 5.2, staining was observed for 3.6 percent of the cells, which was also consistent with Mahller *et al.* [117]. In their article, Guo and his colleagues use two different media complex, namely initial proliferation medium (IPM) and N2 media, to obtain neurospheres from the SVZ and SGZ parts of the brain [118].

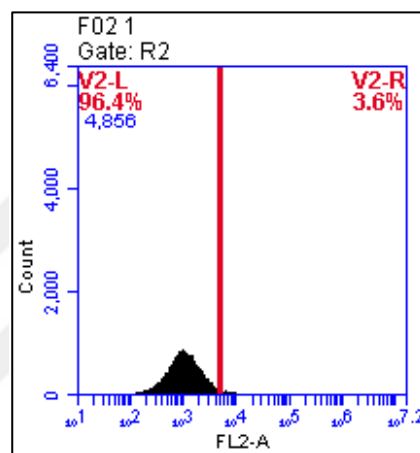


Figure 5.2. Flow cytometric analysis of SKNBE(2) cells for CD133-PE staining

For the assessment of the media composition and cell culture substratum, isolated CD133+ BTICs were cultured with IPM and coated poly-HEMA vs. non-coated culture dishes.

Figure 5.3 shows the representative images for each condition. As seen in Figure 5.3, even the culture medium alone could transform cells to the spheroids regardless of whether they were CD133+ or CD133-. However, they could not keep their form but differentiate when the culture plates were not coated. The attachment of the spheroids to the flasks would give the cells the suitable microenvironment for the differentiation of the cells. Even the attachment without differentiation would lead to the expression of different genes.



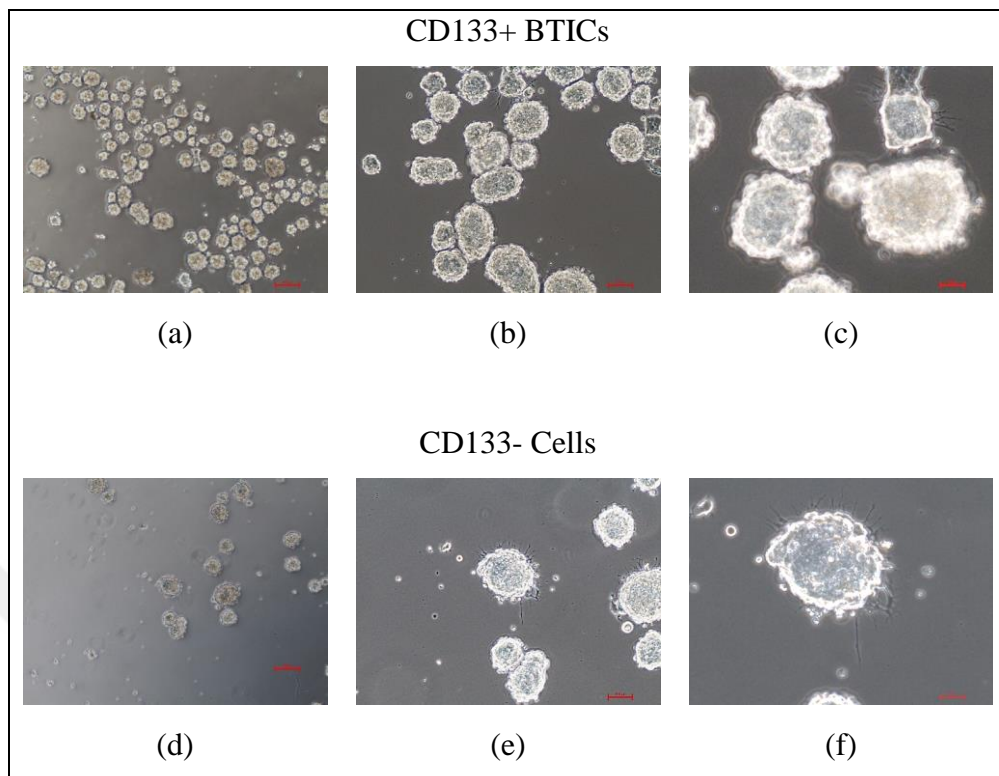


Figure 5.3. SKNBE(2)-derived cells with IPM on non-coated dishes (a) CD133+ BTICs, 4X, non-coated dish, day 4, (b) CD133+ BTICs, 10X, non-coated dish, day 4, (c) CD133+ BTICs, 20X, non-coated dish, day 4; (d) CD133- cells, 4X, non-coated dish, day 4, (e) CD133- cells, 10X, non-coated dish, day 4, (f) CD133- cells, 20X, non-coated dish, day 4.

Figure 5.4 shows the images following the CD133+ BTIC isolation when cells were grown in proper IPM and plates coated with poly-HEMA. Even the starting cell number for the culture of CD133+ BTICs and CD133- cells were the same, the number of resulting spheres were different for each group.

Nevertheless, the formation of tumorspheres stemming from CD133- cells could be an indication of “impurity”. To overcome this idea, CD133 gene expression was checked. According to the CD133 gene expression analysis seen in Figure 5.5, CD133 expression was significantly higher in CD133+ BTICs than that of the CD133- cells. The enrichment of the CD133 group could be achieved.

According to Singh *et al.*, CD133+ BTICs derived from adult GBM patients could form primary xenografts in mice. When those cells were isolated and reinjected to form xenografts again, mice had the tumor.

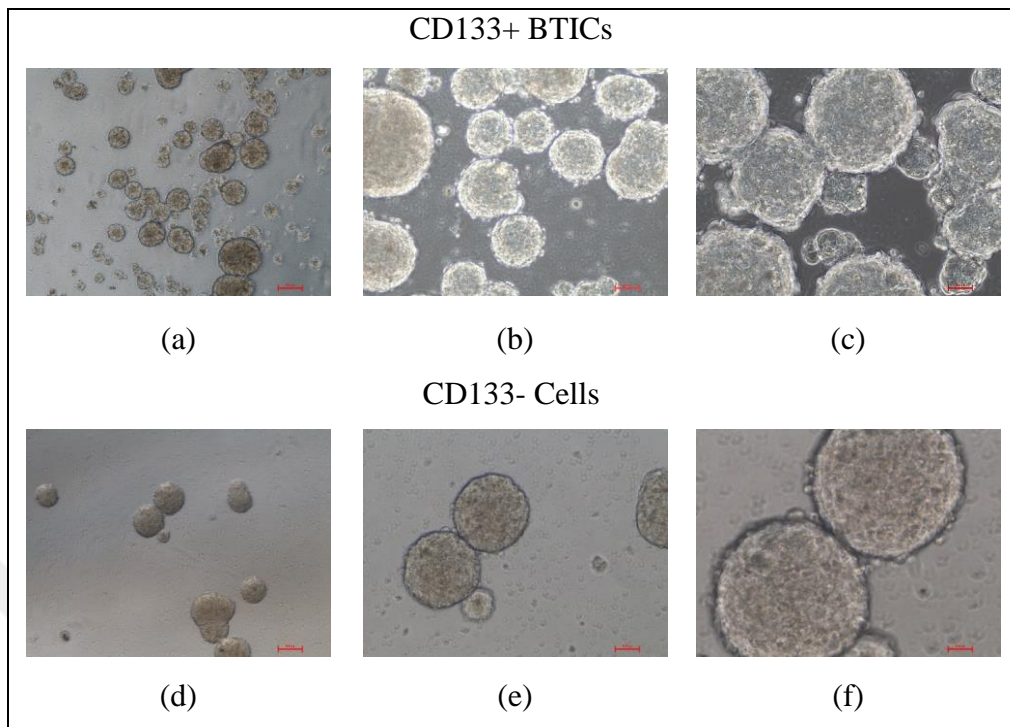


Figure 5.4. SKNBE(2)-derived cells with IPM on coated dishes (a) CD133+ BTICs, 4X, poly-HEMA-coated dish, day 4, (b) CD133+ BTICs, 10X, poly-HEMA-coated, day 4, (c) CD133+ BTICs, 20X, poly-HEMA-coated dish, day 4; (d) CD133- cells, 4X, poly-HEMA-coated dish, day 4, (e) CD133- cells, 10X, poly-HEMA-coated dish, day 4, (f) CD133- cells, 20X, poly-HEMA-coated dish, day 4.

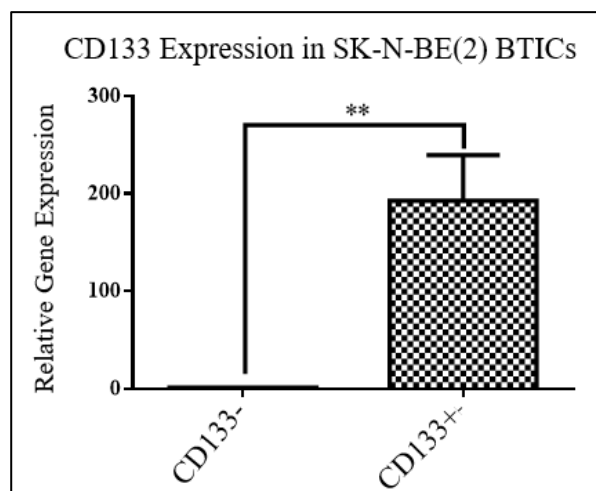


Figure 5.5. CD133 gene expression level comparison following isolation with MACS (Unpaired t-test, \*\* p=0,001)

In the same study, the engraftment of CD133- cells did not result in the formation of tumors. They concluded that CD133+ cells had the capacity of self-renewal [1]. Todaro *et al.* showed that while CD133+ BTICs were insensible to treatment with high doses of chemotherapy drugs, CD133- spheroids had high sensitivity [119].

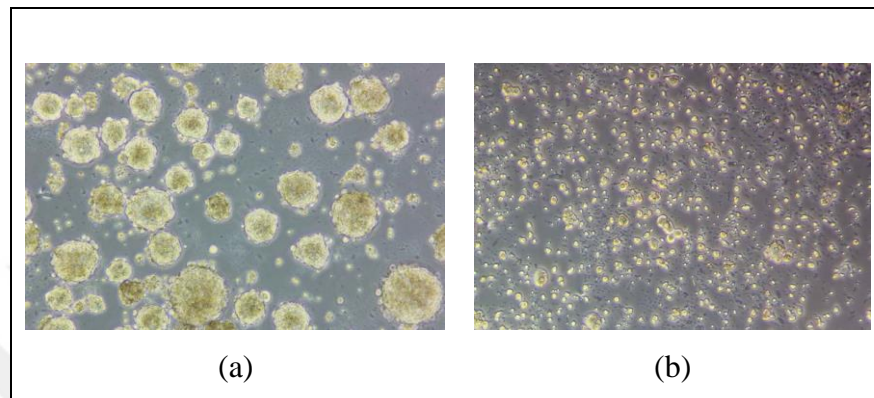


Figure 5.6. First passage, day 4, poly-HEMA coated dish (a) CD133+ BTICs, 20X, (b) CD133- spheroids, 20X

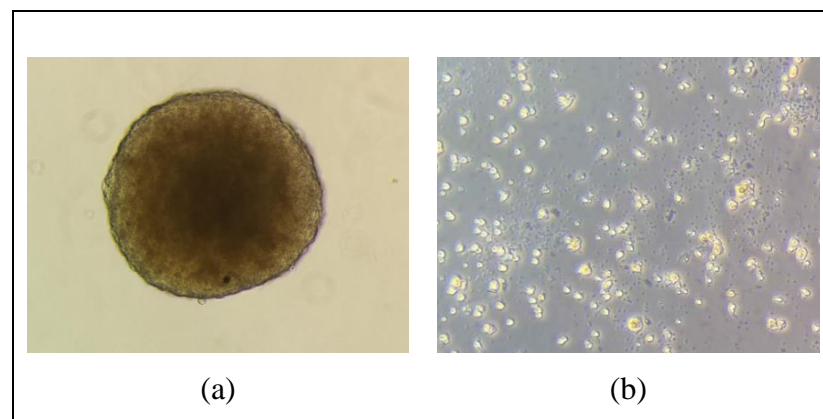
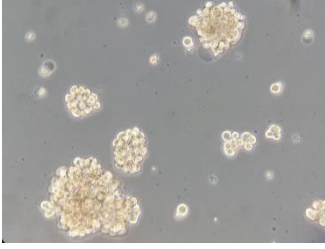
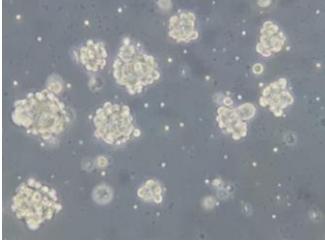
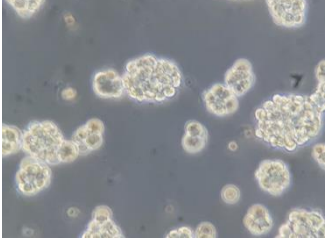
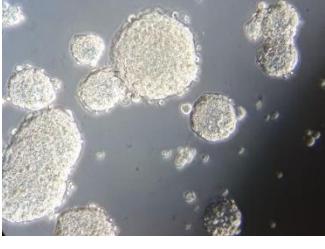
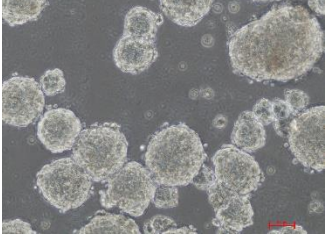


Figure 5.7. Second passage, day 10, poly-HEMA coated dish (a) CD133+ BTICs, 40X, (b) CD133- spheroids, 20X

Serial passaging is a useful technique to check the self-renewal ability of the cells. Together with the difference in gene expression levels of CD133+ BTICs and CD133- spheroids, this led to the idea that isolation was proper and the morphology and the number tumorspheres formed would also be an indicator for the self-renewal properties of CD133- spheroids.

Table 5.1. Tumorsphere morphologies for various cell lines

Cell Line	Tumor Type	Light Microscope, 20X
A172 (ATCC CRL-1620)	Glioblastoma	
T98G (ATCC CRL-1690)	Glioblastoma	
U87MG (ATCC HTB14)	Glioblastoma	
SH-SY5Y (ATCC CRL-2266)	Neuroblastoma	
SKNBE(2) (ATCC CRL-2271)	Neuroblastoma	

CD133+ BTICs could be passaged up to fifth passage whereas CD133- spheroids could only be passaged two times before losing their ability to form spheres. Apart from the isolated CD133+ BTICs and the CD133- spheroids of SKNBE(2) cells, tumorspheres from other cell lines were prepared directly from the monolayer cells that were kept in the same conditions

with the CD133<sup>±</sup> cells. At least 72 hours was necessary until they became “mature” ( $\geq 200$  microns) or they began to die from the very middle (become black (Figure 5.6 and Figure 5.7)).

To keep the continuous EGF and bFGF concentration within the medium before passaging, half of the medium was changed every three-four days. Cells at second passage were used for the experiments.

Lee et al. stated that the maintenance of the CSCs within the tumorspheres of gliomas was possible with EGF and bFGF containing medium. When 10 percent fetal bovine serum was used within the media, the cancer cell lines were losing their capacity of self-renewal and differentiation. In other words, the phenotypic and genetic features of those cell lines could only be sustained with EGF and bFGF supplementation [120].

EGF supplementation activates EGF signaling and activation of EGFR, which in turn promotes gliomagenesis and growth of NSCs [121]. bFGF is a crucial mitogen for NSCs. B27 is a neuronal cell culture supplement that supports the viability of the cells.

Valent *et al.* stated that the use of tumorspheres does not focus on mimicking the cancer tissues, but they are used for the identification of CSC properties. The 3D structure and the niche of a tumor *in vivo* are not completely replicated through sphere models [122]. The use of tumorspheres with or without enrichment together with monolayer cells allowed us to compare the outcomes within the focus of CSCs. Tumorspheres derived from various cell lines led to different sphere morphologies at the same length of incubation as seen in Table 5.1.

### **5.1.2. Transfection of Tumorspheres and CD133<sup>+</sup> BTICs**

To see the effects of over-expression and silencing of ETS family transcription factor Elk-1 on tumorspheres and CD133<sup>+</sup> BTICs, the cells were transiently transfected. Linear polyethyleneimine (PEI, MW 25000, Polysciences) was used for the transfection of monolayer cells within the experiments. The appropriate cell numbers and DNA: PEI ratios were determined by carrying out the necessary optimization experiments for each cell line before starting to use the cell lines for the experiments (Table 5.2).

Table 5.2. PEI transfection setup for each cell line after optimization

Cell Line	DNA:PEI	DNA/cm <sup>2</sup>
SKNBE(2)	1:3	0.3 µg
SH-SY5Y	1:4	0.6 µg
T98G	1:2	0.4 µg
A172	1:2	0.4 µg
U87-MG	1:2.5	0.6 µg

The trials for transfecting tumorspheres and CD133+ BTICs with PEI ended up with low efficiency. DNA and RNAi transfections of CD133+ BTICs and tumorspheres were performed with optimizations with Lipofectamine 2000 (Thermo Fischer Scientific, #11668019) reagent, as often mentioned in the literature.

Trials were made by forming a matrix with the ratios specified in the Lipofectamine 2000 reagent protocol, and it was concluded that the high concentration of Lipofectamine 2000 did not make a significant difference and the transfections were continued with the lowest rate of 1: 2 (Figure 5.8).

When the microarray results and the leading literature survey is considered, Elk-1 should affect the proliferation spheres obtained from both CD133+ BTICs and CD133- spheroids. Figure 5.9 shows the cell culture images following the transfection of CD133+ BTICs and CD133- spheroids with Elk-1 series of plasmids (pcDNA3.1(+), Elk-1, Elk1-VP16, sh-Elk1-GFP (siElk1) and scrRNA).

The constitutive activity of Elk-1 in CD133- spheroids led to an increase in the number of spheres, whereas its repression did not change the cell number significantly. Vice versa, the repression of Elk-1 in CD133+ BTICs led to a decrease in the number of spheres, whereas it does not make a significant change in sphere number when Elk-1 is over-expressed. If Elk-1 were active in the activity of genes related to tumorsphere formation and proliferation, the number of spheroids would change in the way of Elk-1 expression. It should also be noted that, if the effects were not direct or excessive, it would not be possible to make a comparison between the experimental groups.



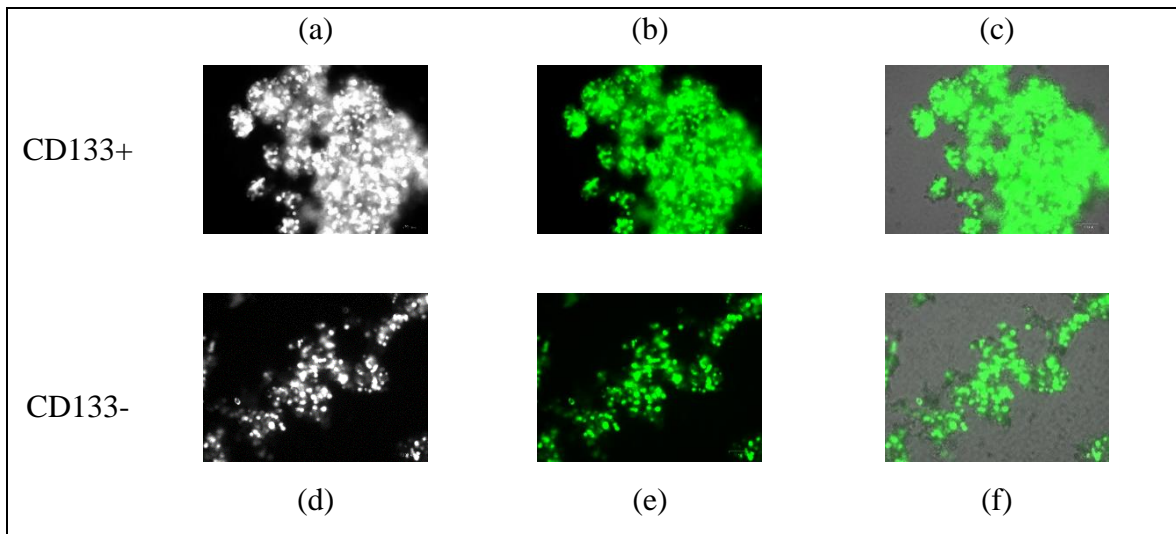


Figure 5.8. EGFP-N2 transfection of CD133+ BTICs with Lipofectamine2000 (a) light microscope, (b) florescent microscope, (c) merged image, 20X. EGFP-N2 transfection of CD133- cells with Lipofectamine2000 (d) light microscope, (e) florescent microscope, (f) merged image, 20X.

Together with these, even the cell number between each group was equal, the number of cells that formed spheres were different for each sphere. That led to heterogeneity between the spheres and groups. These were the first results for evaluating the effect of Elk-1 on CD133+/- cells and further experiments were carried out to see whether it was valid or not.

### 5.1.3. Assessment of Self-renewal Capacity

The studies for the assessment and comparison of colony formation for normal and CSCs date back to sixty years [123]. Following the isolation of CSCs by Bonnet and Dick for the first time through evaluating the self-renewal potentials of groups of leukemia cells [124], CSCs were identified in solid tumors.

In this thesis, the self-renewal potential of CD133+ BTICs and CD133- spheroids together with overexpression or silencing Elk-1 were checked with *in vitro* self-renewal assays, namely limiting dilution assay (LDA) and soft agar assay, designed for BTICs.

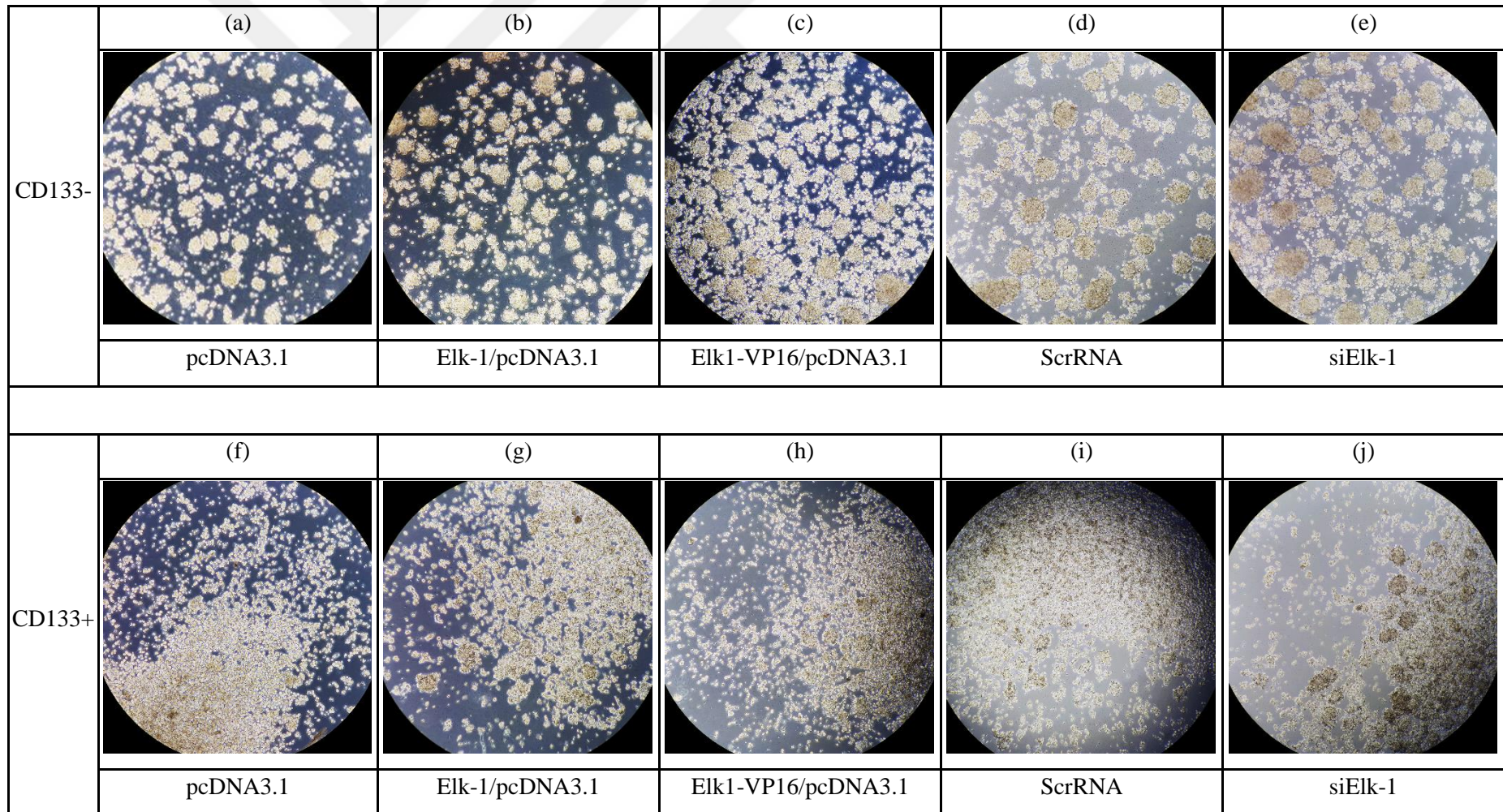


Figure 5.9. CD133+ BTICs and C133- cells after transfecting with Elk-1 series plasmids



### 5.1.3.1. Limiting Dilution Analysis (LDA)

Limiting dilution analysis is an inexpensive assay that can be used for determining the frequency of stem cell formation of brain tumor stem cells. In this thesis, to assess the effect of CD133+ cell enrichment on the formation of BTICs and self-renewal, limiting dilution analysis was carried out. With this aim, after CD133+ BTIC enrichment, both CD133+ and CD133- spheroids were grown in proper IPM culture conditions for three days. On the fourth day; spheres were dissociated to single cells; viable cells were counted with Trypan blue dye and cells were seeded. On the tenth day, the number of wells without spheres were counted, and the results were evaluated through ELDA software. The results can be seen in Figure 5.10.

The results from three independent experiments were included for the calculations for each CD133+ BTIC and CD133- spheroid group making up a pool. For CD133+ cells, one in 16 cells could form BTICs in vitro, whereas up to 230 cells were necessary for the formation of BTICs in the CD133- group. The potential of CD133+ cells to form spheroids was about ten times more than that of the CD133- cells. These results may also be interpreted as the CD133- group was either not totally isolated from CD133+ cells or the incubation time, and conditions following the LDA set-up was supporting the conversion between CD133+ and CD133- populations.

According to Singh *et al.* the stem cell population are in flux; they cannot keep their homogeneity but dilute in time due to asymmetric division. Environmental stress, interactions between the cells and growth factors can cause the transformation of CD133- spheroids into CD133+ BTICs. On the other hand, CD133+ BTICs can be converted to CD133- spheroids either, leading to the idea that BTICs are dynamic, not static [1]. This result was also supported with the slope of the goodness of fit test. The log-dose slope of the test equals one once the ideal model is achieved. In our case, the slope is 0.633, also an indicator of heterogeneity within the population.

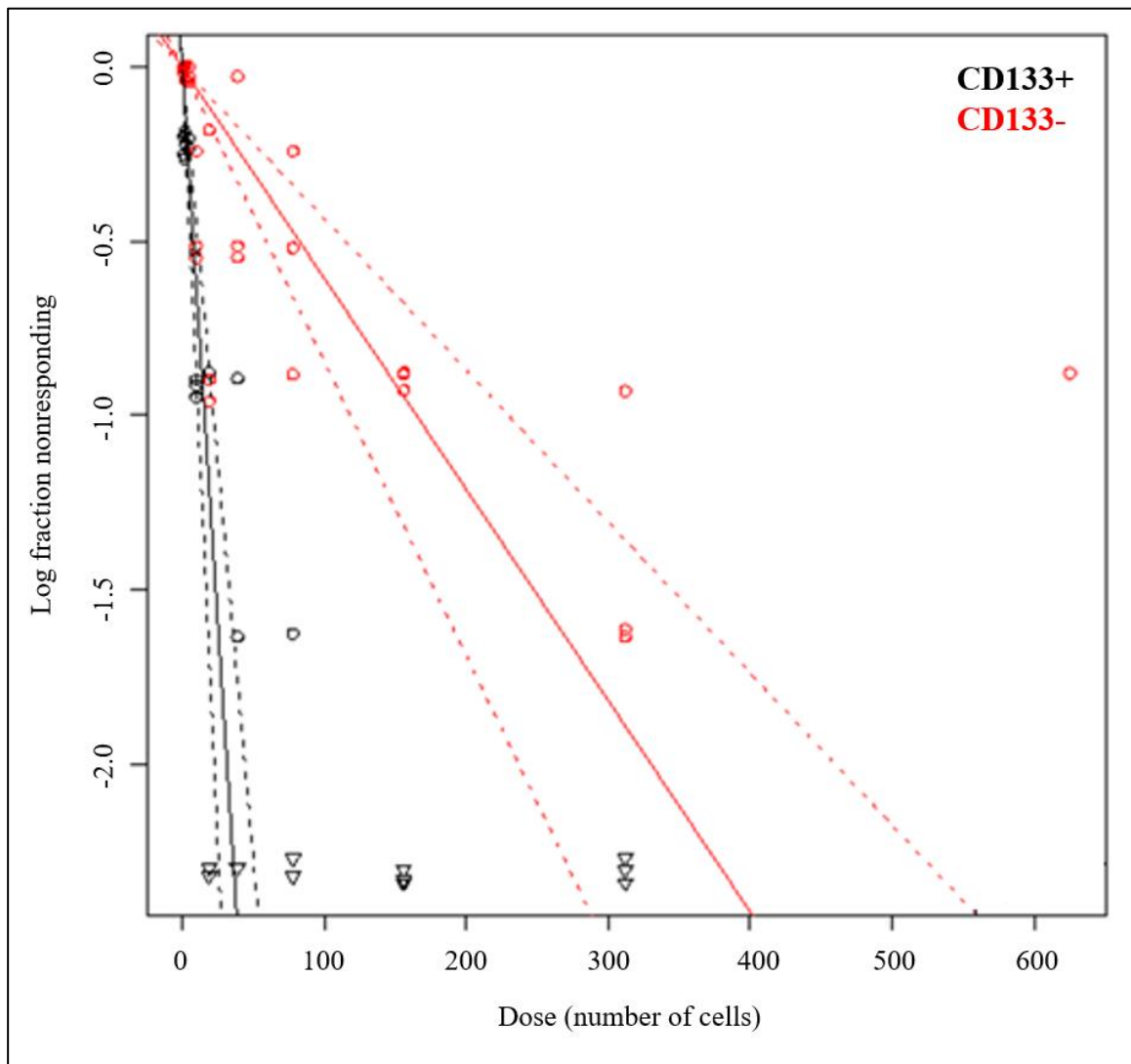


Figure 5.10. The frequency of sphere formation in isolated CD133+ and CD133- cells in BTIC conditions were assessed. LDA experiments were repeated three times. 95% confidence interval is shown by dots. The triangles indicate data value with zero negative (Black: CD133+ group, Red: CD133- group).

### 5.1.3.2. Soft Agar Analysis

Adherent cells form a programmed-cell-death mechanism called anoikis under anchorage-free conditions [125]. Self-renewal of CD133+ BTICs together with anchorage dependence of SKNBE(2) cells and the isolated CD133- spheroids were carried out with soft agar assay. In addition to this, the effect of Elk-1 expression on the self-renewal and independent growth of those cells were evaluated by overexpressing exogenous Elk-1 constructs or knocking

down Elk-1 message. While over-expression of Elk-1 increased the formation of colonies in CD133- spheroids, its repression led to a decrease in the number of colonies in CD133+ BTIC group. The results are given in Table 5.3 for one sample assay setup.

Table 5.3. Soft agar assay colony formation

<b>Cell Group</b>	<b>Transfection</b>	<b>Colonies Formed (mean±SD)</b>
<b>SKNBE(2)</b>	-	25±11
<b>CD133+</b>	-	33±9
<b>CD133-</b>	-	24±11
<b>CD133-</b>	pcDNA3.1	32±3
<b>CD133-</b>	Elk1-VP16/pcDNA3.1	37±10
<b>CD133-</b>	pCMV6-Flag	24±10
<b>CD133-</b>	Elk-1/pCMV6-Flag	50±15
<b>CD133+</b>	scrRNA	26±9
<b>CD133+</b>	siElk-1	18±5

Cells were counted either with staining to confirm the number of colonies grown in each well. For each experimental group, cells were seeded quadruplicates and the colonies  $\geq 20$   $\mu\text{m}$  were counted with care trying to avoid artifacts. The resulting colony numbers are given as mean±SD Table 5.3, and the leading graph is shown in Figure 5.11.

Figure 5.13 shows the representative wells chosen for each group after staining with crystal violet. Cells were grown for fifteen days without replacement or addition of proliferation medium. The grown colonies were not as big as the colonies that would have been grown for fifteen days in proliferation medium in culture dishes. To be able to take photographs of the complete well of the 96-well plate, 4X images are used in Figure 5.12, the representative photos of colonies grown in LMP agar were shown.

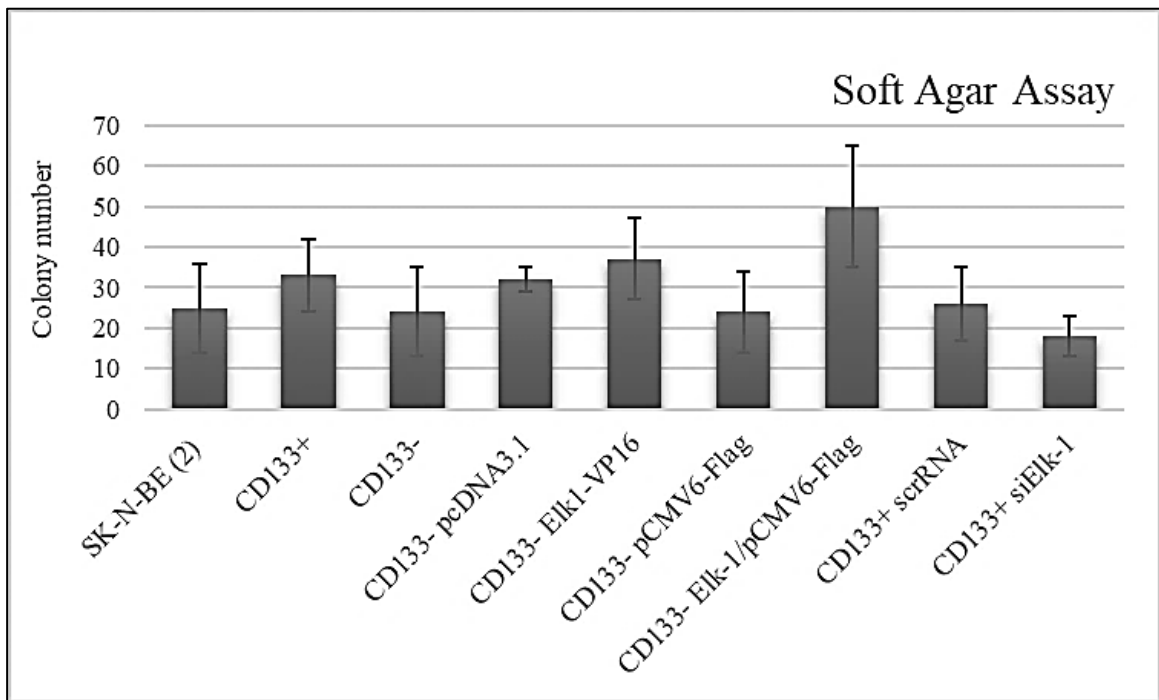


Figure 5.11. Colony numbers following soft agar assay

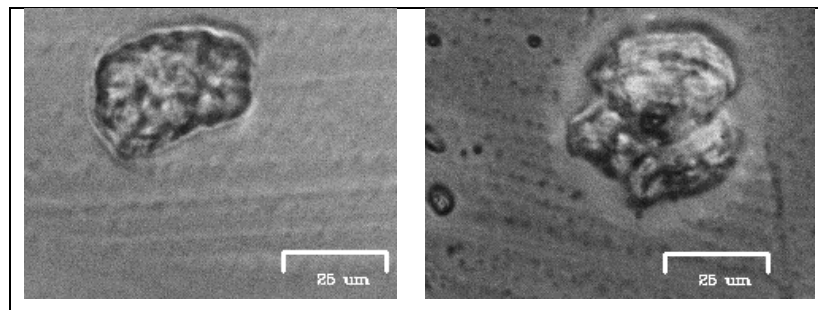


Figure 5.12. Colonies formed in LMP soft agar

The transfection of spheroids with Elk-1 plasmids were the preliminary results related to the effect of Elk-1 expression on the morphology of the spheroids. With limiting dilution analysis it was seen that the enrichment of CD133+ cells were done successfully, about ten times at a time. Then, the 3D microenvironment was mimicked together with Elk-1 transfection to see the possible tumorigenic effect without attachment to the matrix. These results were subtle, however they were precious.

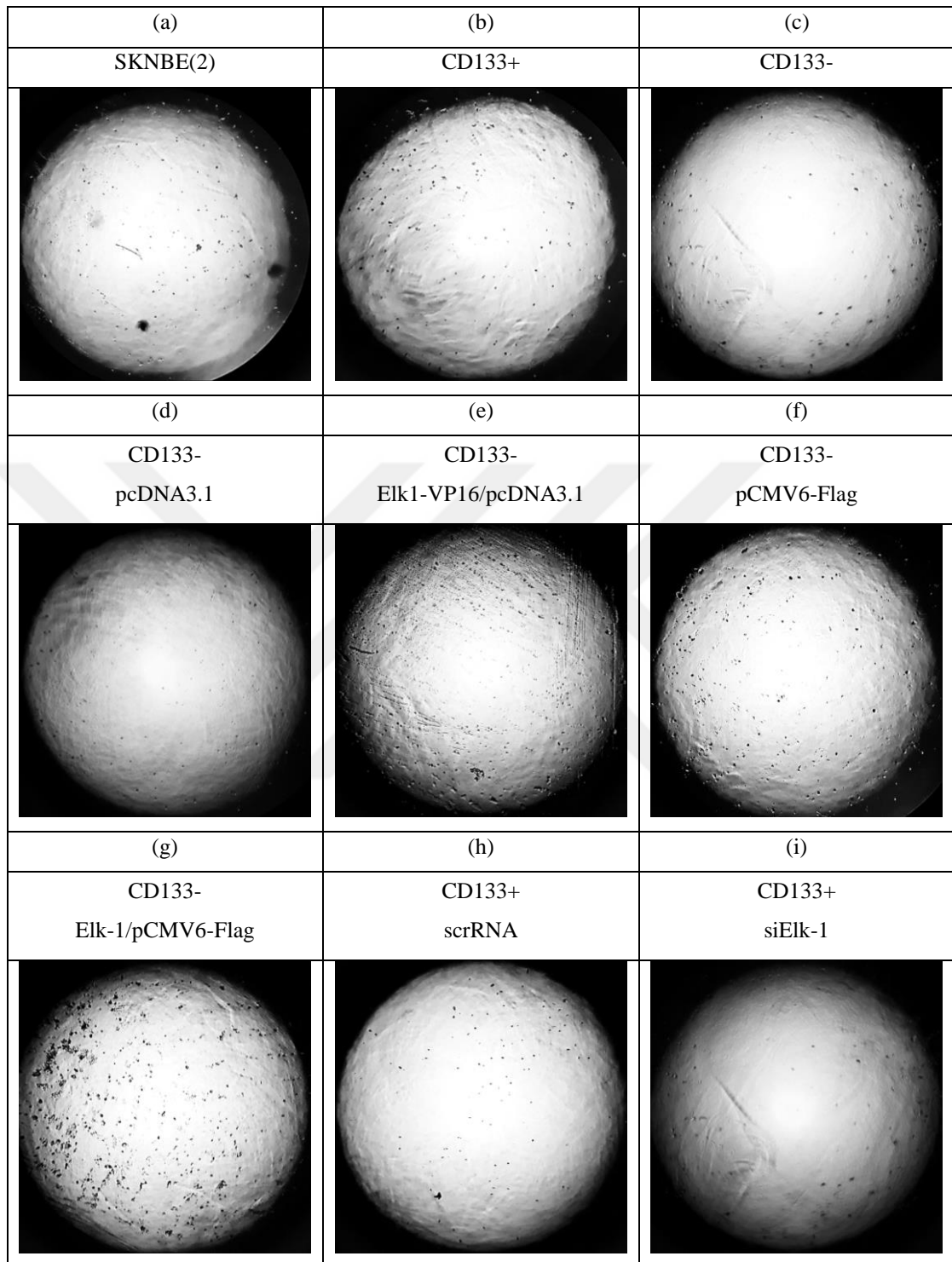


Figure 5.13. Crystal violet-stained photos of soft agar assay groups, 4X.

#### 5.1.4. Characterization of BTICs by CSC-related Gene Expression and Protein Levels

Even though an array of studies has been conducted for the identification of a universal marker, the characterization of CSCs still depends on the co-expression of intracellular and extracellular markers. For the characterization of CD133+ BTICs and tumorspheres, the gene expression levels and protein levels of BTICs and tumorspheres were assessed. For this, Nestin, Sox2, Pou5f1, Nanog, CD133 expressions and protein levels were analyzed. The effect of Elk-1 on the expressions of stemness genes was also determined.

The expression of the Nestin protein was checked for the determination of the stem-cell-like characteristics of the tumorspheres and CD133+ BTICs. Nestin, first identified in 1990 as a NSC/progenitor cell marker by Lendahl *et al.*, is a class VI intermediate filament protein [126]. When the stem cells/progenitor cells in the central nervous system are differentiated and transformed into neurons or glial cells, the level of expression of Nestin lowers. The change in Nestin protein level can be observed both *in vitro* and *in vivo* in adult central nervous system stem cells. To be sure about the expression of stem-cell-related markers, protein lysate was prepared from both monolayer cells grown in DMEM High Glucose (4.5 g/L) medium and tumorspheres were grown in IPM for 72 hours. 25 microgram protein was loaded to the SDS-PAGE gel and wet-transfer was conducted for 1h 20 minutes as Nestin is a *big* protein with a molecular weight of 177 kDa and its transfer to the membrane could not be achieved with the semi-dry system (Figure 5.14).









	(a)	(b)	
A172			Anti-Nestin (177 kDa)
T98G			
U87MG			
SH-SY5Y			

Figure 5.14. Nestin expression in neuroblastoma and glioblastoma cells that were kept either (a) in DMEM High Glucose (4.5 g/L) or (b) IPM for 72 h. 25 microgram protein was loaded.

In all four cell lines, an increase in Nestin expression was observed following 72 hours of incubation in IPM medium. Nevertheless, the expression was more apparent in A172 glioblastoma and SH-SY5Y neuroblastoma cell lines.

Nestin expression is indirectly related to the potential aggressiveness of some tumor types, and in some cases, its expression together with CD133 can be used for the prognosis of glioma patients [127]. The difference between the Nestin expression of different cell lines may be the result of their tumorigenic character.

Figure 5.15 shows the comparison of Nestin expressions in SKNBE(2) cell lysate, CD133-spheroids isolated from SKNBE(2) cells, passage 1 and 2 CD133+ BTICs. Nestin was not detected in monolayer SKNBE(2) and CD133- spheroids, which is parallel to the cell lines used for tumorsphere formation without CD133 isolation. There was a decrease in the expression of Nestin in CD133+ with increasing passage number. As the CD133+ BTICs were used at passage two at most in this thesis, Nestin expression was checked for two passages.

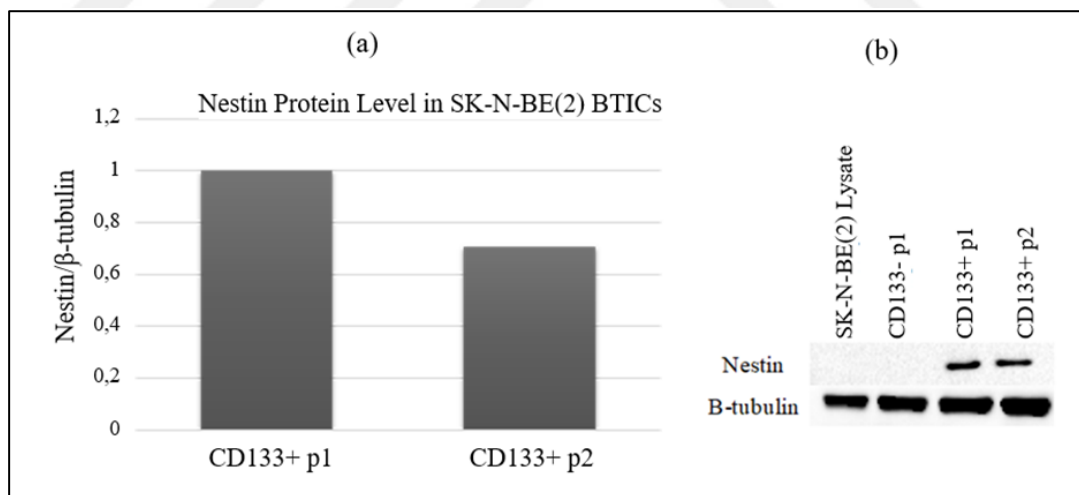


Figure 5.15. Nestin expression in SKNBE(2) CD133+ BTICs , 25 microgram protein lysate.

The decline in Nestin expression due to the passage number may be the result of an inter-conversion between CD133+ and CD133- cells as indicated in the study of Feng *et al.* for colon cancer SW620 cell line [128]. According to that study, the CD133+ and CD133- cell populations are reversible and dynamic, and there exists a specific ratio between each subset.

In other studies, cancer cells without stem cell characteristics could be converted to a stem-like state dynamically, or the phenotypic equilibrium was sustained through inter-conversion [129] [130]. These findings challenge the CSC hypothesis which states that via asymmetrical cell division two daughter cells either a stem cell or non-stem cell characteristics are formed.

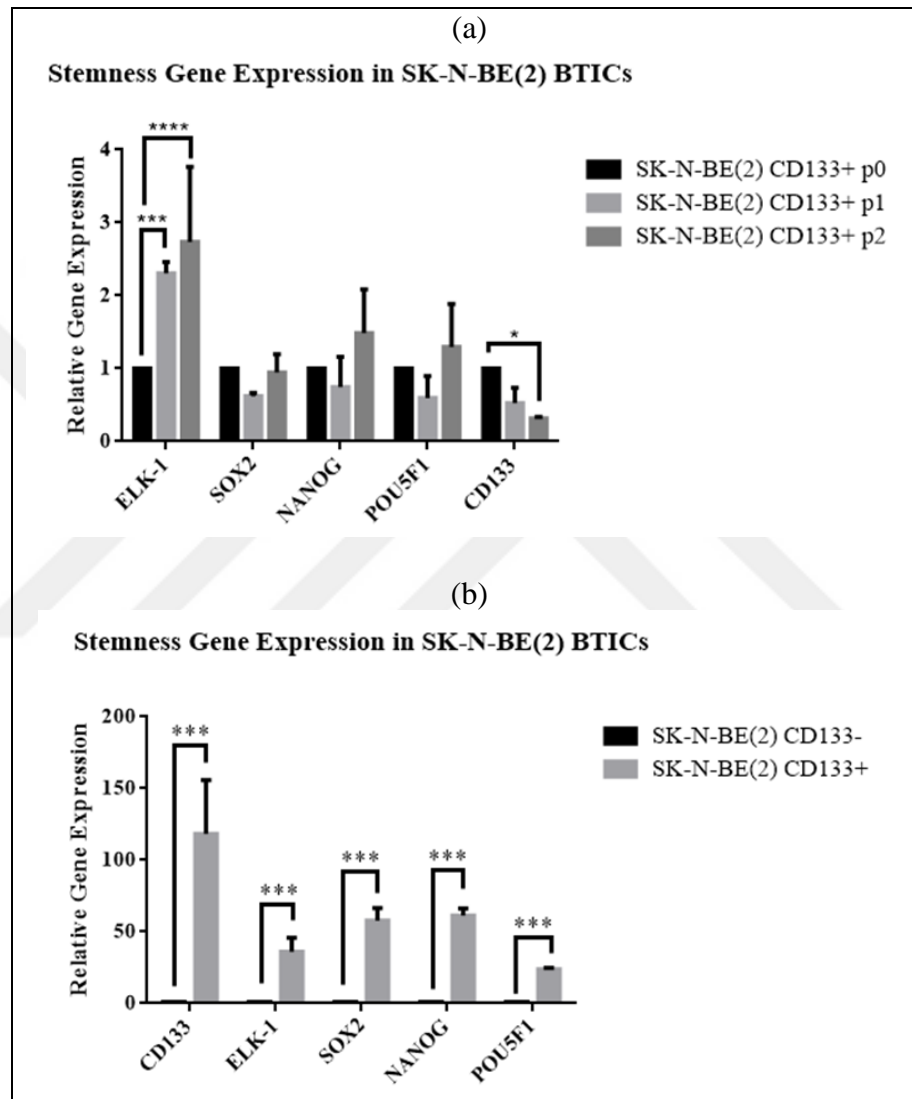


Figure 5.16. Stemness gene expression analysis of (a) SKNBE(2) passage 0, passage 1 and passage 2 cells, (One-way ANOVA, \*  $p < 0.5$ , \*\*\* $p < 0.001$ , \*\*\*\* $p < 0.0001$ ); (b) SKNBE(2) CD133+ BTICs vs CD133- spheroids, (Unpaired t-test, \*\*\* $p < 0.001$ ).

If CD133 is not a genuine marker for the enrichment of BTICs, why are there that many research articles on its usage in CSCs? This question can be answered in different ways. The primary function of CD133 cannot be fully understood yet. However, it appears to be



involved in the creation of a response to the changes in the extracellular environment through its terminal tail and the eventual signal transduction. It has been shown that CD133 roles in MAPK/ERK signaling brain tumor cells [131].

To check the gene expression pattern in different passage numbers of BTICs and to make a comparison between CD133<sup>-</sup> spheroids and CD133<sup>+</sup> BTICs in their stemness gene expression qPCR analysis were done as shown in Figure 5.16. In Figure 5.16 (a), it is clear that while CD133 expression decreases with increasing passage number parallel to Figure 5.15, Elk-1 expression increases in the opposite direction. The expression levels of SOX2, POU5F1 and NANOG transcripts fluctuate between the passages. The change in NANOG and POU5F1 expressions are parallel to each other which may be a result of the direct interaction of NANOG to POU5F1 promoter [132].

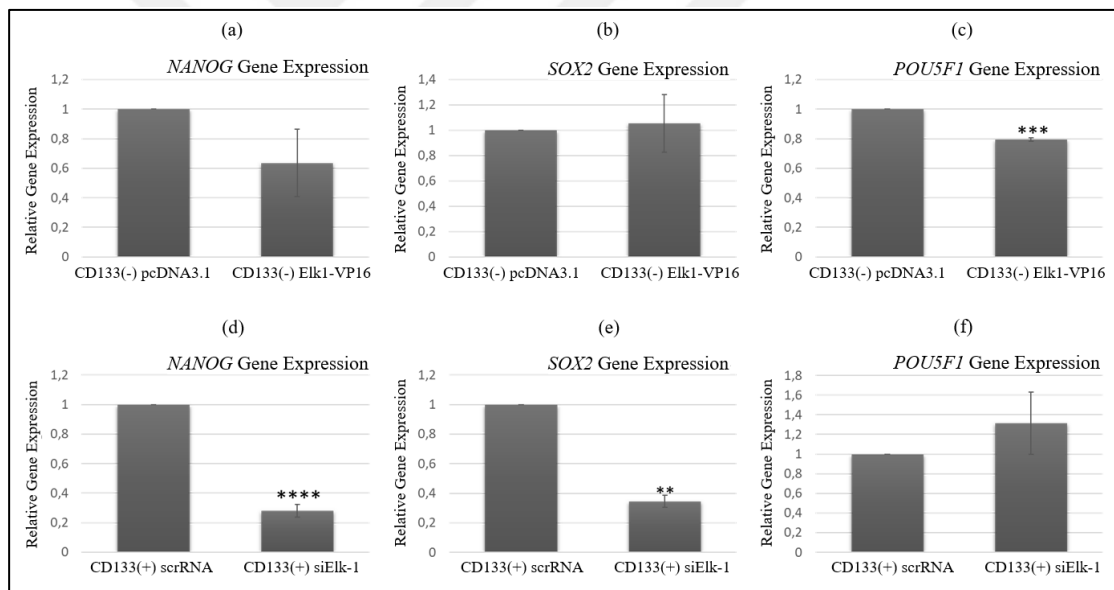


Figure 5.17. Stemness gene expressions related to Elk-1 over-expression vs. silencing (Unpaired t-test; \*\*\*\*p<0.0001, \*\*\*p<0.001, \*\*p=0.0051)

According to the results given in Figure 5.17, Elk-1 over-expression in CD133<sup>-</sup> spheroids did not make any significant difference in the expression of stemness genes. However, the expression of *NANOG* and *SOX2* expression significantly decreased with Elk-1 knockdown. The change in *POU5F1* expression was not significant. Elk-1 may not upregulate the stemness genes on its own directly, yet, the results clearly show that Elk-1 has a role in the regulation of *NANOG* and *SOX2*. That is also consistent with the finding of Ma *et al.* in

which the role of Erk signaling was discussed in mouse ESCs [133]. In that study, Erk depletion led to *Nanog* and *Pou5f1* upregulation within 48 hours. However, their levels decreased in time. They underline that for mouse ESCs, Erk signaling is essential for self-renewal but how the regulation is controlled is a question mark.

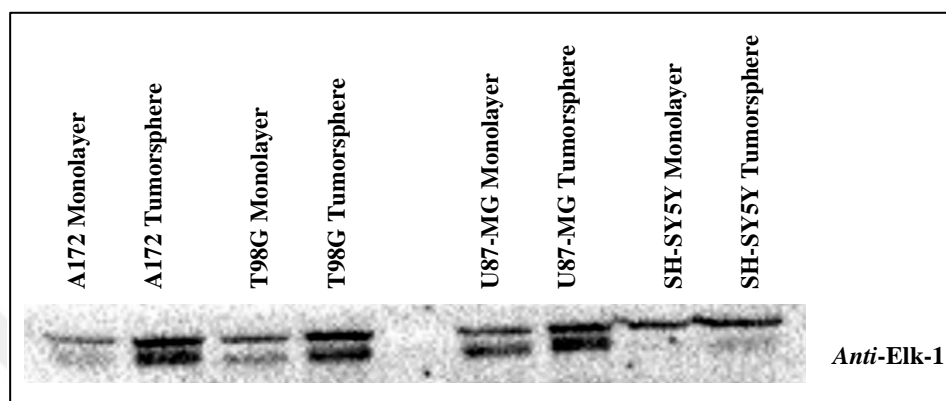


Figure 5.18. Western blot analysis for the tumorspheres

The tumorspheres derived without CD133 isolation were also checked for the Elk-1 expression as shown in Figure 5.18. Elk-1 expression was increased with respect to that of the monolayer versions of each tested cell line. This result is parallel to the increase in Elk-1 gene expression in CD133+ BTICs shown in Figure 5.16. The expression of Elk-1 increased when tumorspheres were formed from monolayer cells that were grown with complete DMEM medium (with serum) for many passages.

## 5.2. THE MOLECULAR ANALYSIS OF POTENTIAL GENE TARGETS OF ELK-1 IN NORMOXIA AND HYPOXIA

### 5.2.1. Verification of Hypoxia

Physiological oxygen levels change within the body depending on the anatomical location ranging between 1-14 percent oxygen. In the brain, the partial pressure of oxygen is lower than the other parts of the body. However, also depending on the location, the oxygen level changes within the brain. For instance, while the substantia nigra, CA1, thalamus, and cortex have lower oxygen pressure in rat brain, lateral ventricles and dentate gyrus need more

oxygen levels [134]. Thus, specific tissues have specific oxygen tensions, and this is known as physioxia. By definition, hypoxia is the oxygen tension below the physioxia for a specific tissue [135].

Transcriptional responses in low oxygen levels are regulated by hypoxia-induced factors (HIFs). HIFs are the main oxygen level sensors within the cells, and they regulate of many crucial processes through activation of many genes that function in glycolysis, reactive oxygen species (ROS) formation, angiogenesis, and remodeling. The decrease in the oxygen levels leads to pathological conditions due to a significant change in the microenvironment that results in the change of the activated signaling pathways. The increase in the expression of HIF-1 $\alpha$  is found to be related to the radiotherapy resistance in tumors [136].

The protein level of HIF-1 $\alpha$ , the indicator of hypoxia, was checked with Western blot using Elk-1 over-expressed and silenced SKNBE(2) cells incubated in hypoxia for six hours at one percent O<sub>2</sub>, five percent CO<sub>2</sub> to confirm the hypoxic environment provided in the experiments as seen in Figure 5.19.

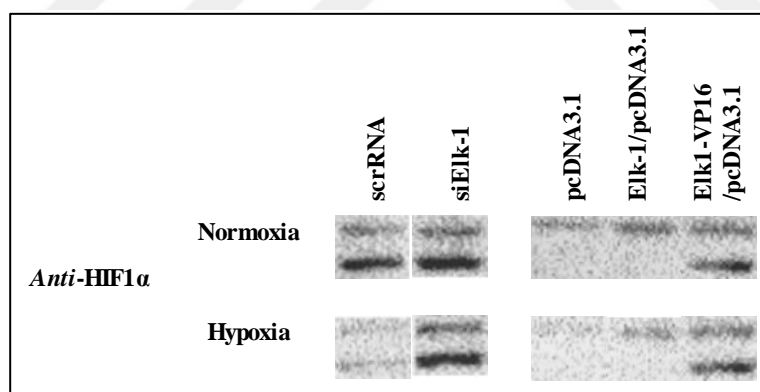


Figure 5.19. Protein expression of HIF1 $\alpha$  (SantaCruz, sc-10790) in normoxia and hypoxia

However, as opposed to the expectations at 132 kDa, the bands were observed at 55-70 kDa. Through a literature survey, it is concluded that these bands are not fully-characterized yet, but they are the products of HIF1 $\alpha$  degradation or truncation. As a second possibility, these bands could be seen due to competitive binding of the antibody to these products as it was polyclonal and as a result, causing the HIF1 $\alpha$  products not to display thoroughly. Therefore, HIF-1 $\alpha$  protein was not used alone, and a secondary control was necessary.

*VEGF* is the direct transcriptional target of both HIF-1 $\alpha$  and HIF-2 $\alpha$  [137]. Taking this into account, *VEGF* mRNA expression was evaluated with qPCR using both non-transfected SKNBE(2) cell line (Figure 5.20) and Elk-1 series transfected SKNBE(2) cells to confirm hypoxia (Figure 5.21). According to this, six hours hypoxia treatment to the SKNBE(2) cells led to a very significant increase in *VEGF* expression by responding to the hypoxia treatment (Figure 5.20).

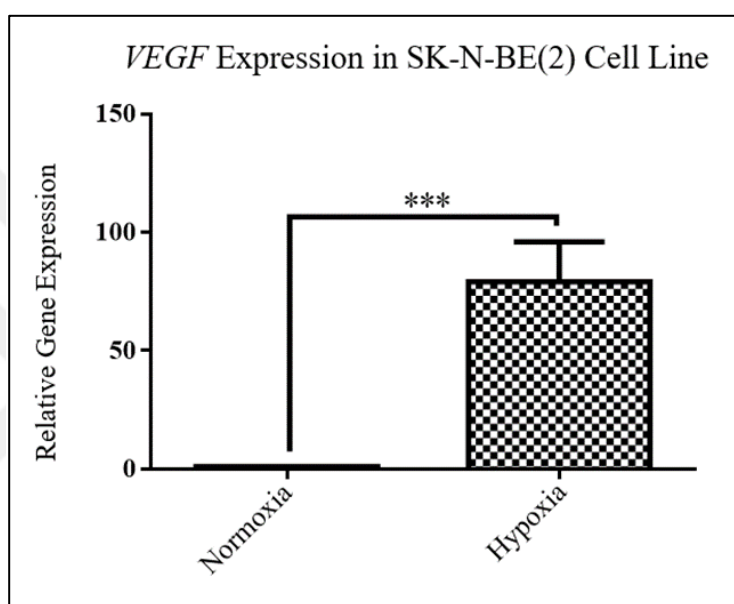


Figure 5.20. *VEGF* expression in normoxic vs. hypoxic conditions in SKNBE(2) cell line (Unpaired t-test, \*\*\*  $p < 0.001$ )

Muller *et al.* showed that under hypoxia Elk-1 is phosphorylated through the MAPK pathway, and Elk-1 may be acting as a sensor for redox status within the cell [104]. Aprelikova *et al.* used Elk-1 knock-down by siRNA to test the effect on HIF-2-dependent genes and to exclude the possible interaction with HIF-1-regulated genes they chose genes with promoters that have Elk-1 binding sites on them [106]. *VEGF* was one of those evaluated genes, and the qPCR results showed no change in *VEGF* gene expression concerning Elk-1 in their ability to react to hypoxia. Although in the promoters of the target genes within the hypoxia-responsive elements (HREs), the same DNA sequence is recognized by both HIF-1 and HIF-2, they do not compensate for each other. Their functions are not redundant [106]. In Figure 5.21 (a), the analysis of putative binding sites of Elk-1 on *VEGF* promoter through Eukaryotic Promoter Database (EPD) is shown. Even there are Elk-

1 binding sites on the *VEGF*; there is not a direct interaction that changes the *VEGF* expression directly with the increased expression of Elk-1. These findings support the stable *VEGF* expression levels in Figure 5.21 (b).

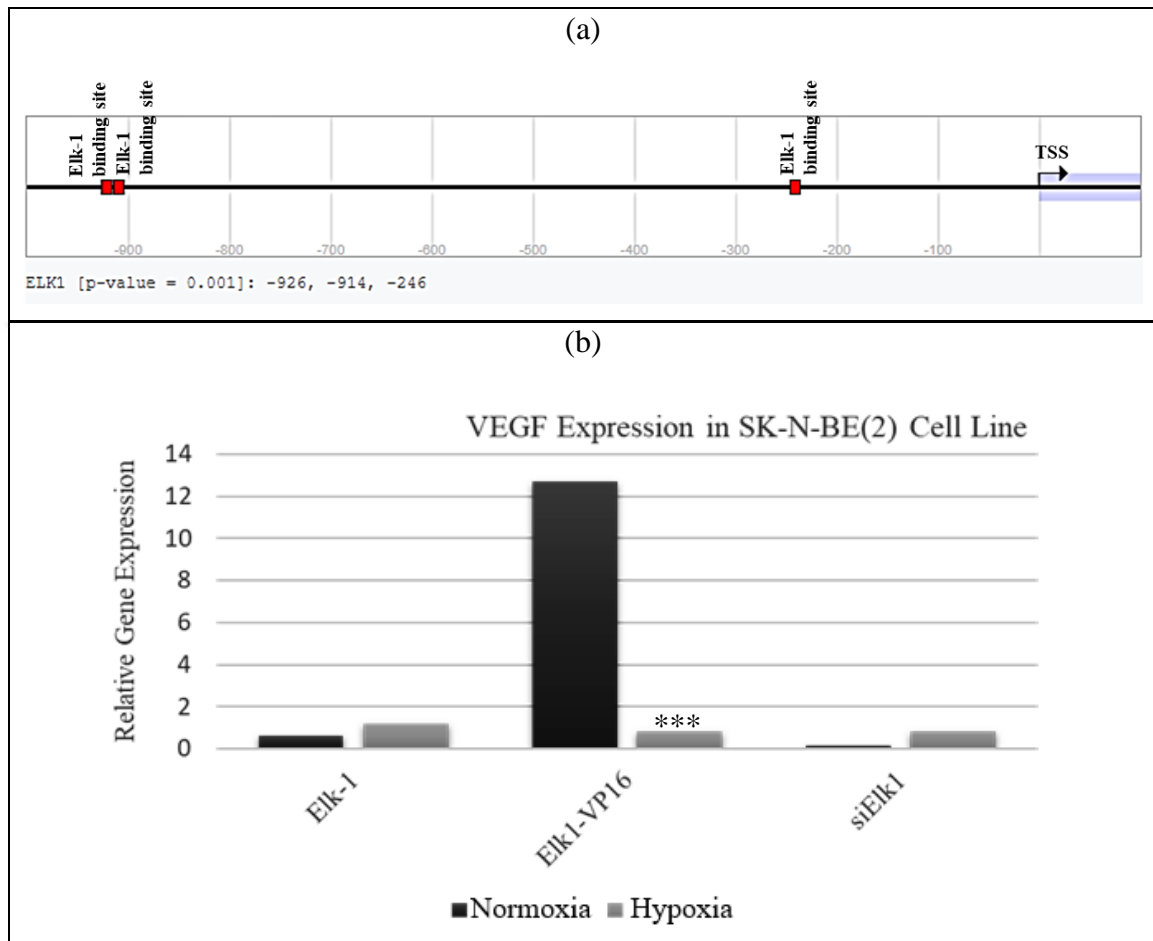


Figure 5.21. (a) *VEGF* promoter analysis for Elk-1 binding, (b) *VEGF* expression in normoxic vs. hypoxic conditions in Elk-1-transfected SKNBE(2) cells (Unpaired t-test, \*\*\* p<0.001)

The increase in *VEGF* expression with Elk-1 over-expression and the reduction in expression through Elk-1 knockdown may be related to the activation of the miR-17-92 cluster with Elk-1 (Figure 5.21 (b)). This cluster takes a role in the induction of tumor angiogenesis and suppression of apoptosis of cancer cells together with supporting the cell proliferation [138]. Elk-1 activates this miRNA cluster in endothelial cells [139].

### 5.2.2. Gene Expression Levels of Elk-1 and Target Genes in Normoxia and Hypoxia

Hypoxia creates a critical microenvironment for the survival and progression of CSCs. The idea that hypoxia, hypoxia-inducible factor (HIF) expression, and the CSC phenotype is related through some complex mechanisms supported by experimental evidence. Soeda et al. showed that CD133+ cell ratio of cells cultured in hypoxia increased through activation of HIF1 $\alpha$  [140]. In a study conducted by the Yamanaka group, which succeeded in the establishment of iPSCs, it was stated that the iPSC generation was significantly supported by hypoxia [141]. However, Ohnishi *et al.* carried out a study to identify the possible mechanisms for the activity of CSC marker protein CD133 by HIF-1 $\alpha$  and HIF-2 $\alpha$  and found out that CD133 promoter activity was regulated through ETS transcription factors. They did not bind to the hypoxia response element (HRE) binding sites, but ETS binding sites (EBS) [142].

To analyze the effect of hypoxia on the regulation of both Elk-1 and stemness genes, tumorspheres were derived from SKNBE(2) cells in favorable conditions, and the dishes were then transferred to the hypoxia incubator (one percent oxygen) for various time intervals. At the end of each time interval cells were collected immediately, total RNA was isolated for each sample and cDNA was synthesized. The qPCR results of hypoxia were normalized to the normoxia counterparts of each time interval are shown in Figure 5.22.

The expression of all the tested genes increased in the first nine hours in response to hypoxia. While the expression of *NANOG* and *POU5F1* genes continued to increase, *ELK-1* and *SOX2* expression decreased in the tumorsphere samples. The change in *NANOG* and *POU5F1* expressions are parallel to each other which may be a result of the direct interaction of *NANOG* to *POU5F1* promoter [132]. A strict decrease was observed in all the samples of Figure 5.22 at 24 hours of hypoxia treatment. The results of 24-hour treatment were not included in the graphs.

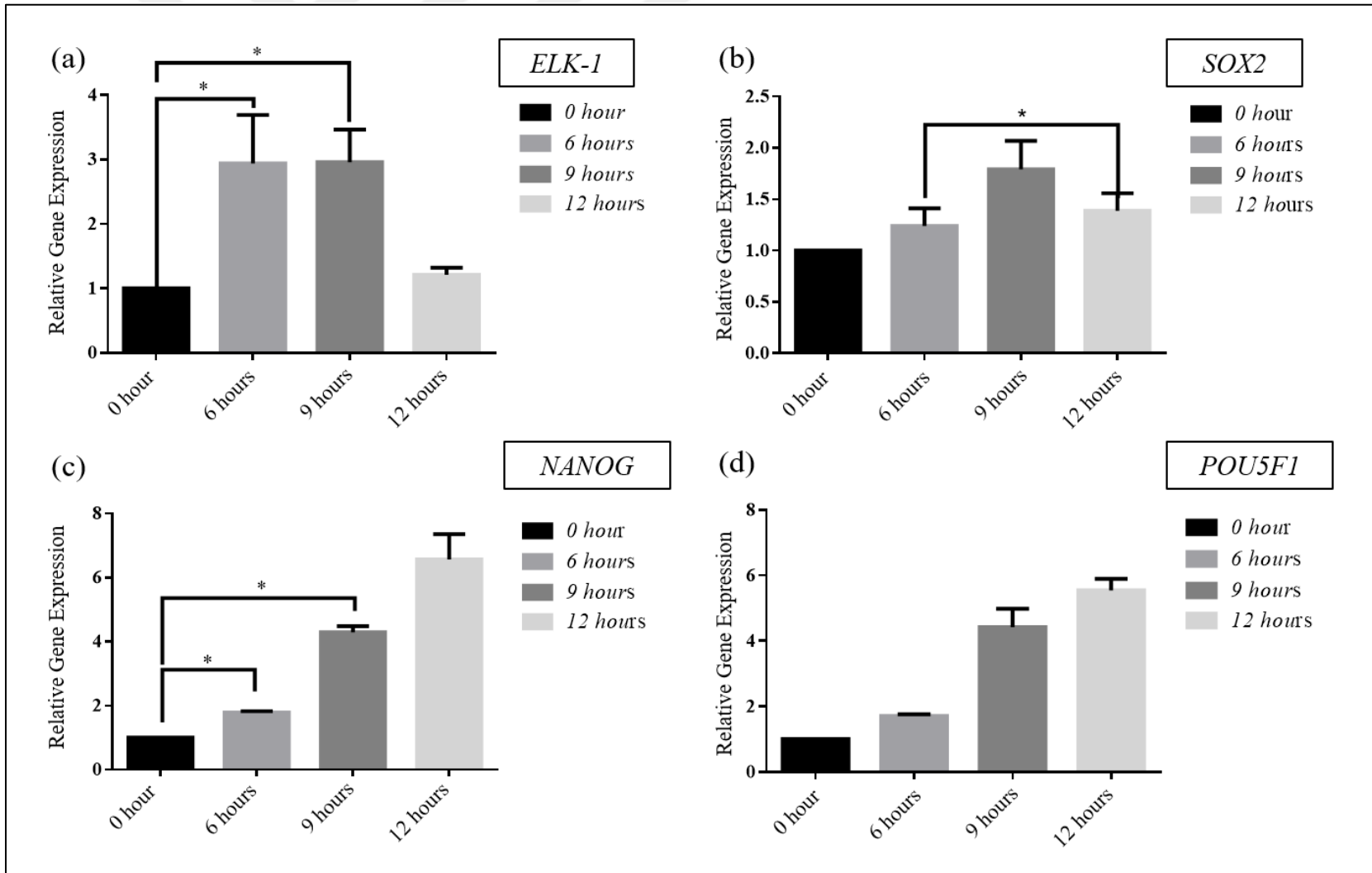


Figure 5.22. Quantitative gene expression analysis of stemness genes following intervals of hypoxia treatment (One-way ANOVA, \* p<0.5)

When the gene expression of CSC markers in SKNBE(2) cell line and tumorspheres derived from SKNBE(2) were compared, it was interesting that the CD133 expression pattern was opposite for the monolayer and the tumorsphere cells as shown in Figure 5.23 (a) and (b).

The results were seemingly contradictory. CD133 is involved in the maintenance of CSCs, and there are various studies indicating hypoxia increases the expression of CD133 and the stem cell characteristics glioblastomas. Nevertheless, there is not a study carried on neuroblastoma cells. In several other cell lines including colorectal, gastric and lung cancer, it was shown that severe hypoxia (0.1 percent O<sub>2</sub>) led to a decrease in CD133 expression [143]. From another perspective, as hypoxia supports the stem cell formation, the level of CD133 expression increases in time in SKNBE(2) monolayer cells. Tumorspheres, being spheroids, may be regulated by other stemness genes but not CD133 in hypoxia. These studies give an idea about the O<sub>2</sub>-dependent transcriptional regulation of CD133; however, this specific condition is yet to be explained.

The change in the *SOX2* expression per time interval for both the monolayer (2D) and tumorsphere (3D) cultures was quite the same for the first twelve hours (Figure 5.23 (c) and (d)). When *SOX2* protein level of SKNBE(2) cells concerning Elk-1 over-expression and silencing at normoxia and hypoxia was evaluated with a Western blot, it can be seen that Elk-1 expression does affect the *SOX2* expression in protein level. Upregulation in Elk-1 leads to also upregulation in *SOX2* protein level in either normoxia or hypoxia.

The downregulation of Elk-1 increased *SOX2* protein level significantly in hypoxia. Nevertheless, neither CD133+ BTICs nor CD133- spheroids reacted to the downregulation of Elk-1 with upregulating *SOX2* gene expression Figure 5.26. These results show the difference in the outcome of the same conditions to the 2D vs. 3D cell cultures of the same cell line *in vitro*.



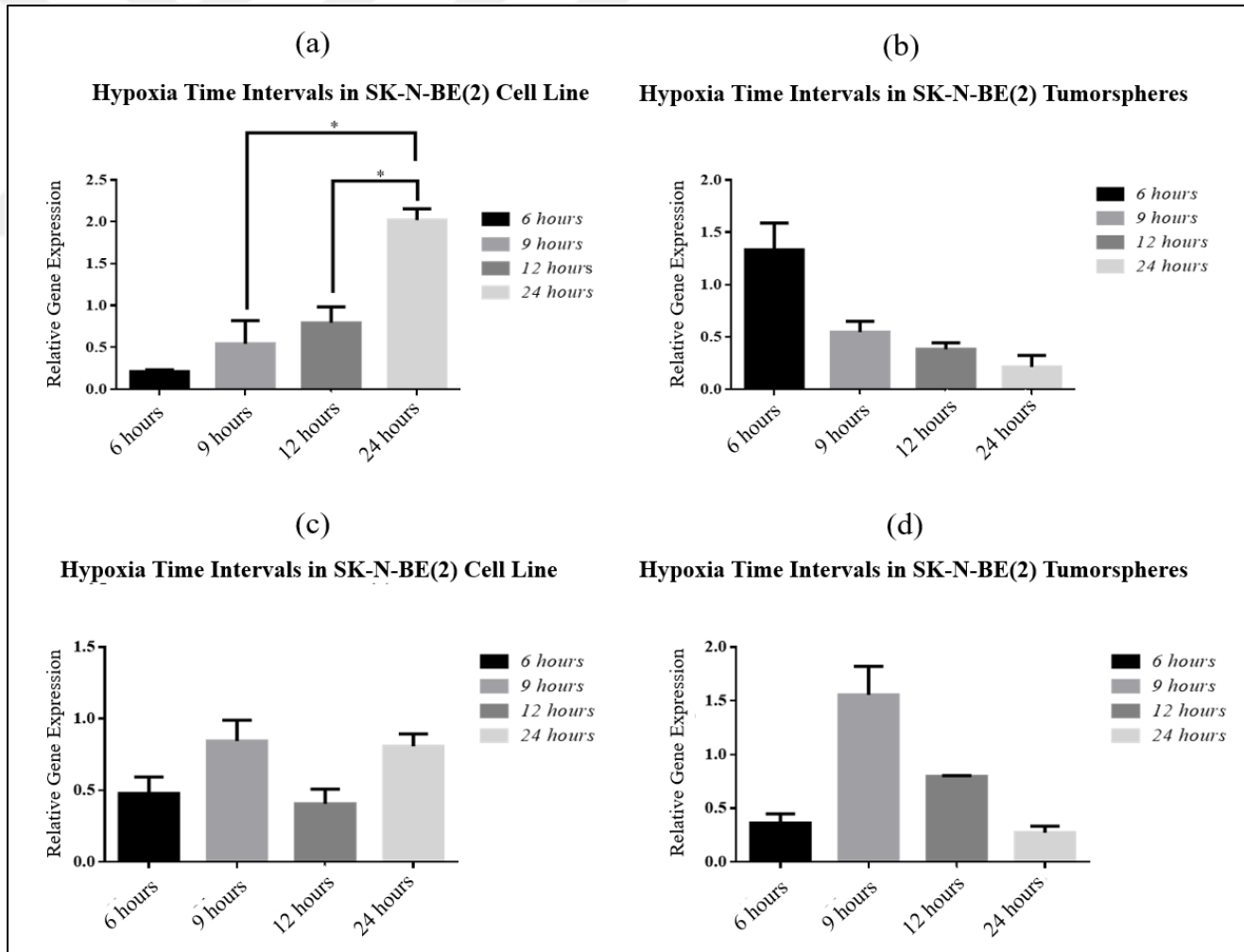


Figure 5.23. Gene expression of CSC markers in SKNBE(2) monolayer cells and tumor cells at hypoxic conditions

(One-way ANOVA, \* p<0.5)

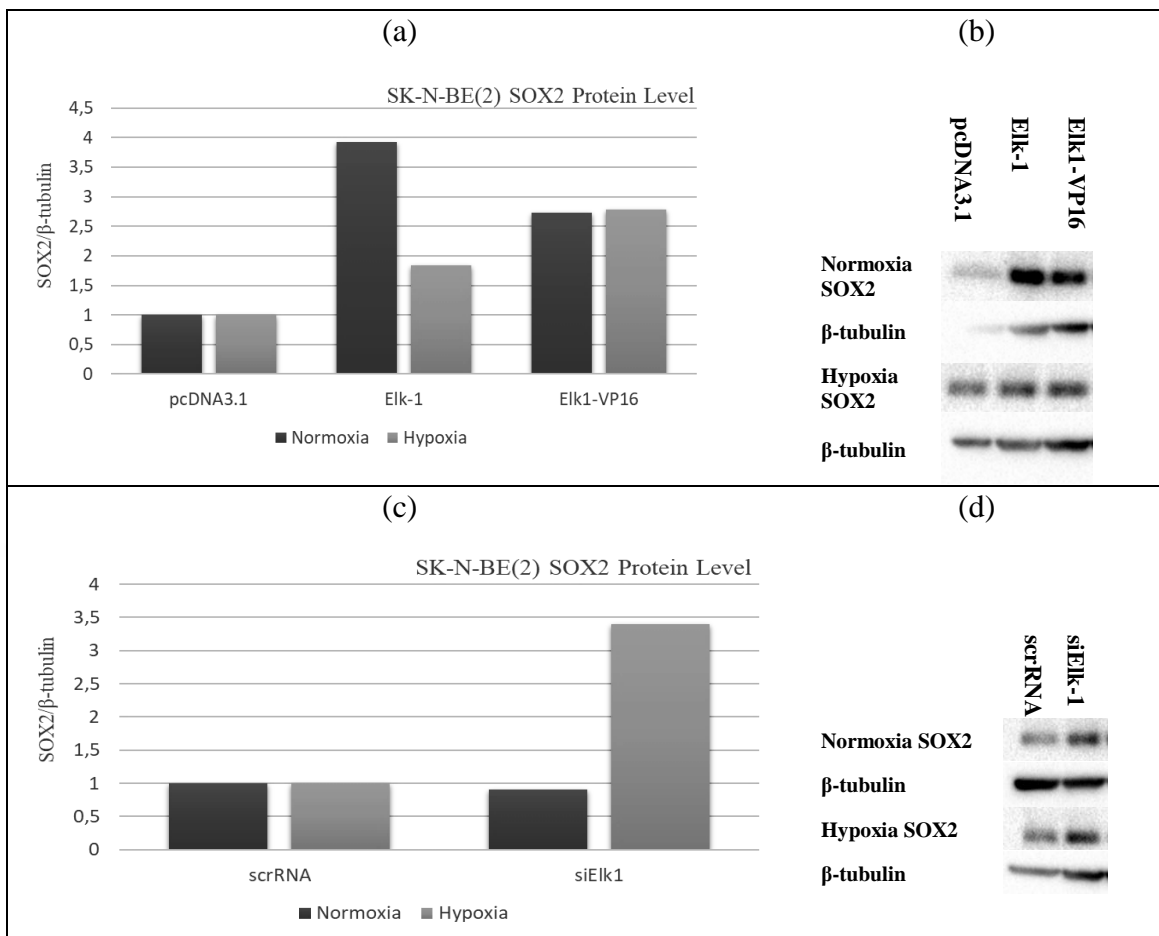


Figure 5.24. Anti-SOX2 Western blot with Elk-1 over-expressed/repressed SKNBE(2) cells at normoxia and hypoxia

This is a puzzle with many dimensions that depends on many parameters. Apart from regulation at transcriptional level; microRNAs, post-translational modifications as well as long non-coding RNAs take a role in the expression and activity of SOX2 [144]. For this reason, reducing the research question to “is there a direct control between Elk-1 and SOX2 or not” would not be proper.

To continue, the stemness gene expressions were analyzed for CD133+ BTICs and CD133- spheroids when Elk-1 was either over-expressed or silenced in normoxic vs. hypoxic conditions as shown in Figure 5.25 and Figure 5.26, respectively. According to Figure 5.25, moderate hypoxia (one percent oxygen) could elevate *ELK-1* expression in both CD133+ BTICs and CD133- spheroids. However, the level of increase in CD133- spheroids was significantly higher than that of the CD133+ BTICs. Interestingly, the expression level of

all three stemness genes, namely *SOX2*, *NANOG*, and *POU5F1*, decreased with hypoxia regardless of the spheroid type. In CD133- spheroids, in normoxia, the level of stemness genes was lower than the CD133+ BTICs as expected. In CD133- spheroids with hypoxia treatment the level of *SOX2* expression increased.

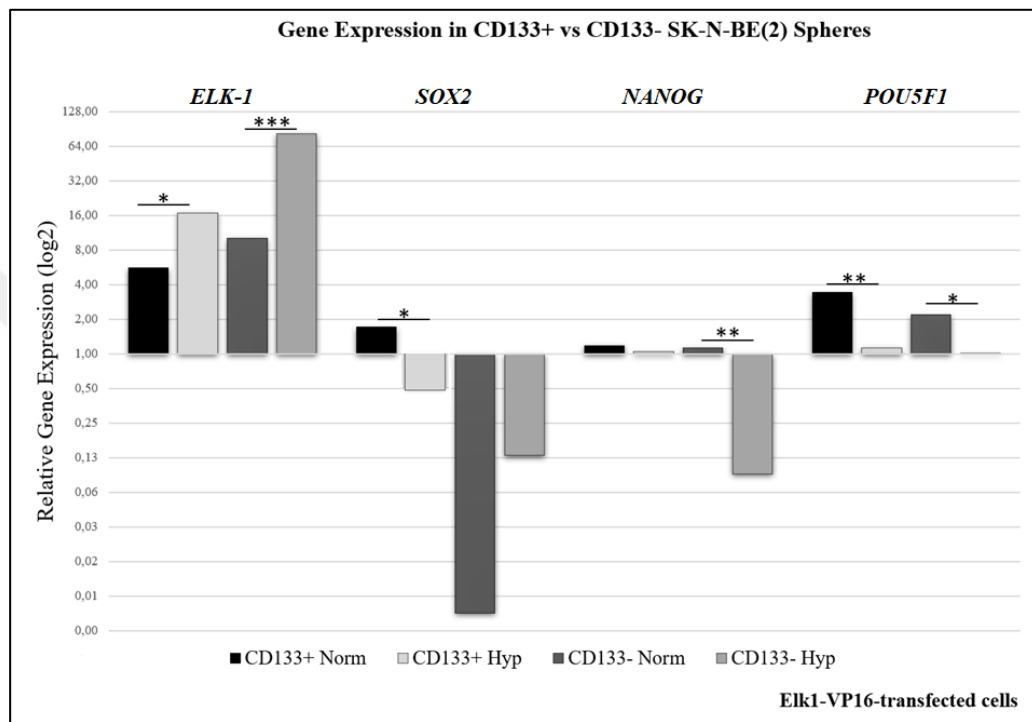


Figure 5.25. Stemness gene expressions in CD133+ BTICs and CD133- spheroids with Elk-1 over-expression at normoxic vs. hypoxic conditions (Unpaired t -test; \*\*\* $p < 0.0001$ , \*\* $p < 0.001$ , \* $p < 0.01$ )

In Figure 5.26, *ELK-1* expression was repressed in both CD133+ BTICs and CD133- spheroids in either normoxic or hypoxic conditions. ELK-1 silencing did not change the pattern of *SOX2* expression in CD133+ BTICs but that of the CD133- spheroids was reversed. *SOX2* expression was significantly increased in CD133- spheroids that were incubated in normoxic conditions in siElk-1-transfected cells. The pattern of *NANOG* expression was almost the same with Elk1-VP16-transfected cells in both CD133+ BTICs and CD133- spheroids, but the expression of *POU5F1* increased in siElk-1-expressing cells with respect to Elk1-VP16-expressing cells.

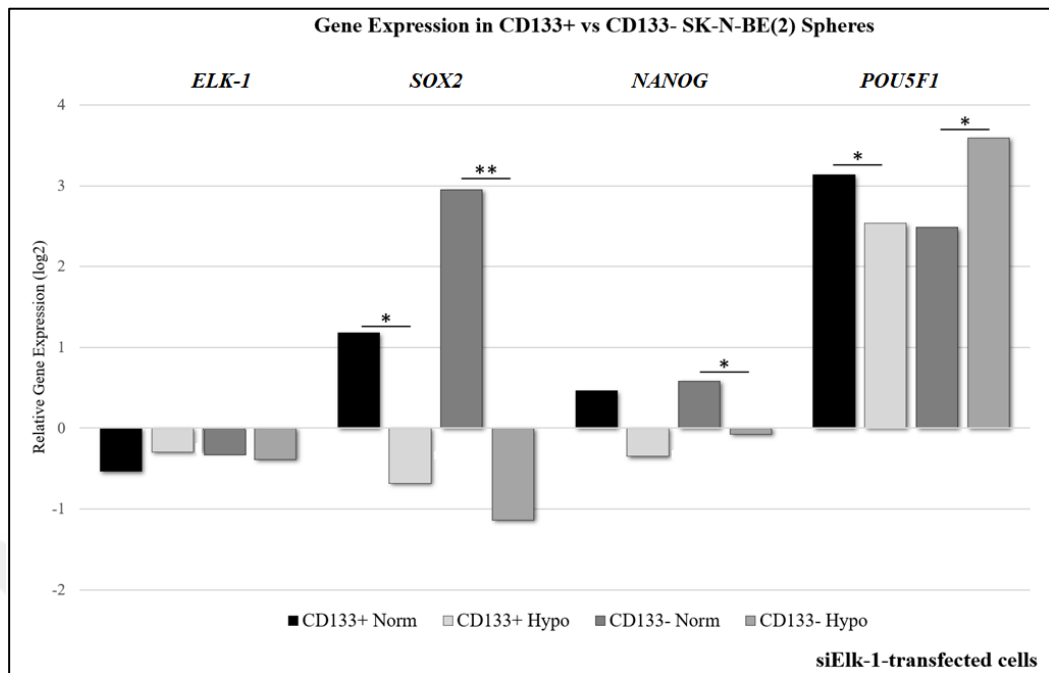


Figure 5.26. Stemness gene expressions in CD133+ BTICs and CD133- spheroids with Elk-1 repression at normoxic vs. hypoxic conditions (Unpaired t -test, \* $p < 0.5$ , \*\* $p < 0.001$ )

Setting up the hypoxia incubator to one percent oxygen may not thoroughly reflect the real oxygen tension the CSCs face at the cell level. There is an array of parameters that has to be taken into account for analyzing the effect of hypoxia on spheroids including depth of medium, the  $O_2$ -gradient created from the periphery to the center, pH changes throughout the hypoxic treatment and cell density [145].

It was shown that the culture of glioma cells for extended passages *in vitro* in normoxic (20 percent oxygen) condition could lead to *de novo* epigenetic changes and increase in CD133-cell number [120].

On the other hand, the exposure to atmospheric oxygen and the change in oxygen levels are also critical conditions those cells have to cope with at the end of the hypoxia experiments. These are the limitations to keep in mind when assessing the results of the hypoxia experiments.

### **5.3. THE EFFECT OF ELK-1 OVER-EXPRESSION OR SILENCING ON THE PROLIFERATION OF THE CD133+ BTICs AND CD133- SPHEROIDS**

The effects of hypoxia on neurodegeneration-neurogenesis/proliferation/tumorigenesis-neuroprotection axis and the events at the molecular level have not been fully understood, yet. There are different opinions about the role of Elk-1 in the survival-apoptosis axis in neurons. Our laboratory hypothesizes that Elk-1 regulates survival in neurons by Elk-1 expression, alteration of localization and/or phosphorylation. In a previous study by our group, the activation of Elk-1 by MAPK and PI3K pathways was shown to contribute to the proliferation of Glioblastoma Multiforme (GBM) cells [146]. Also, in the 2-month sabbatical study, Prof. Dr. Isil Kurnaz showed that CD133 + BTICs, as well as CD133+ fetal human NSCs, were found to have higher expression of Elk-1 than their CD133- counterparts (Kurnaz 2009, Singh lab, McMaster University, data not shown).

The assays used for proliferation analysis of the cells *in vitro* can be grouped in four main groups including fluorometric assays, dye-exclusion assays, luminometric assay, and colorimetric assay. In this thesis, the XTT assay was used for the assessment of the proliferation difference between different experimental groups of cells.

The XTT assay requires incubation of the cells with the reagent 2-24 hours, depending on the cell type and the setup. In this case, various incubation times were checked, and four hours of incubation was found to be suitable for this setup. The results of the proliferation experiments for Elk-1 over-expression and silencing of CD133+ BTICs and CD133-spheroids in normoxia and hypoxia after four hours of incubation with XTT reagent are as shown in Figure 5.27.

There was no significant difference in SKNBE(2) monolayer cell proliferation between the Elk-1 over-expressed or silenced groups as seen in Figure 5.27 (a) and (b). In normoxic conditions, with Elk-1 silencing the proliferation of CD133+ cells increased, while in hypoxia their proliferation fell to the control level and below CD133- cells. The decrease in CD133+ cell proliferation with Elk-1 silencing in normoxia was supported with the expression of Elk1-EN dominant negative form of Elk-1. However, this is not the case with hypoxia.

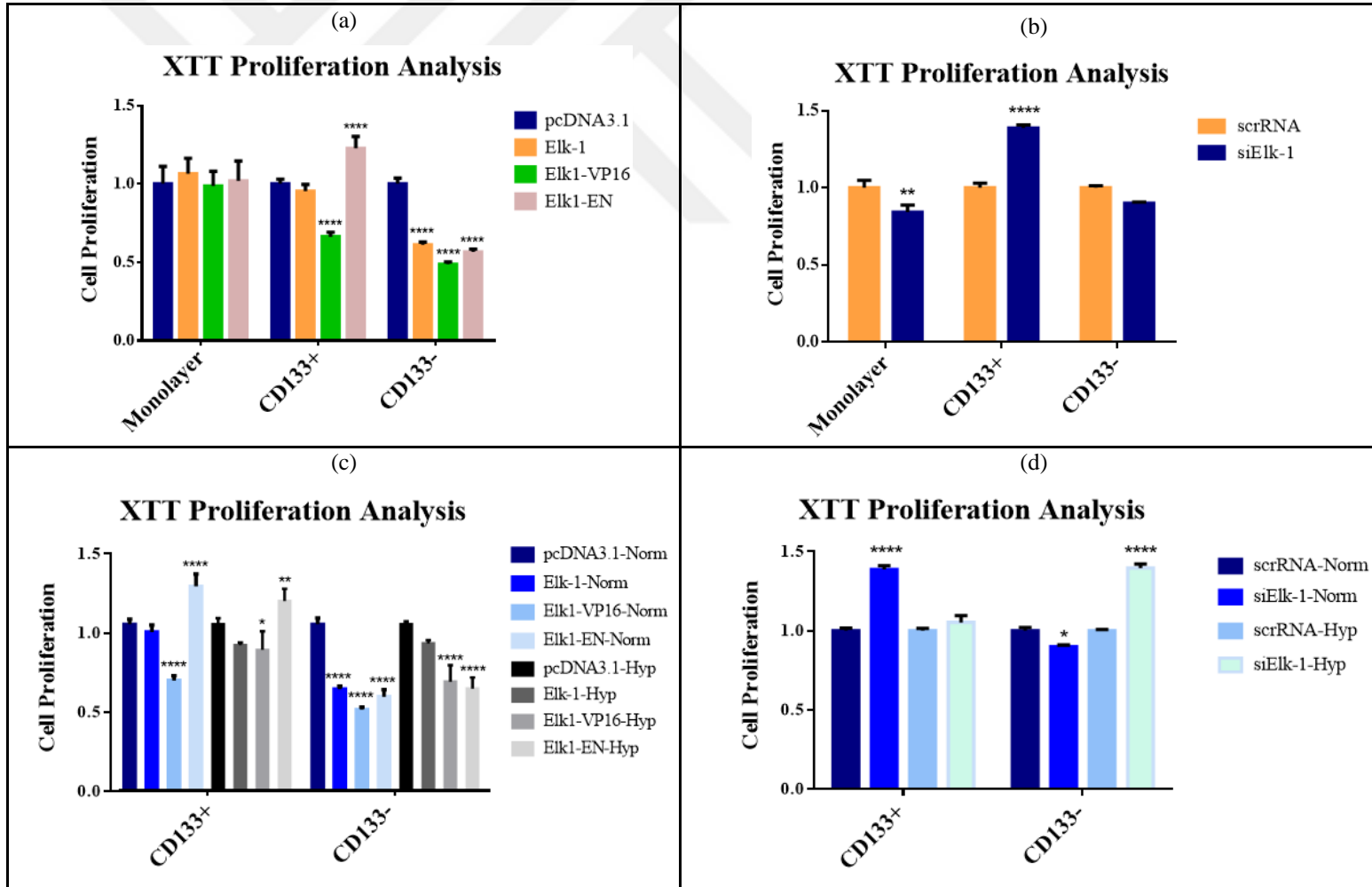


Figure 5.27. Evaluation of cell proliferation in CD133 + BTICs and CD133- spheroids at normoxia and hypoxia by XTT analysis (Two-way ANOVA; \*\*\*\*p<0.0001, \*\*p<0.01, \*p<0.05)

The results are not promising, yet, they are not only related to the transient transfection of various Elk-1 forms but also to the XTT assay itself. XTT assay analyzes the proliferation rate through assessing the reductive capacity of the cells with mitochondrial dehydrogenase activity. This reduction may be affected by many factors such as pH, environmental factors and cell cycle variation. In our case, the reagents used for the transfection of the cells, hypoxia and the inevitable changes in the pH of the medium might have affected the final readings. These experiments were supported with LDA and soft agar assays, and the effect of Elk-1 on colony formation was analyzed.

#### **5.4. THE REGULATION OF PLURIPOTENCY GENES BY ELK-1**

To assess the potential role of Elk-1 in the regulation of pluripotency genes, luciferase reporter assay, and chromatin immunoprecipitation (ChIP) assay were used. Using the primers shown in Table 4.2 reporter plasmids were prepared for luciferase assays. Deletion mutations were done on Elk-1 binding sites of cloned promoters with site-directed mutations using the designed primers shown in Table 4.7.

NANOG homeobox protein has two isoforms, namely NANOG isoform 1 and NANOG isoform 2. While NANOG isoform 1 codes for a longer transcript, NANOG isoform 2 uses an alternative in-frame splice site leading to a shorter transcript. For the promoter clonings of luciferase reporter assay, the promoter sequence of NANOG isoform 1 that was retrieved from the TRED website (-700/+299) was used, and the eventual clone was named NANOG-*luc*/pGL3. The analysis of the NANOG promoter sequence from TRED led to one Elk-1 binding site, and that site was deleted by site-directed mutation, and the leading clone was named NANOG $\Delta$ -*luc* /pGL3. For ChIP assays, both isoforms and Eukaryotic Promoter Database (EPD) were analyzed for Elk-1 binding sites, and three potential Elk-1 binding sites were detected – two sites from isoform 1 (NANOG*ets*1, NANOG*ets*2), one site from isoform 2 (NANOG*ets*3).

POU domain, class 5, transcription factor 1 (POU5F1) has four isoforms, and POU5F1 isoform 1 encodes the longest isoform. For the promoter clonings of luciferase reporter assay, the promoter sequence of POU5F1 isoform 1 that was retrieved from the TRED website (-700/+299) was used, and the eventual clone is named POU5F1-*luc* /pGL3. The analysis of the POU5F1 promoter sequence from TRED led to three potential Elk-1 binding

sites, and those sites were deleted by site-directed mutation, and the leading clones were named POU5F1 $\Delta$ 1-*luc*/pGL3, POU5F1 $\Delta$ 2-*luc* /pGL3 and POU5F1 $\Delta$ 3-*luc*/pGL3. For ChIP assays, both TRED and EPD were analyzed for potential Elk-1 binding sites, and four potential Elk-1 binding sites were detected – three sites from TRED (POU5F1*ets*1, POU5F1*ets*2, POU5F1*ets*3), one site from EPD (POU5F1*ets*4).

SRY-box 2 (SOX2) transcription factor does not have any isoform. For the promoter clonings of luciferase reporter assay, the promoter sequence of SOX2 that was retrieved from the TRED website (-700/+299) was used, and the clone is named SOX2-*luc*/pGL3. The analysis of the SOX2 promoter sequence from TRED led to two Elk-1 binding sites, and those sites were tried to be deleted by site-directed mutation; however, SDM could not be achieved. For ChIP assays, both TRED and EPD were analyzed for Elk-1 binding sites, and five potential Elk-1 binding sites were detected – two sites from TRED (SOX2*ets*1, SOX2*ets*2) and three sites from EPD (SOX2*ets*3, SOX2*ets*4, and SOX2*ets*5).

#### **5.4.1. Functional Assessment with Luciferase Reporter Assay**

It is challenging to analyze the effect of TFs within the cells as they are multifaceted. A luciferase reporter assay is a useful tool for studying the role of Elk-1 on the expression of pluripotency genes. For this, the promoter sequences of *NANOG*, *POU5F1*, and *SOX2* genes were cloned to the downstream of the regulatory DNA sequence in the pGL3-Basic vector (Promega). The cloned *Firefly*-luciferase plasmids, Elk-1 over-expression or silencing plasmid (Elk-1 over-expression (Elk-1/pcDNA3.1), Elk-1 constitutively active form (Elk1-VP16), Elk-1 dominant negative form (Elk1-EN), Elk-1 silencing (siElk-1) and scrambled RNA (scrRNA)) and the control vector *Renilla*-luciferase were co-transfected and the effect of Elk-1 expression on the activity of promoter of interest was evaluated. For RNA interference studies, scrRNA and siElk-1 transfections were repeated 24 hours after the first transfection to ensure the silencing of Elk-1. The normalization of the *Firefly* results with *Renilla* results would enable to overcome the possible discrepancies due to leakage or transfection efficiency differences between the groups and the experiments.



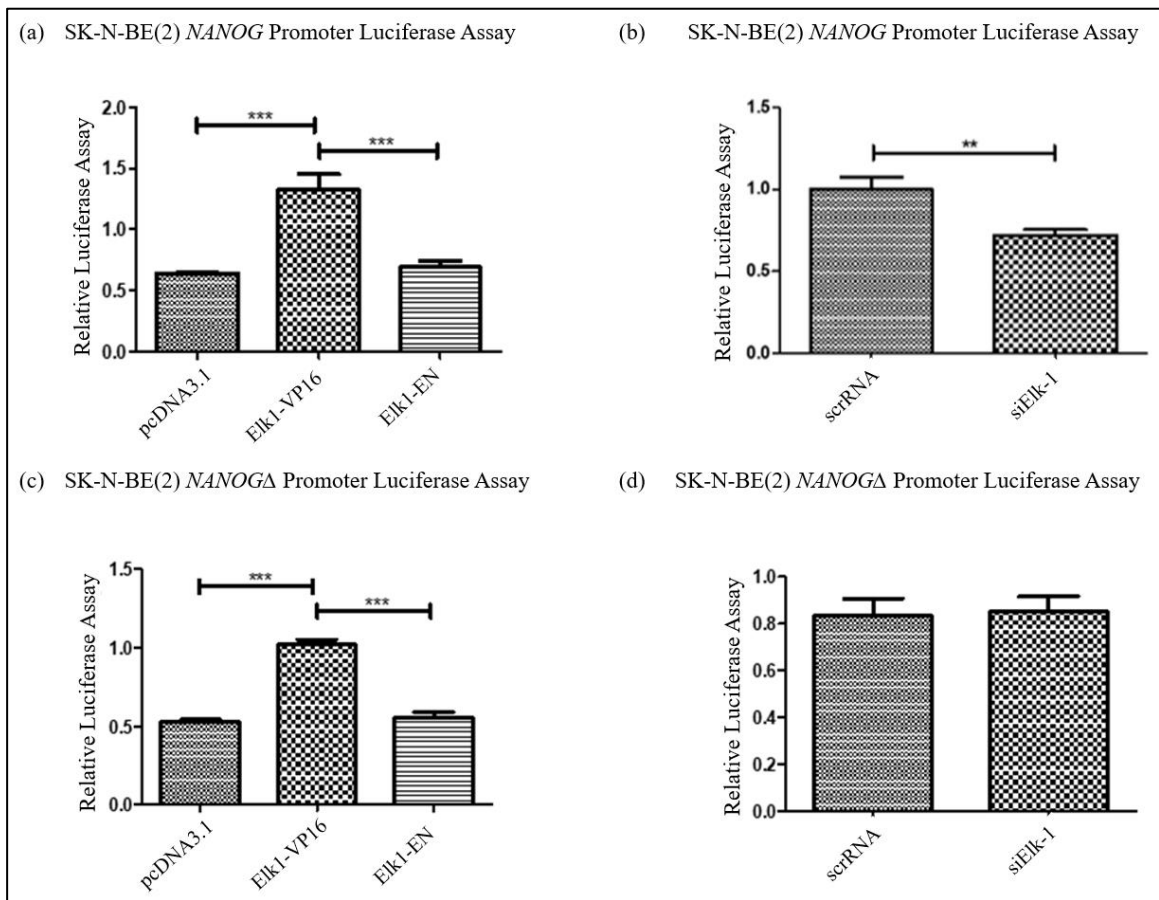


Figure 5.28. Luciferase assay for *NANOG*-Luc and *NANOGΔ*-Luc reporters in SKNBE(2) cells after transfection of expression plasmids with Elk1-VP16, Elk1-EN or empty control plasmid pCDNA3.1, siElk-1 or scrRNA control plasmid (a) *NANOG*-Luc, (b) *NANOG*-Luc, (c) *NANOGΔ*-Luc reporter; (d) *NANOGΔ*-Luc reporter cells. Luminometric measurements were normalized to Renilla-luc activity. ANOVA, Tukey's multiple comparative tests, \*\*\* $p < 0.001$  for (a) and (c); unpaired two-tailed t-test, \*\* $p < 0.01$  was done for (b) and (d).

The effect of the change in Elk-1 expression on *NANOG*, *NANOGΔ*, *POU5F1*, *POU5F1Δ1*, *POU5F1Δ2* and *POU5F1Δ3* promoters was investigated in SKNBE(2) and SH-SY5Y neuroblastoma cell lines as well as U87-MG glioblastoma cell line. Experiments with wild-type promoters would give information about the linkage between the Elk-1 transcription factor and the related promoters while the experiments with mutant promoters would allow the determination of whether the association was carried out directly through the Elk-1 binding site or not.

*NANOG* is a homeobox transcription factor that binds to DNA, which plays a role in the proliferation, renewal, and maintenance of pluripotency of ESCs. While it inhibits the differentiation of ESCs, it also automatically suppresses its own expression in differentiated cells. ESCs and CSCs are thought to carry the same phenotypic characteristics. For example, both cell types are characterized by rapid growth and high telomerase activity. The excess of telomerase activity causes these cells to acquire immortality. Over-expression of *NANOG* in CSCs results in apoptosis inhibition and cell proliferation, while that provides specific differentiation in ESCs [147].

Figure 5.28 shows the results of luciferase assays for *NANOG* and *NANOG* $\Delta$  promoters in SKNBE(2) cell line. It looks like there is a significant correlation between Elk-1 transcription factor and wild-type *NANOG* gene promoter in SKNBE(2) cells in Figure 5.28 (a) and (b). Nevertheless, the deletion of the Elk-1 binding site from the wild-type promoter did not change the results (Figure 5.28 (c)).

Table 5.4. ETS transcription factor family binding site profiles for the selected pluripotency gene promoters

ETS Family Transcription Factors	Pluripotency Gene Promoters (# binding sites)		
	<i>SOX2</i>	<i>NANOG</i>	<i>POU5F1</i>
<b>ETS1</b>	15	11	14
<b>ETS2</b>	4	6	4
<b>ELK-1</b>	2	1	3
<b>PEA3</b>	1	-	-
<b>ELF-1</b>	1	-	-
<b>MEF-2A</b>	-	2	-
<b>HIF*</b>	1	-	-

On the other hand, as the study concentrated on the effect of Elk-1, the promoter analysis was getting through Elk-1 binding site, and the mutants were prepared according to those sites in Table 5.4. (\* Even it is not a member of the ETS Family Transcription Factor Family, HIF is included into the table). However, when the promoters of interest were checked for

all the ETS family members, the leading TFs from other subfamilies were also detected on the promoters.

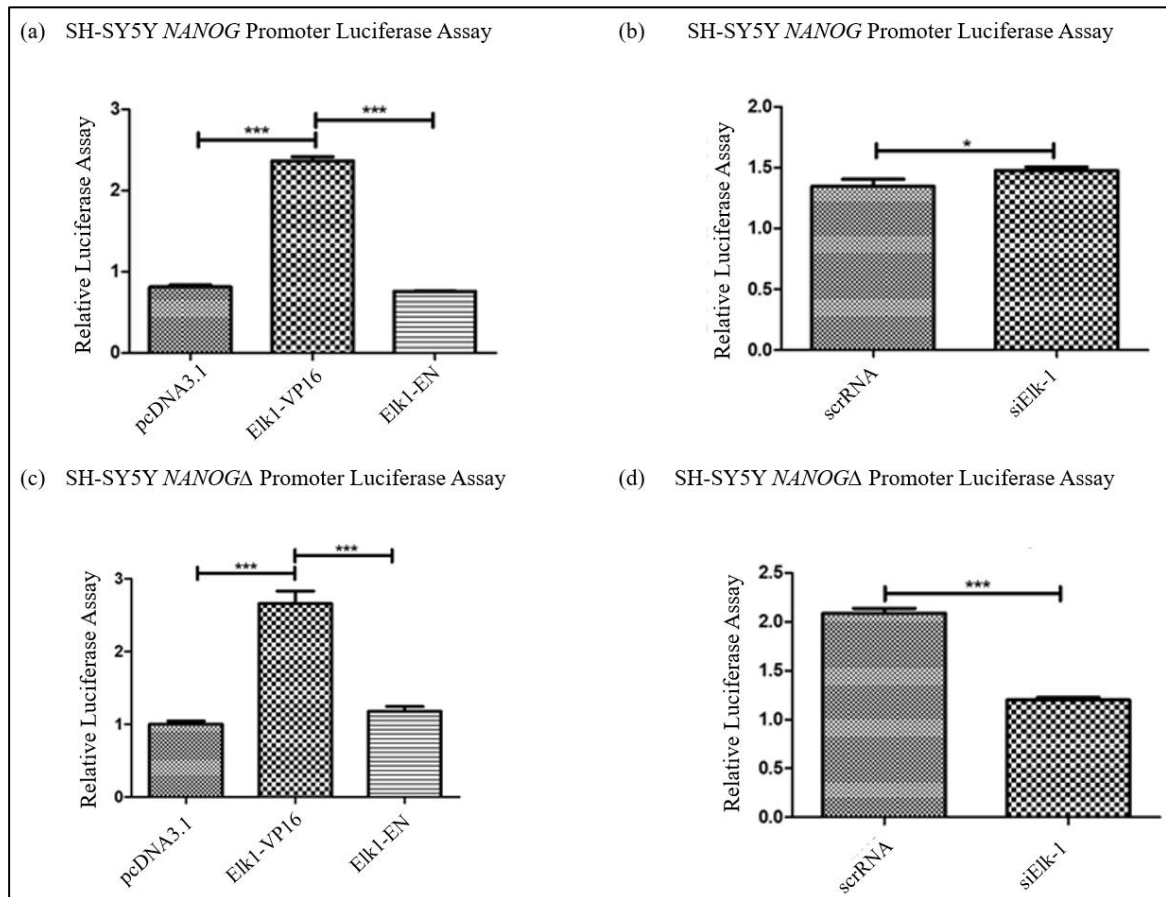


Figure 5.29. Luciferase assay for *NANOG*-Luc and *NANOGΔ*-Luc reporters in SH-SY5Y cells after transfection of expression plasmids. Luminometric measurements were normalized to *Renilla*-luc activity. ANOVA, Tukey's multiple comparative tests, \*\*\* $p < 0.001$  for (a) and (c); unpaired two-tailed t-test; \* $p < 0.5$ , \*\*\* $p < 0.001$  for (b) and (d).

Especially the binding motifs for ETS1 and ETS2 transcription factors were high in number, and they were intersecting with the Elk-1 binding motifs on the promoters. The dominant negative Elk-1 construct could have prevented the function of other ETS factors, leading a decrease in promoter activity [148]. That may be an explanation for the decrease in promoter activity with Elk1-EN expression, while siElk-1 expression did not change the promoter activity significantly. Therefore, it may be concluded that ETS factors function in the promoter activity of the chosen promoters of interest.

With the mutated plasmid, the silencing of Elk-1 kept the promoter activity at the control level. However, with RNAi, the idea is to repress a functional transcript to prevent function, whereas, with dominant-negative, the function is knocked-down at the primary source. It means, in this case, the change in the promoter activity between Figure 5.28 (b) and (d) may not be directly the result of Elk-1 expression. This suggests that there may a reciprocal mechanism allowing the interaction between NANOG promoter and Elk-1 transcription factor to continue similarly following Elk-1 binding site deletion.

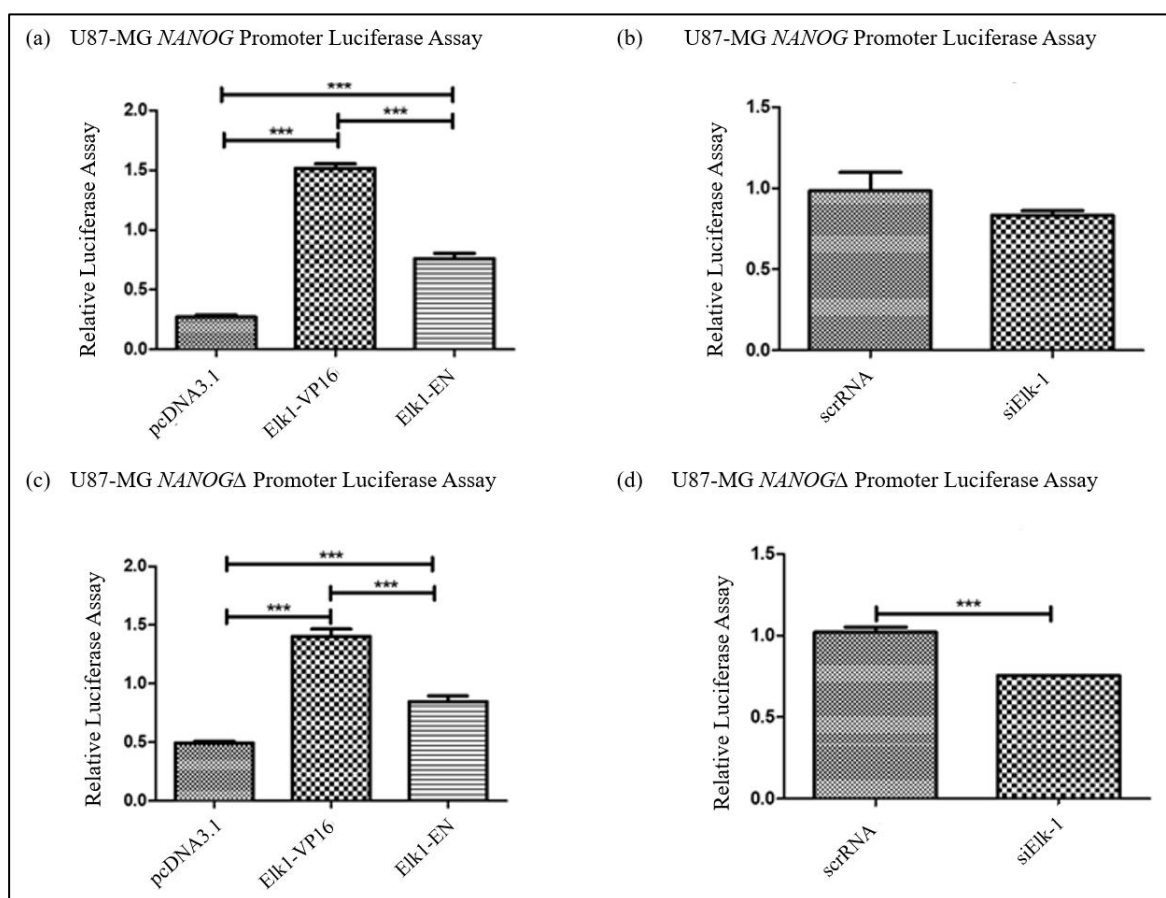


Figure 5.30. Luciferase assay for NANOG-Luc and NANOG $\Delta$ -Luc reporters in U87-MG cells after transfection of expression plasmids Elk1-VP16, Elk1-EN, siElk-1 or scrRNA control plasmid (a) *NANOG*-Luc, (b) *NANOG*-Luc, (c) *NANOGΔ*-Luc reporter, (d) *NANOGΔ*-Luc reporter. Luminometric measurements were normalized to *Renilla*-luc activity. ANOVA, Tukey's multiple comparative tests, \*\*\* $p < 0.001$  for (a) and (c); unpaired two-tailed t-test, \*\*\* $p < 0.001$  was done for (b) and (d).

Figure 5.29 and Figure 5.30 show the results for SH-SY5Y neuroblastoma and U87-MG glioblastoma cell lines, respectively. In these two cell lines, the deletion of Elk-1 binding site did not change the promoter activity profile when the cells were transfected with Elk-1 over-expression and dominant-negative plasmids.

Even the type of cancer cell and the the leading processes within the cells were different, their reactions to the given genes were about the same for these cell lines. In both cell lines, silencing Elk-1 through RNA interference made a more prominent effect in mutant *NANOG* promoters leading to a significant decrease in promoter activity.

Figure 5.31 shows the results of luciferase assays for wild-type *POU5F1* and mutant *POU5F1* promoters in SKNBE(2) cell line. It looks like there is a significant correlation between Elk-1 transcription factor and wild-type *POU5F1* gene promoter in SKNBE(2) cells. The results of the luciferase assay are interpreted as a relative activity. In the case of *POU5F1*, the deletion of each of the Elk-1 binding sites affected the promoter activity relative to the control group.

However, the main pattern remained constant. The difference in promoter activity of *POU5F1* $\Delta$ 2 promoter was prominently different from the wild-type and other mutants. Nevertheless, the deletion of one Elk-1 binding site did not have a strictly deleterious effect of ceasing the *POU5F1* promoter activity entirely.

The deletion of all the Elk-1 or in general, ETS sites, on the promoter could have such a sharp effect on the activity. In this case, it can be concluded that Elk-1 have a role in the regulation of *POU5F1*, probably indirectly and this can be checked with other means.

Figure 5.32 and Figure 5.33 show the results for wild-type and mutant *POU5F1* promoter activity in SH-SY5Y neuroblastoma and U87-MG glioblastoma cell lines, respectively. In these two cell lines, the deletion of Elk-1 binding site did not change the promoter activity profile when the cells were transfected with Elk-1 over-expression and dominant-negative plasmids.

However, in both cell lines, silencing Elk-1 through RNA interference made a noticeable effect in mutant *POU5F1* promoters leading to a significant change in promoter activity. Different TFs (possibly still from the ETS transcription factor family) could be activated or compensated over a different pathway.

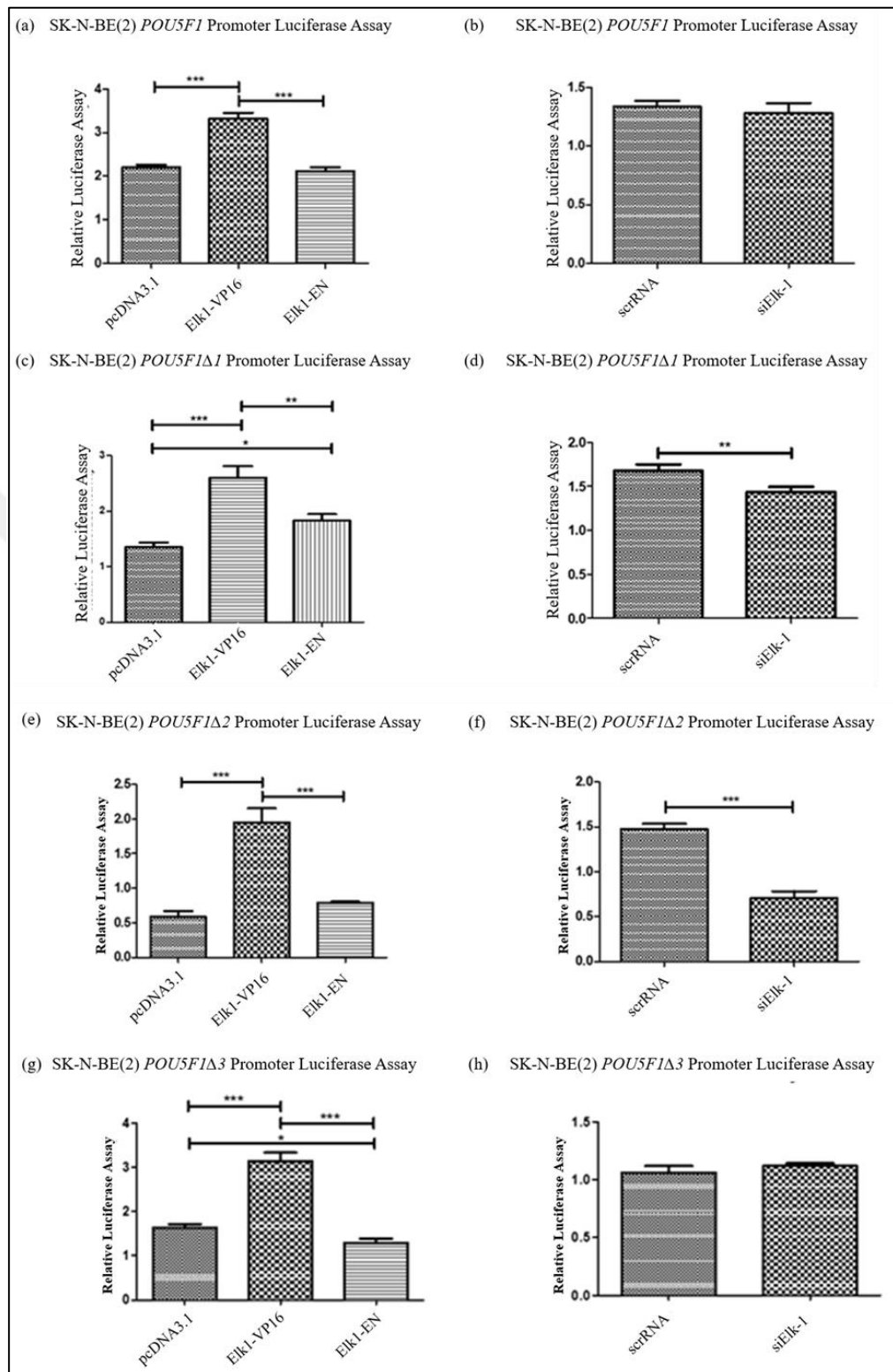


Figure 5.31. Luciferase assay for wild-type *POU5F1*-Luc and its deletion mutant reporters in SKNBE(2) cells. Luminometric measurements were normalized to *Renilla*-luc activity. ANOVA, Tukey's multiple comparative tests, \*\* $p < 0.01$ , \*\*\* $p < 0.001$  for (a), (c), (e) and (g); unpaired two-tailed t-test, \*\* $p < 0.01$  and \*\*\* $p < 0.001$  for (b), (d), (f) and (h).

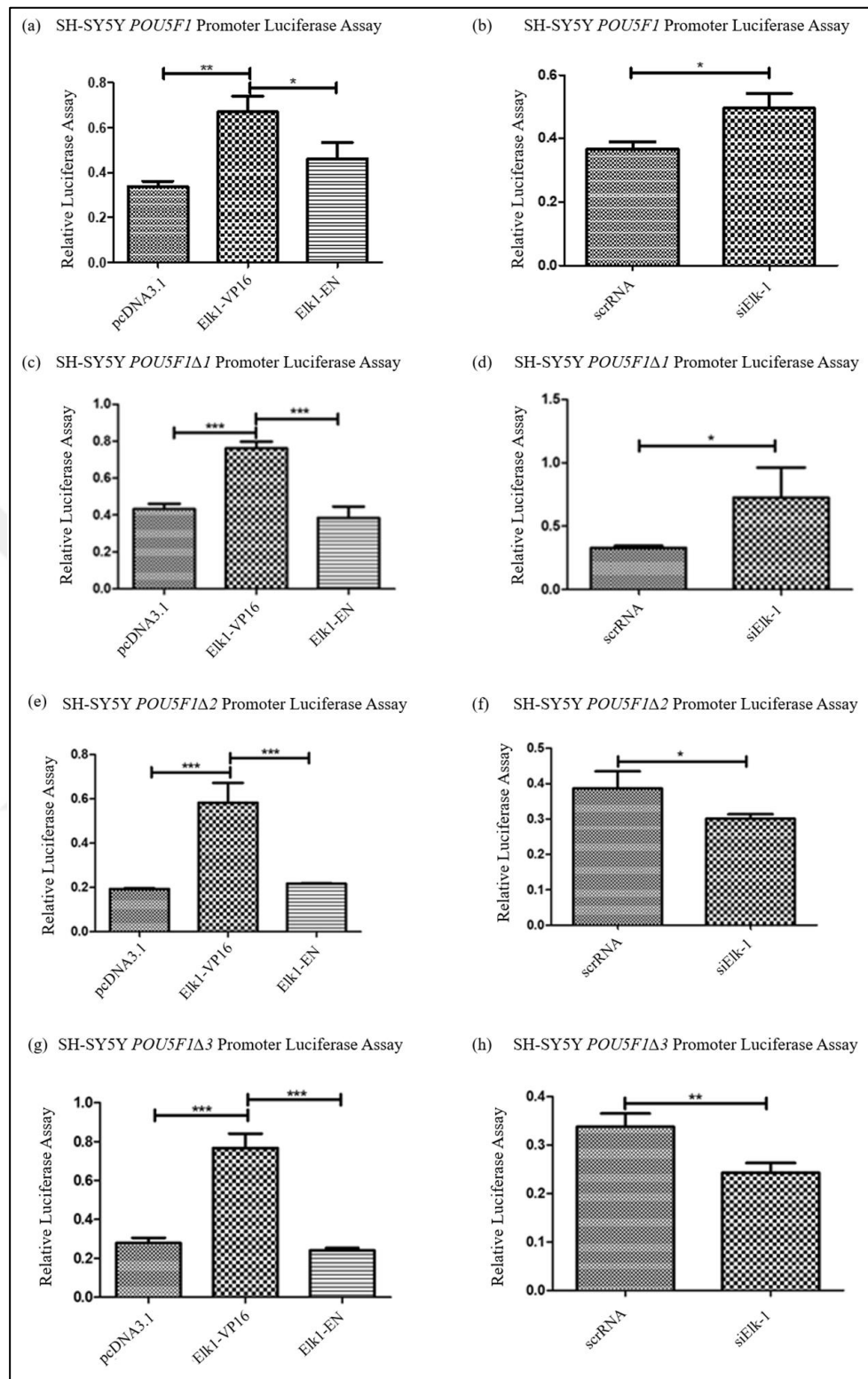


Figure 5.32. Luciferase assay for wild-type POU5F1-Luc and its deletion mutant reporters in SH-SY5Y cells. Luminometric measurements were normalized to *Renilla-luc* activity. ANOVA, Tukey's multiple comparative tests, \* $p < 0.5$ , \*\* $p < 0.01$ , \*\*\* $p < 0.001$  for (a), (c), (e) and (g); unpaired two-tailed t-test, \* $p < 0.5$ , \*\* $p < 0.01$  was done for (b), (d), (f) and (h).

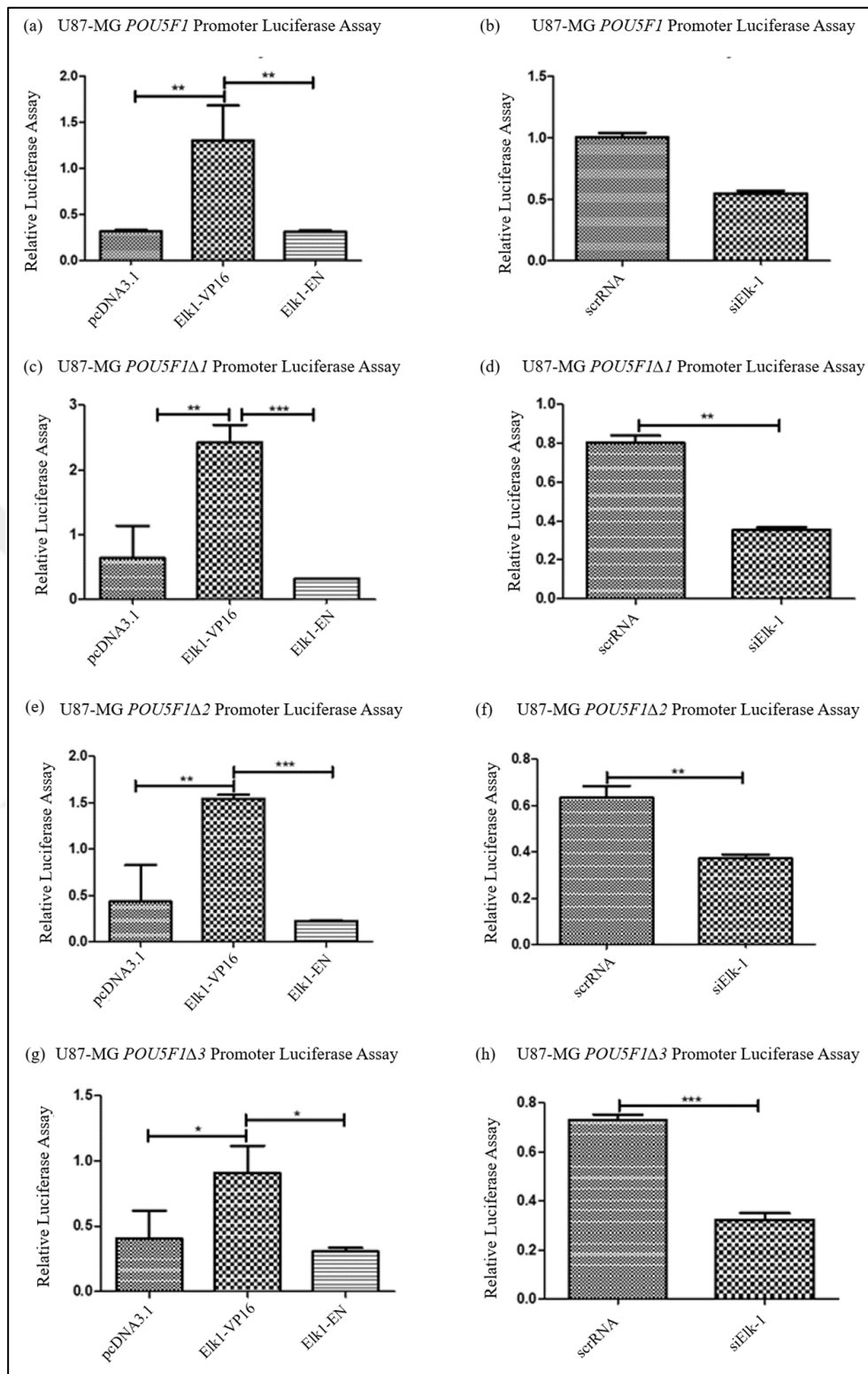


Figure 5.33. Luciferase assay for wild-type POU5F1-Luc and its deletion mutant reporters in U87MG cells. Luminometric measurements were normalized to *Renilla*-luc activity. ANOVA, Tukey's multiple comparative tests, \* $p < 0.05$ , \*\* $p < 0.01$ , \*\*\* $p < 0.001$  for (a), (c), (e) and (g); unpaired two-tailed t-test, \*\* $p < 0.01$ , \*\*\* $p < 0.001$  for (b), (d), (f) and (h).



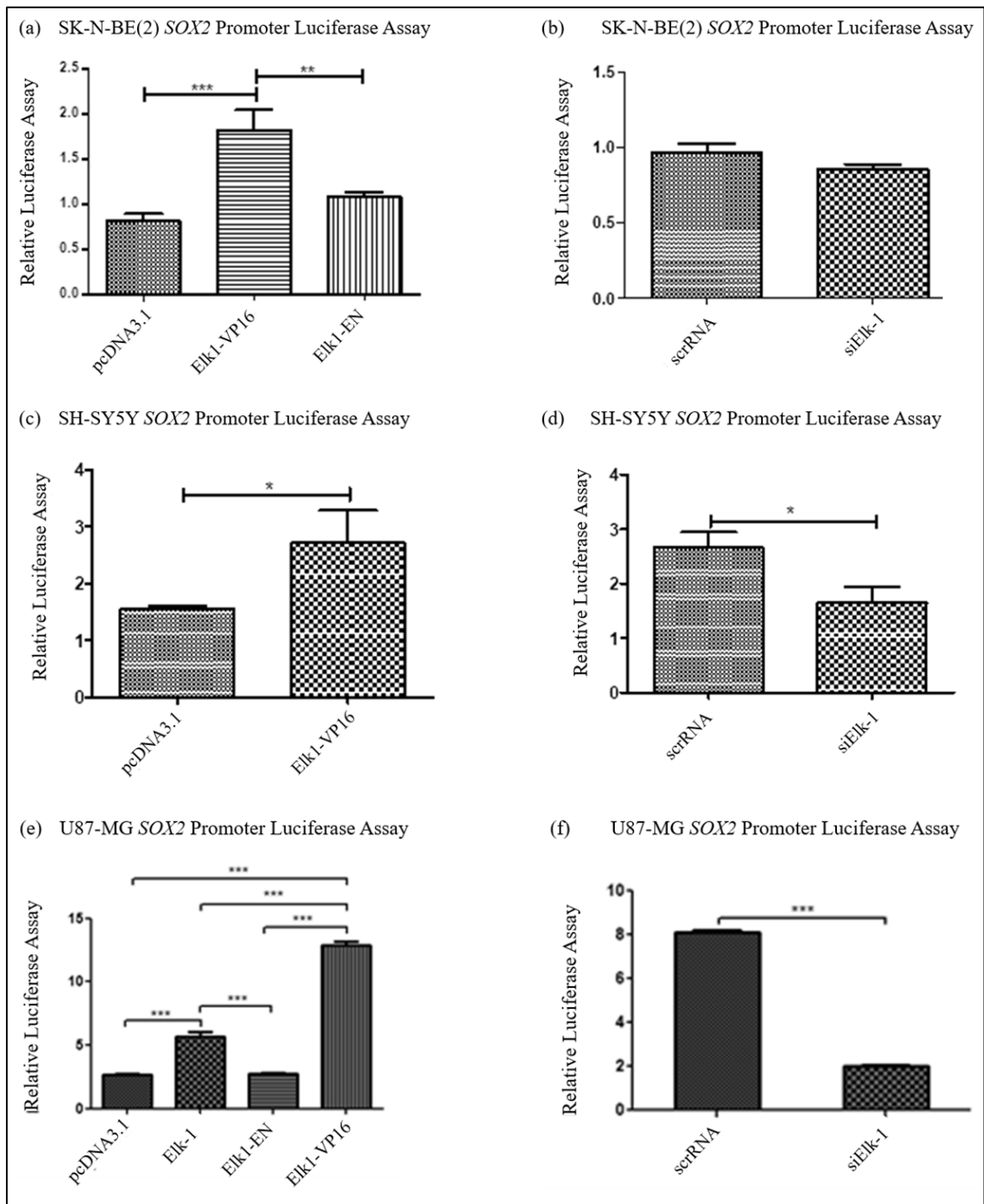


Figure 5.34. SOX2 promoter activity analysis with respect to ELK-1 over-expression and silencing in (a,b) SKNBE(2), (c,d) SH-SY5Y, (e,f) U87-MG cell lines. Luminometric measurements were normalized to *Renilla*-luc activity. ANOVA, Tukey's multiple comparative tests, \* $p < 0.5$ , \*\* $p < 0.01$ , \*\*\* $p < 0.001$  for (a), (c), (e); unpaired two-tailed t-test, \* $p < 0.5$ , \*\*\* $p < 0.001$  was done for (b), (d), (f).

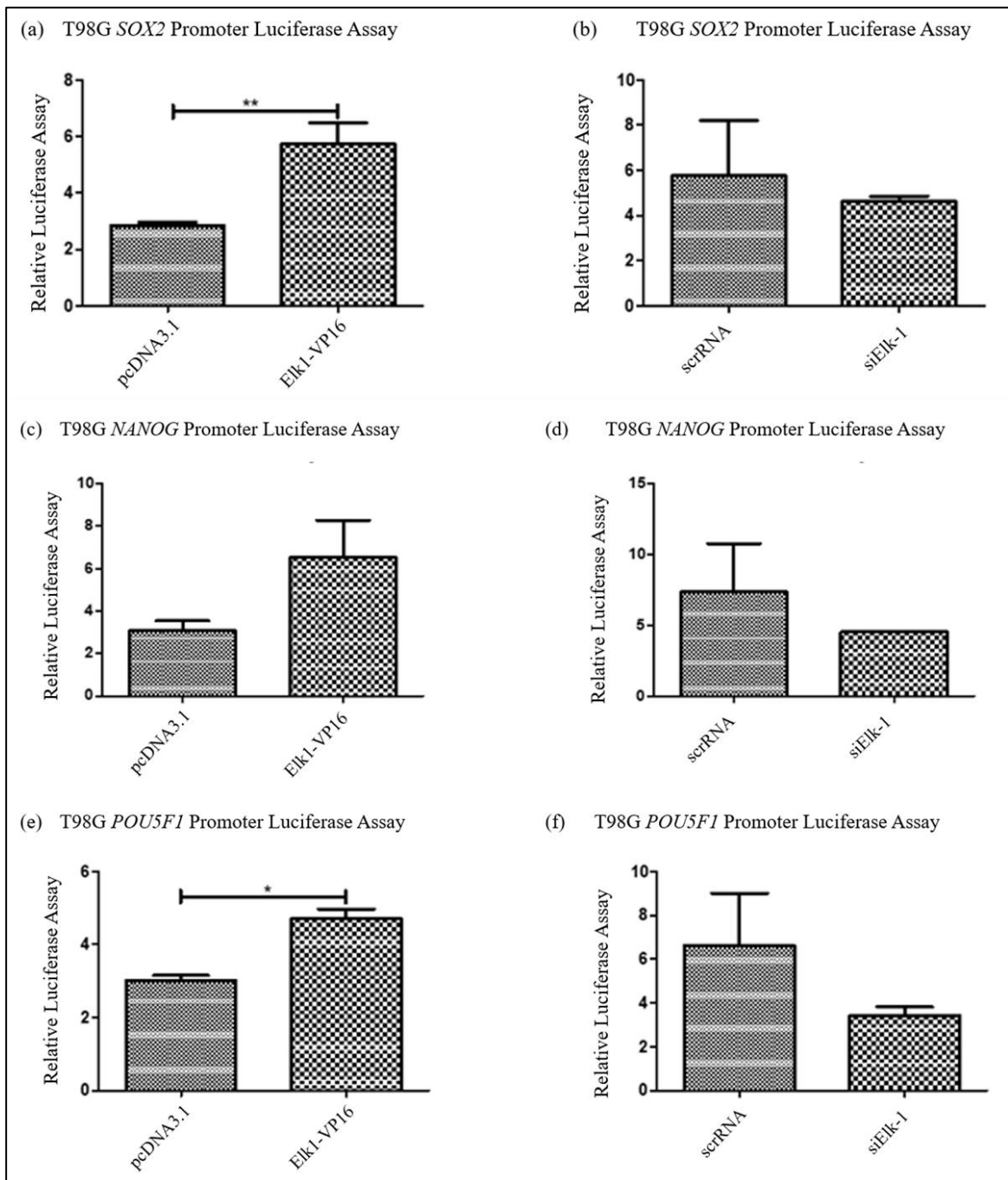


Figure 5.35. *SOX2*, *NANOG* and *POU5F1* promoter activity analysis with respect to ELK-1 over-expression and silencing in T98G cell line. Luminometric measurements were normalized to *Renilla-luc* activity. ANOVA, Tukey's multiple comparative tests, \* $p < 0.5$ , \*\* $p < 0.01$ , for (a), (c), (e); unpaired two-tailed t-test was done for (b), (d), (f).

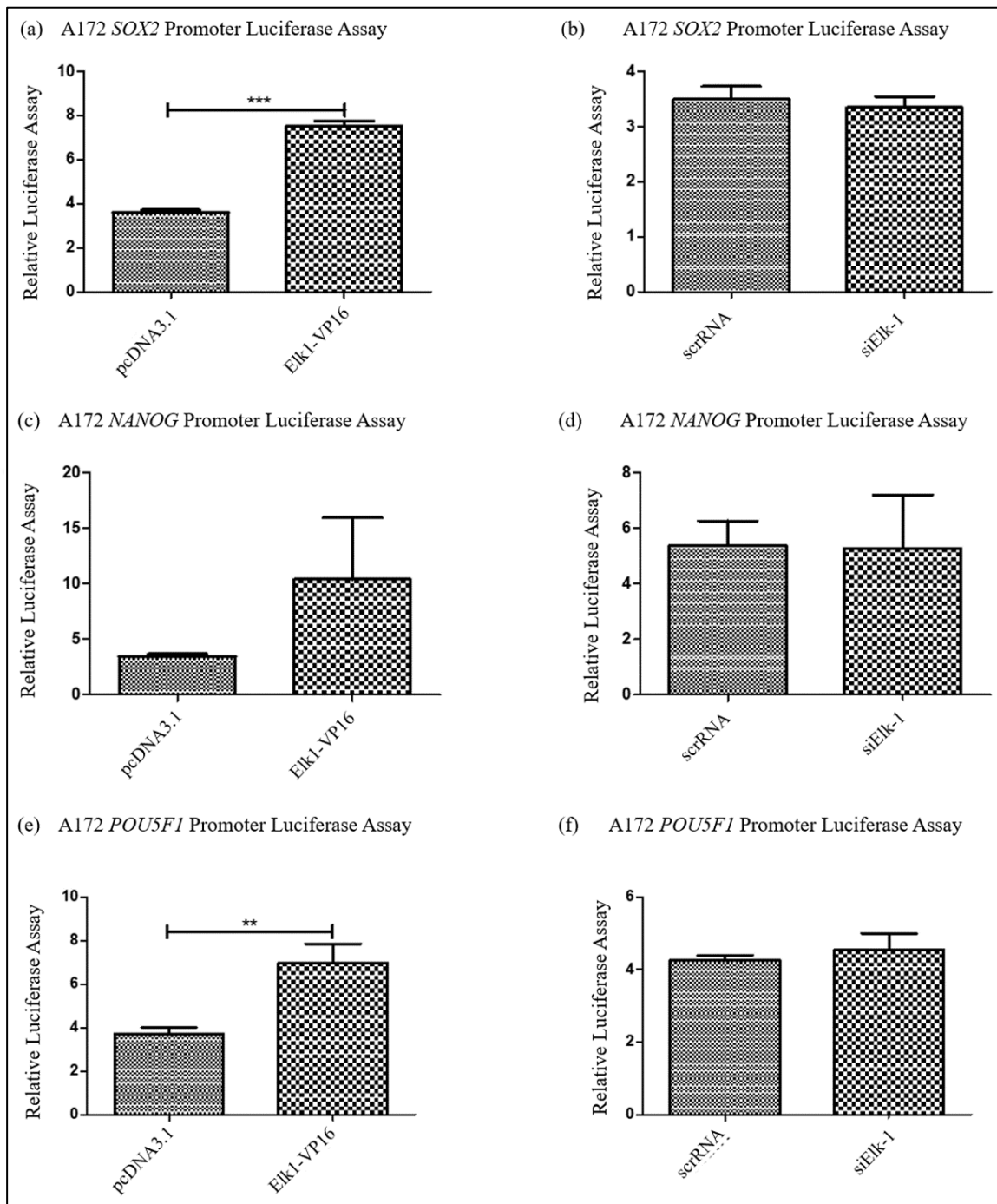


Figure 5.36. *SOX2*, *NANOG*, and *POU5F1* promoter activity analysis with respect to ELK-1 over-expression and silencing in A172 cell line. Luminometric measurements were normalized to *Renilla-luc* activity. ANOVA, Tukey's multiple comparative tests; \*\*p < 0.01, \*\*\*p < 0.001 for (a), (c), (e); unpaired two-tailed t-test was done for (b), (d), (f).

The wild-type *SOX2* promoters were investigated with respect to Elk-1 over-expression and silencing in neuroblastoma and glioblastoma cell lines as seen in Figure 5.34. On the other

hand, when the activity of pluripotency promoters in T98G and A172 glioblastoma cell lines were investigated, the results were not as significant as they were with neuroblastoma and U87 glioblastoma cell lines. Only *SOX2* activity and at a degree *NANOG* activity was prominent when Elk-1 was over-expressed

Elk-1 silencing did not result in a significant change in promoter activities in those cell line. Different transcription factors (possibly still from the ETS transcription factor family) could be activated or compensated over a different pathway.

#### 5.4.1.1. The Analysis of the Target Promoter Activities in Hypoxia

Hypoxia-inducible factors (HIFs) regulate and respond to hypoxic stress through binding to hypoxia-responsive elements (HREs). HREs are cis-regulatory elements, and through the consensus binding sites on the promoters, they mediate hypoxic response [149]. The Elk-1 binding sites on *NANOG*, *POU5F1* and *SOX2* promoters (-700/299) for HREs revealed that there is one HIF1 binding site on the *SOX2* promoter as shown in Figure 5.37 and Table 5.4.

GGGGAGTGATTATGGGAAGAAGGTTAGTAAGGAACAAAACAATGCACCGT	-651	50 HIF-1 [T01609]
TTTGTAAGATAATAAATGGAACGTGGCTGGTAGATACTATTTCAGTACAT	-601	
TTTCTTAGGGTGAGTAAGGGTAGACCAGGGGAGGAGGGGGCGGAGAGAGT	-551	
GTTACAGAAGAAAGAAAATAAGTAACCTGATGGTTTAAGCCCTTTATAA	-501	
AAAAGAAATGGCATCAGGTTTTTTTTCTTTATTCCCCCCCACCCACCC	-451	
TTTGTAGTCAAGTGCATTTTAGCCACAAGATCCCAACAAGAGAGTGGAA	-401	Sequence TGCTGC
GGAAACTTAGACGAGGCTTTGTTGACTCCGTGTAGCGACAACAAGAGAA	-351	Dissimilarity 0.91%
ACAAAACCTACCTATTTGTAACGGACGTGCTGCATTGCGCTCCGCATTGA	-301	
GCGCTACCTATTGAAATCTTTACGTCGGGACAATGGGAGAGCGGCTAAA	-251	
ATTACCCTCTGGGTCTGGGCGGGCAAGATTCTTGAGCCCCACCCCG	-201	
CCCCATCTCATCCTCCTCTAACCCGGGCTTGCTGGGCTCCCCCTTCCC	-151	
CAGTCCCGGCCCTTCTCCAGTGTGCGCTGCCTGCACCTGTGCCTGGA	-101	
GAGCATCGACCCCGCTCCAGGCCTTGAGCCCTTTGCGGGCAGCCCC	-51	
AGCCTTGCGCGGCTGGGCTTTGCGGCCACCAATGGAATCTACGGGG	-1	
AAAATGCCAGGGCTGTTCTGCTGGAGTCTGGGAATCTGCGTGGGAGG	49	
GAGTTGTGACTGCGGCCAAAAGCCACCTCCATACAGTGCCGTGGGATG	99	
CCAGGAAGTTGAAATCACCCCTCCCATCGCCTGCACCTTTGAGCGCCCT	149	
TCCGTCTGTGCTTTCCCCAGCCCCATTTGAAAGCCGACGACCGAAAC	199	
CCTTCTTACGGGGAGGCATGGGATGGGAATGGGGAGTGGGGGCAGACAGT	249	
AGAAGCATCCCCCTTGTACGGTTGAATGAAGACAGTCTAGTGGGAGATG	299	

Figure 5.37. HIF1 binding site on *SOX2* promoter

The dissimilarity rate for potential HIF binding site on *SOX2* promoter was below one. In other words, it is highly possible for that site to be the HIF binding site on *SOX2* promoter. Taking this into consideration, direct hypoxic effect and/or Elk1-related effects are considered for evaluating the results of hypoxia studies.

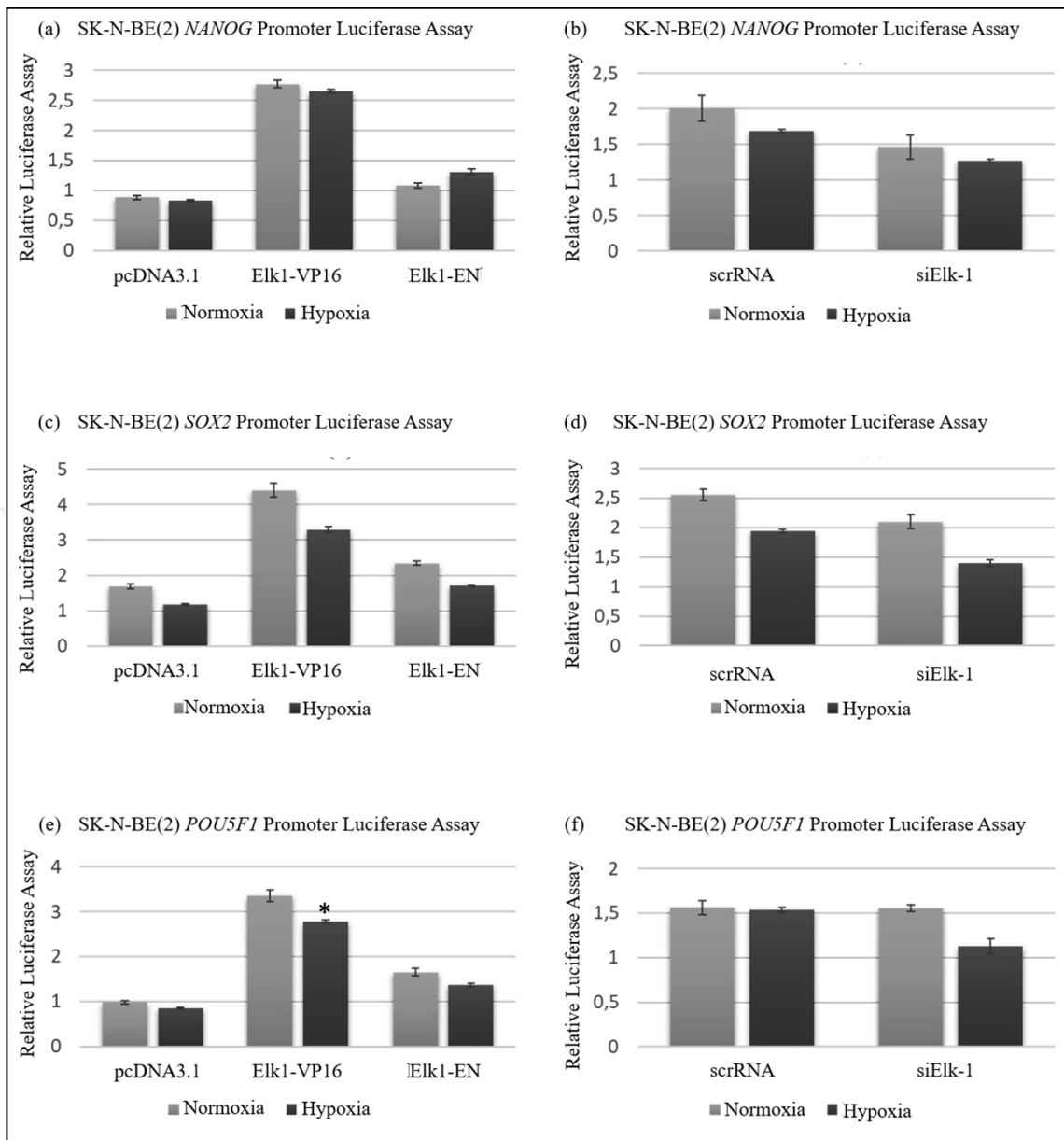


Figure 5.38. The promoter activities in normoxic vs. hypoxic conditions following transient transfection for Elk-1 over-expression vs. silencing ((Unpaired t -test, \* $p < 0.5$ )

The promoter activities were investigated for all three wild-type pluripotency genes as well as the mutant forms of *NANOG* and *POU5F1* genes in SKNBE(2). Nevertheless, hypoxia (one percent oxygen, six hours) did not change the interaction pattern significantly in SKNBE(2) cells as seen in Figure 5.38 Figure 5.39 and Figure 5.40 shows a change in promoter activities due to hypoxia on both wild-type and mutant promoters. However, the results were quite the same for both normoxia and hypoxia; there was no significant change between the groups of different conditions.

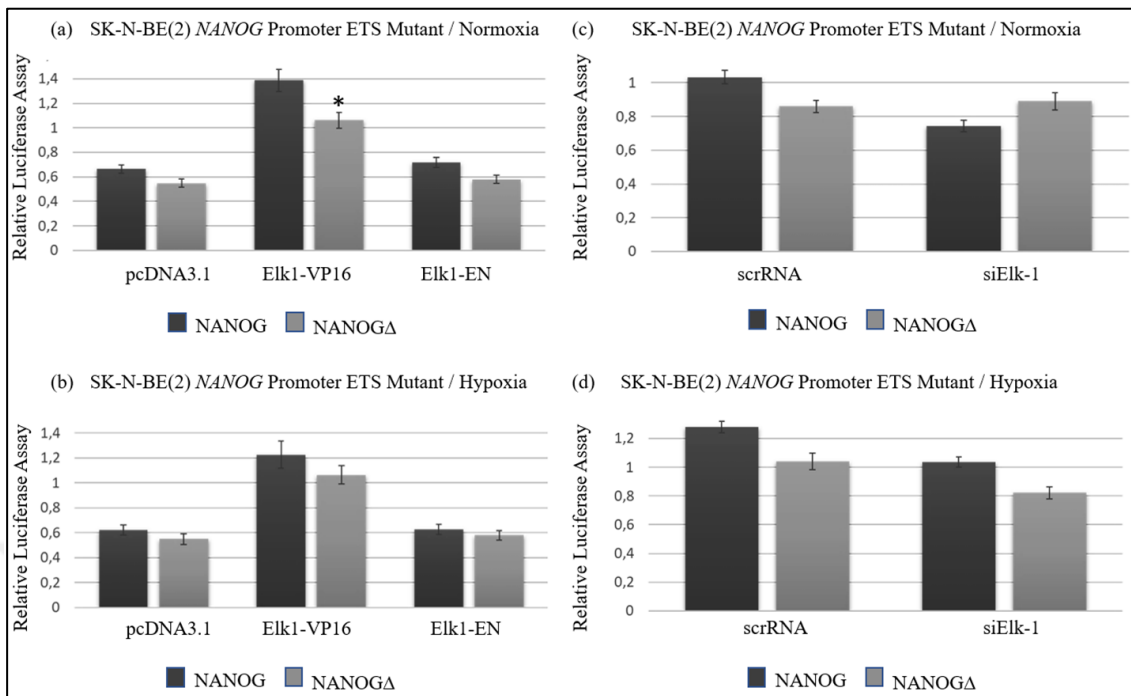


Figure 5.39. Luciferase assay results for NANOG vs. NANOG $\Delta$  in normoxic vs. hypoxic conditions in SK-N-B (2) cell line. (Unpaired t -test, \*p < 0.05).

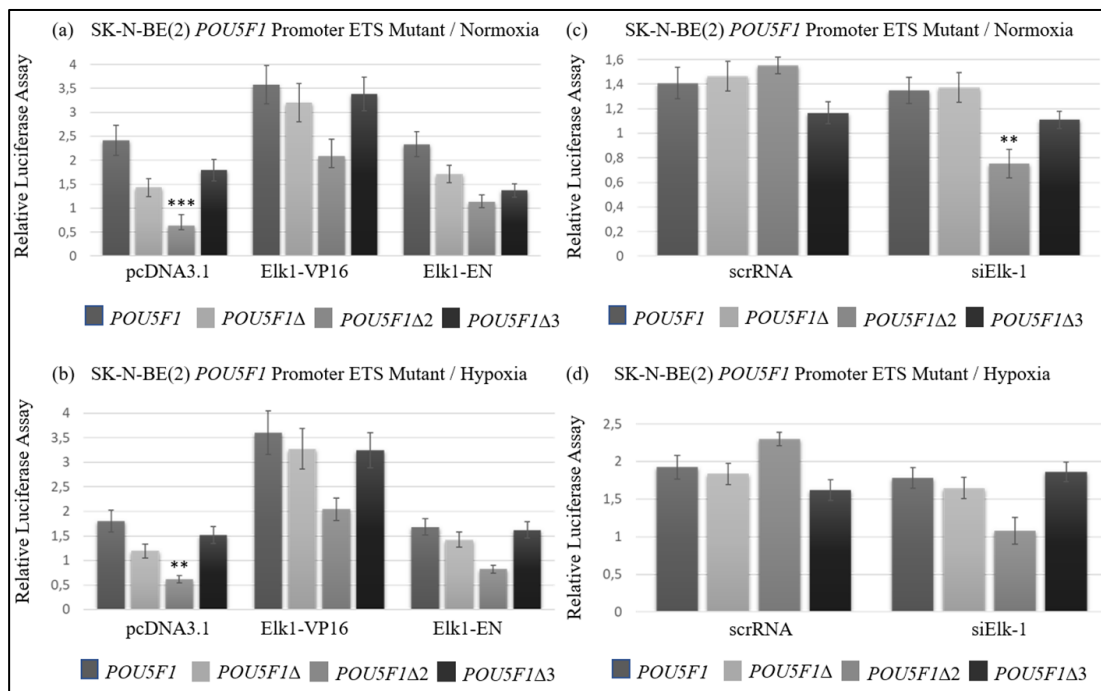


Figure 5.40. Luciferase assay results for wild-type POU5F1 vs. mutants in normoxic vs. hypoxic conditions in SKNBE(2) cell line. (One-way ANOVA; \*\*p < 0.01, \*\*\*p < 0.001).

The similarities between the normoxia and hypoxia groups may be related to the setup of the Dual-Glo Luciferase assay. Throughout the assay, the cells pass through various steps and incubated at least 15 minutes for each of the *Firefly* and *Renilla* luciferase activities. This time could have restored the hypoxia stress, and the relative luciferase activities might have been similar.

#### **5.4.2. Analysis of Pluripotency Promoter Occupancies by Chromatin Immunoprecipitation (ChIP)**

ChIP is a powerful technique for the identification of binding of TFs to a particular region of the genome within the natural chromatin context of the cell. To support the findings from luciferase assay, ChIP assay was performed. To verify Elk-1 transcription factor interactions with the promoters of pluripotency factors as well as promoters of other potential target genes that were detected with microarray results, ChIP was suitable. Specific primers spanning the Elk-1 binding sites on the promoter of interest were used to investigate the promoter occupancy. *In silico* PCR was used to confirm the regions the designed primers would amplify on the genome.

Myeloid Cell Leukemia (*MCL-1*), one of the target genes of Elk-1 in SH-SY5Y neuroblastoma cells [33], and Serum Response Factor (*SRF*), the binding partner of Elk-1 [150] were used as a positive control for the ChIP assay. Figure 5.41 (a) shows the results for three independent ChIP assays. The potential binding sites were positive for Elk-1 interaction with different fold changes. Figure 5.41 (b) shows the agarose gel electrophoresis run after the ChIP-qPCR.

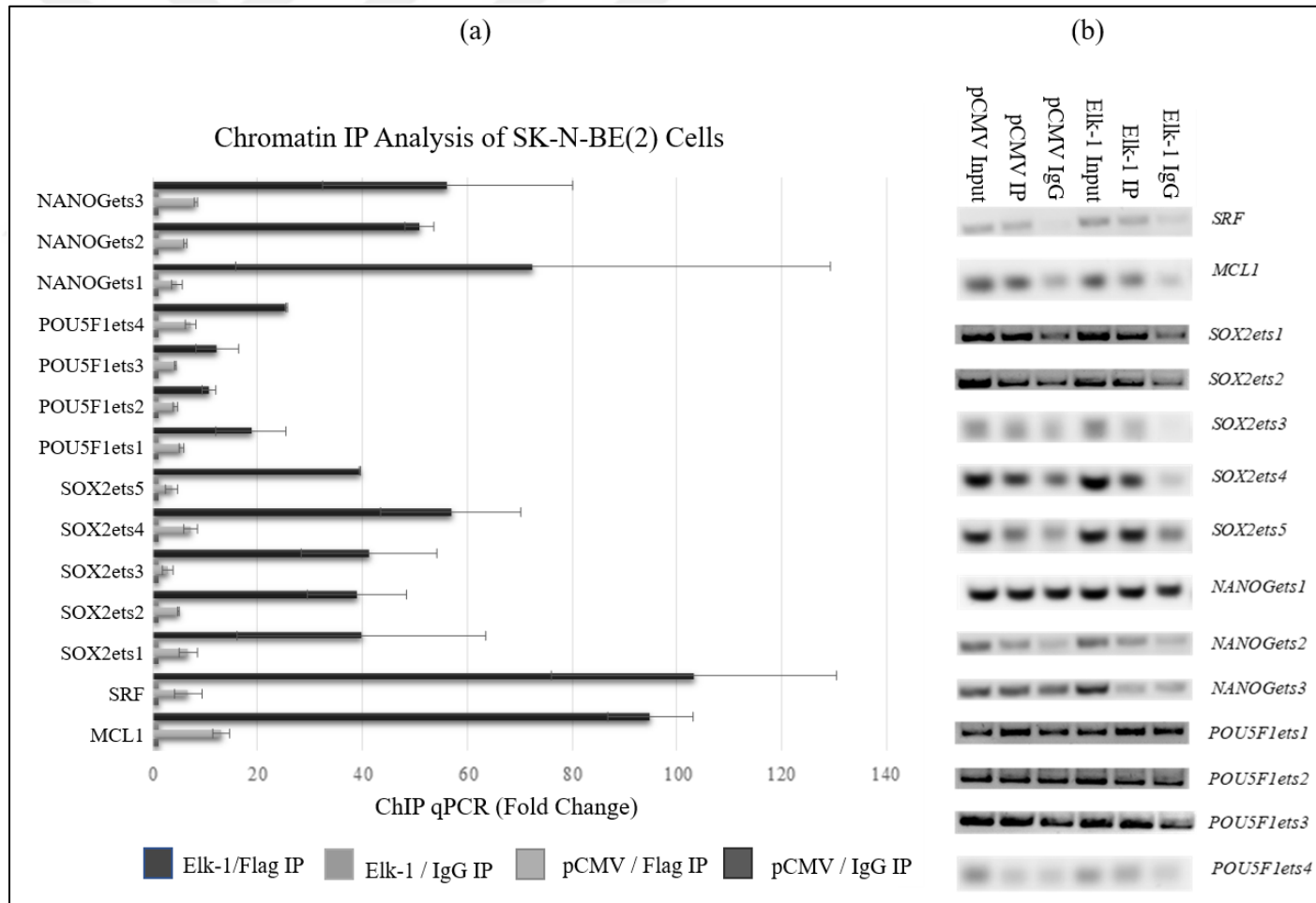


Figure 5.41. ChIP for the identification of Elk-1 binding sites on the target pluripotency gene promoters pCMV-transfected vs. Elk-1 over-expressing SKNBE(2) cells, immunoprecipitated with either Flag antibody (Flag IP) or IgG (IgG IP). (a) ChIP-qPCR, (b) agarose gel electrophoresis.



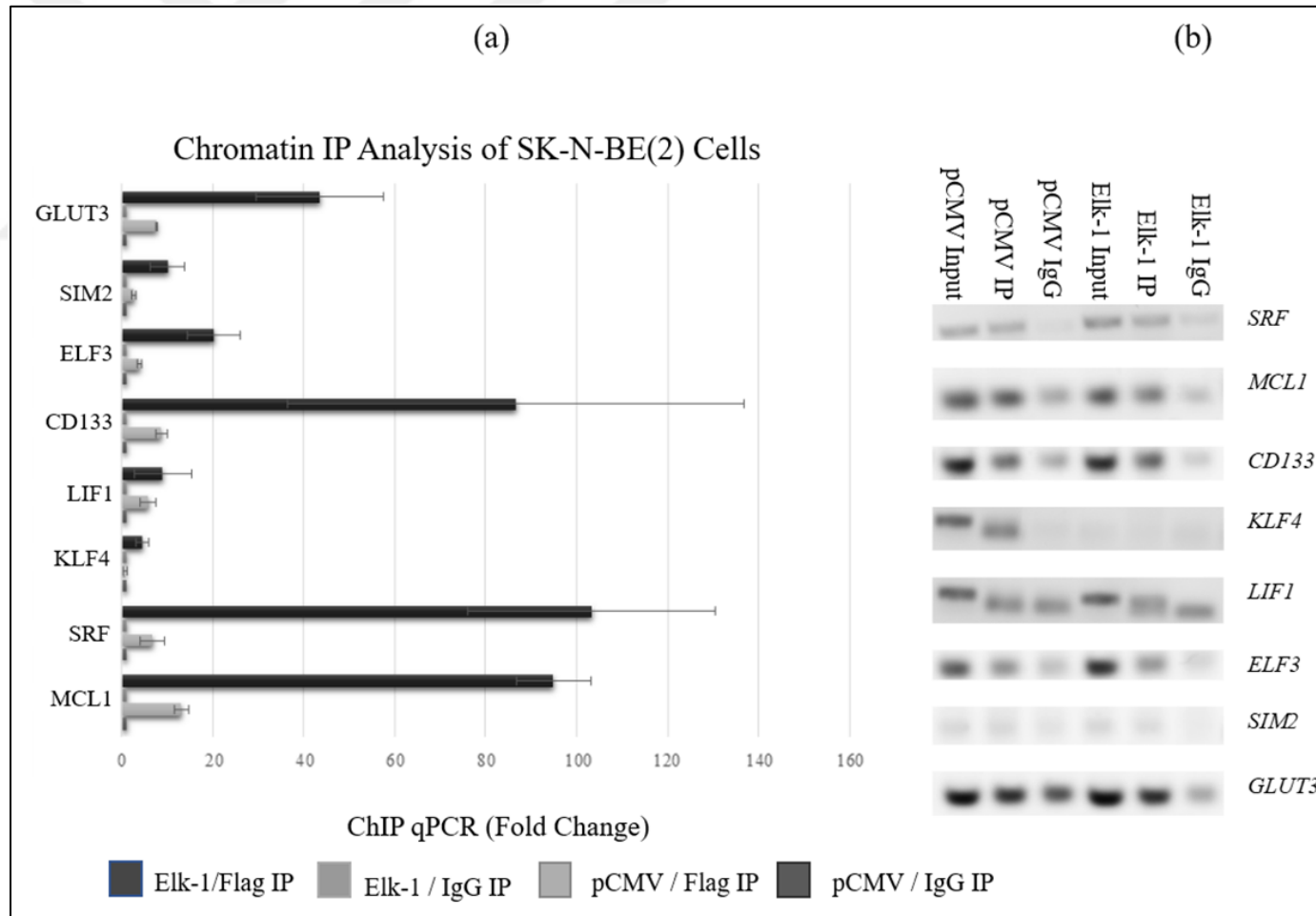


Figure 5.42. ChIP-qPCR results for the identification of Elk-1 binding sites on the target gene promoters pCMV-transfected vs. Elk-1 over-expressing SKNBE(2) cells, immunoprecipitated with either Flag antibody (Flag IP) or IgG (IgG IP). (a) ChIP-qPCR, (b) agarose gel electrophoresis.

When the results in Figure 5.41 (a) and (b) are evaluated together, it can be concluded that Elk-1 occupies pioneering stem cell promoters at various sites in SKNBE(2) cell line. Figure 5.42 shows the results of ChIP assay that was performed to check the binding of Elk-1 transcription factor to the potential target promoters.

Kruppel-like factor 4 (KLF4) and leukemia inhibitory factor (LIF) are usually shown in the pluripotency factors group together with *SOX2*, *NANOG*, and *POU5F1*. For the reprogramming of somatic cells to pluripotency state Yamanaka et al. used four factors, namely *SOX2*, *POU5F1*, *c-MYC* and *KLF4* [46].

When ESCs are considered, Pou5f1 together with LIF/Stat3 can activate Kruppel factors to maintain the self-renewal [151] and it was shown that LIF signaling sustains pluripotency of mouse ESCs [152]. The role of ETS transcription factor in the activation of CD133 promoter in hypoxia was shown by Ohnishi et al. [142]. E74-like factor-3 (Elf3) is also an ETS transcription factor family protein that is involved in tumorigenesis, metastasis, and differentiation.

The HSA21 encoded Single-minded 2 (SIM2) transcription factor occupy promoter of pioneering *SOX2*, *POU5F1*, *NANOG* or *KLF4* in pluripotent mouse ESCs [153]. In cancers, a phenomenon known as the Warburg Effect is recognized. Tumor cells start to rely on anaerobic yet glucose-intensive glycolysis pathway rather than oxidative phosphorylation. It was shown that nutrient restriction supports brain tumor-initiating cell phenotype and the profound stem cell regulators induced upon nutrient restriction [154].

When the results in Figure 5.42 (a) and (b) are evaluated together, it can be concluded that *CD133*, *LIF1*, *ELF3*, and *GLUT3* promoters are occupied with Elk-1 transcription factor in SKNBE(2) cell line. The same assays were also performed for T98G glioblastoma cell line to compare the possible differences in interaction. In general, the standard deviation between the biological groups for T98G setup was high. When the fold change graph is analyzed together with the agarose gel bands, it can be concluded that Elk-1 has at least one binding site on the pioneering stem cell promoters in T98G glioblastoma cell line, just like SK-N-BE neuroblastoma cell line (Figure 5.43). Parallel to the SKNBE(2) results, it can be concluded that *CD133*, *LIF1*, *ELF3*, and *GLUT3* promoters are occupied with Elk-1 transcription factor in T98G glioblastoma cell line (Figure 5.44).

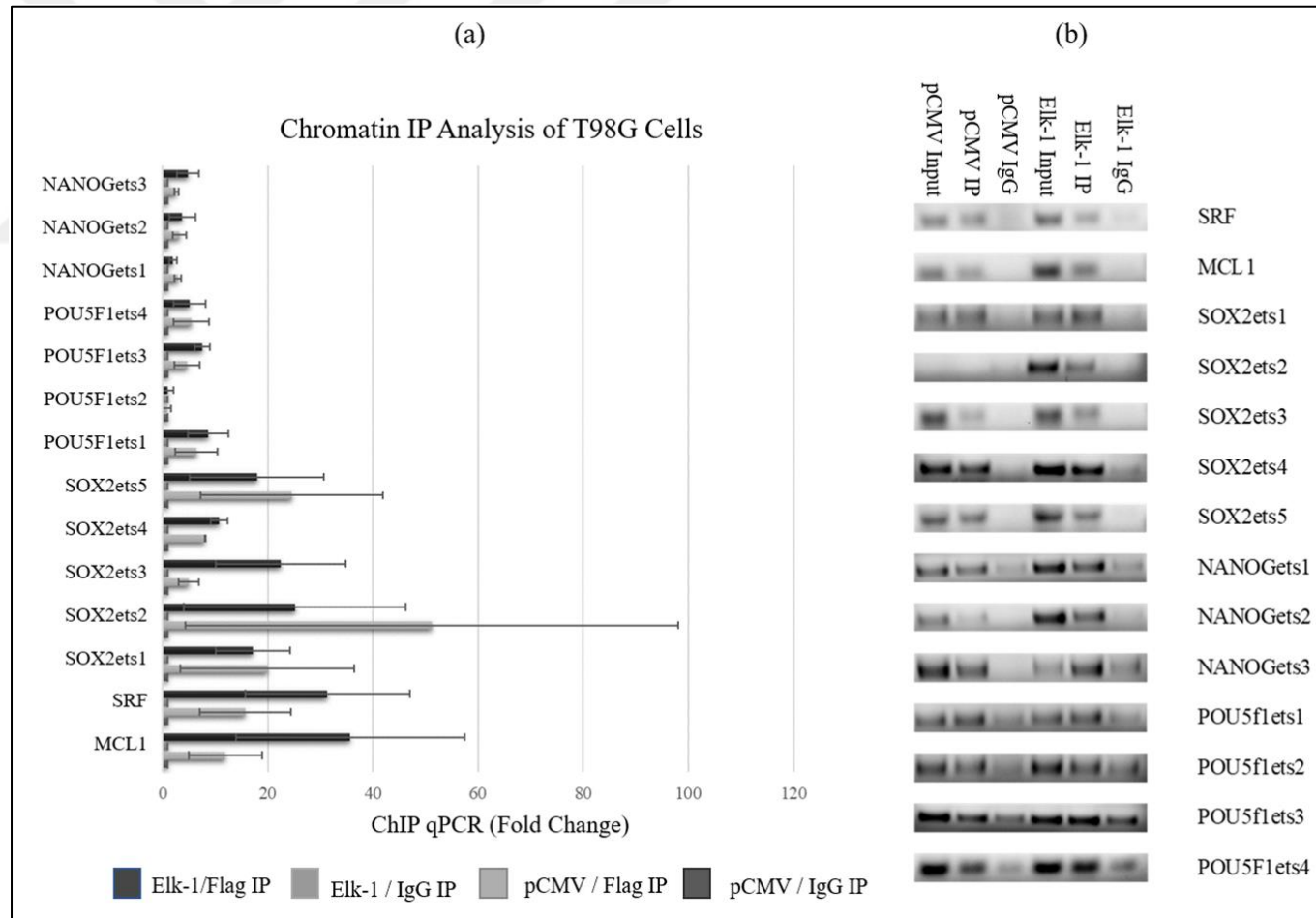


Figure 5.43. ChIP for the identification of Elk-1 binding sites on the target pluripotency gene promoters in pCMV-transfected vs. Elk-1 over-expressing T98G glioblastoma cells immunoprecipitated with either Flag antibody (Flag IP) or IgG (IgG IP). (a) ChIP-qPCR, (b) agarose gel electrophoresis.

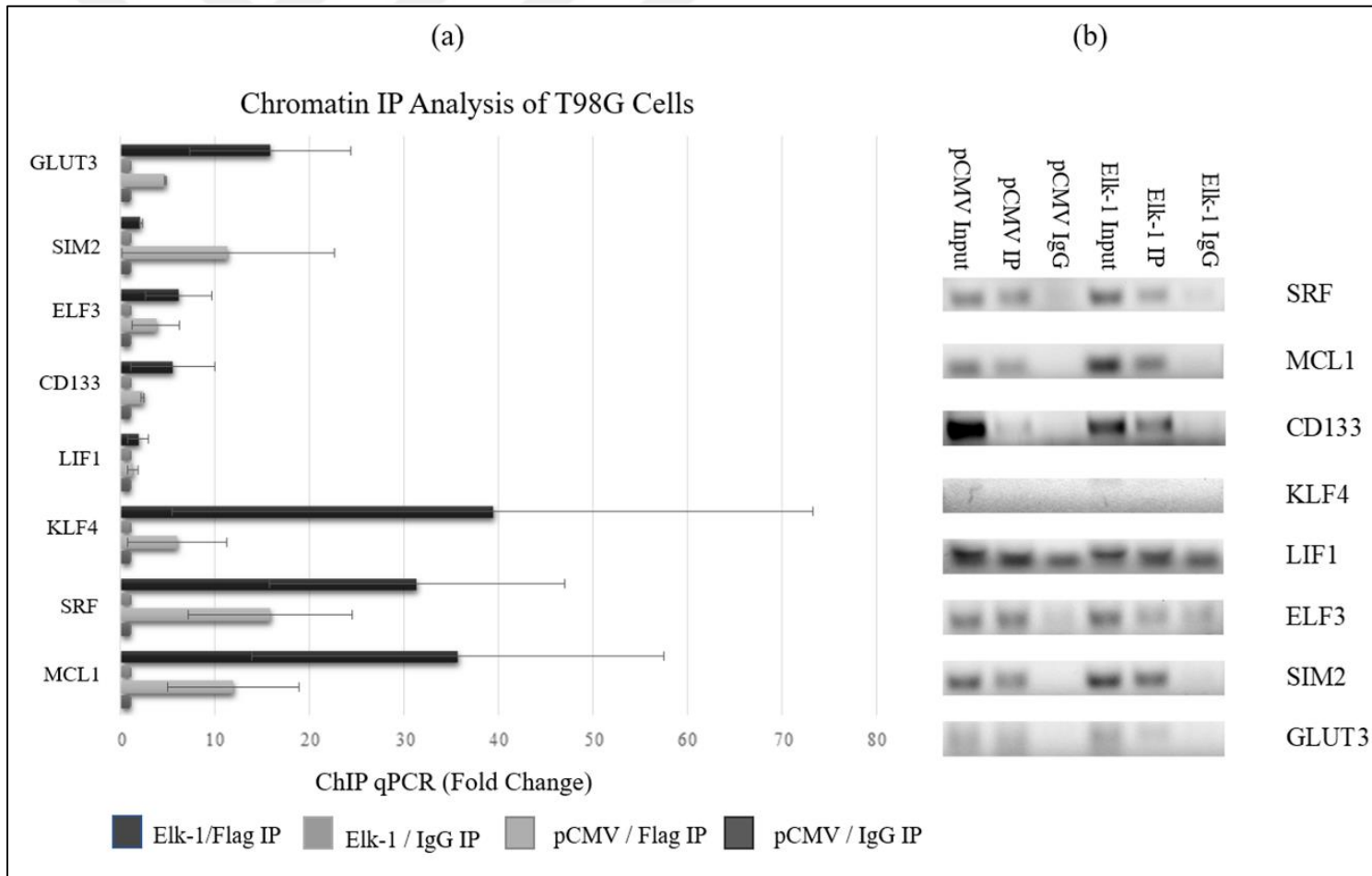


Figure 5.44. ChIP-qPCR results for the identification of Elk-1 binding sites on the target gene promoters in pCMV-transfected vs. Elk-1 over-expressing T98G glioblastoma cells, immunoprecipitated with either Flag antibody (Flag IP) or IgG (IgG IP). (a) ChIP-qPCR, (b) agarose gel electrophoresis.

When analyzing the ChIP results, it should be mentioned that with ChIP assay the direct binding of the TF to the chromatin cannot be demonstrated, but only the occupancy can be detected. That is an important limitation for ChIP assay. Occupancy means there exists an interaction between the protein and the chromatin; however, that interaction may be through a protein complex. As all the proteins crosslink to the chromatin at the same time, this may lead to discrepancies. To overcome this problem, electrophoretic mobility shift assay (EMSA) can be used, and the direct binding can be further characterized.

### 5.5. ROLE OF ELK-1 IN THE REGULATION OF EARLY NERVOUS SYSTEM DEVELOPMENT AND STEMNESS-RELATED GENES

In the microarray carried out within the scope of the COST project (211T167) in AxanLab, target genes for Elk-1 were determined in SH-SY5Y cell line. Genes were clustered and the ones that are related to early nervous system development and stemness were detected, and further expression analysis was performed with both neuroblastoma and glioblastoma cell lines.

Table 5.5. The expression of selected potential Elk-1 target genes after Elk1-VP16 over-expression in neuroblastoma cell lines

<b>Gene ID</b>	<b>SH-SY5Y (fold change)</b>	<b>SKNBE(2) (fold change)</b>	<b>Microarray Data (fold change)</b>
<i>LIFR</i>	-0,91	-1,52	-2,01
<i>GLUT3</i>	1,62	0,07	2,43
<i>RHO</i>	-3,56	-1,07	2,27
<i>TCF7L1</i>	0,79	0,56	2,34
<i>MEF2B</i>	0,09	-0,41	-2,74
<i>WNT3A</i>	-2,11	0,53	2,25
<i>NOTO</i>	-2,94	0,18	2,15
<i>IRAK3</i>	2,78	0,51	1,70
<i>FRZB</i>	1,21	-0,72	1,91
<i>RXRΒ</i>	1,01	0,66	5,95

<i>NODAL</i>	2,33	0,66	1,64
<i>PAX6</i>	-1,54	-0,28	2,61
<i>CREB3</i>	-0,01	N/A	-1,92
<i>SIX3</i>	-1,94	N/A	-5,72
<i>FGF11</i>	-0,23	N/A	-2,40
<i>FRAT1</i>	0,17	N/A	1,82
<i>GSK3B</i>	-0,22	N/A	-1,61
<i>BRACHYURY</i>	N/A	0,32	1,54
<i>ZIC1</i>	N/A	1,53	2,26

The differences in stemness gene expressions following Elk-1 over-expression in various cell lines cultured as monolayer were shown in Table 5.5 and Table 5.6. The results obtained with SH-SY5Y cell line were in parallel with the values obtained from the microarray analysis (especially in the genes related to pluripotency such as *SOX2*, *NANOG*, *POU5F1*, *RXRβ*, *GLUT3*, *TCF7L1*, *NODAL*, and *CREB3*). The *SOX2* gene exhibited similar behavior to Elk-1 in all cell types, while the *NANOG* and *POU5F1* genes showed an increase in Elk1-VP16 over-expression in SH-SY5Y and T98G cells, and a reduction with Elk-1 silencing. In SKNBE(2) and A172 cell lines, the profile was not consistent.

Table 5.6. The expression of selected potential Elk-1 target genes after Elk1-VP16 over-expression in glioblastoma cell lines

<b>Gene ID</b>	<b>T98G (fold change)</b>	<b>A172 (fold change)</b>	<b>Microarray Data (fold change)</b>
<i>LIFR</i>	-0,84	-0,08	-2,01
<i>GLUT3</i>	0,83	0,92	2,43
<i>CREM</i>	-0,91	1,40	-2,27
<i>CREB3</i>	0,83	0,46	-1,92
<i>ALS2</i>	-0,45	0,60	-6,06
<i>ARC</i>	0,44	1,67	-6,87
<i>RHO</i>	-2,26	N/A	2,27
<i>TCF7L1</i>	0,15	N/A	2,34

<i>MEF2B</i>	-1,19	N/A	-2,74
<i>WNT3A</i>	0,11	N/A	2,25
<i>NOTO</i>	-0,34	N/A	2,15
<i>IRAK3</i>	-0,46	N/A	1,70
<i>FRZB</i>	-0,86	N/A	1,91
<i>SIX3</i>	0,61	N/A	-5,72
<i>HES7</i>	0,68	N/A	-1,77
<i>FGF11</i>	N/A	0,28	-2,40
<i>GLI4</i>	N/A	0,695	-3,81
<i>NOTCH4</i>	N/A	3,56	3,39
<i>SOX10</i>	N/A	2,94	2,41
<i>MAPK6</i>	N/A	0,76	1,64
<i>SMAD6</i>	N/A	-0,29	-3,78

*RHO* and *LIFR* expressions decreased in all cell types with Elk1-VP16 over-expression, while *GLUT3* and *TCF7L1* increased; *PAX6* and *RXR*B only showed a significant reduction in SH-SY5Y and SKNBE(2) neuroblastoma cell lines. The expression of *ARC* increased significantly in A172 and T98G cells. Other than these genes (*IRAK3*, *MEF2B*, *WNT3A*, etc.) exhibited very different profiles according to the cell type. The results are summarized in Table 5.5, Table 5.6 and Figure 5.45.

Table 5.7. The expression of selected potential Elk-1 target genes after siElk-1 silencing in neuroblastoma cell lines

<b>Gene ID</b>	<b>SH-SY5Y (fold change)</b>	<b>SKNBE(2) (fold change)</b>	<b>Gene ID</b>	<b>SH-SY5Y (fold change)</b>	<b>SKNBE(2) (fold change)</b>
<i>LIFR</i>	-0,53	0,48	<i>RXR</i> B	0,45	0,31
<i>GLUT3</i>	-0,67	-0,46	<i>ZIC1</i>	N/A	1,07
<i>RHO</i>	-0,20	-0,30	<i>BRACHYURY</i>	N/A	-0,25
<i>TCF7L1</i>	-0,29	-0,25	<i>GSK3B</i>	-0,12	N/A
<i>MEF2B</i>	-0,19	-0,33	<i>FGF11</i>	0,48	N/A

<i>WNT3A</i>	0,86	-1,11	<i>SIX3</i>	1,56	N/A
<i>NOTO</i>	1,05	-0,08	<i>HES7</i>	0,12	N/A
<i>IRAK3</i>	-0,23	-0,81	<i>FRIT1</i>	-0,34	N/A
<i>FRZB</i>	-2,20	-1,34	<i>CREB3</i>	0,09	N/A
<i>NODAL</i>	-0,66	-0,26	<i>CREM</i>	-0,51	N/A
<i>PAX6</i>	1,18	-1,62			

Table 5.8. The expression of selected potential Elk-1 target genes after siElk-1 silencing in glioblastoma cell lines

<b>Gene ID</b>	<b>T98G (fold change)</b>	<b>A172 (fold change)</b>	<b>Gene ID</b>	<b>T98G (fold change)</b>	<b>A172 (fold change)</b>
<i>LIFR</i>	-0,12	-0,82	<i>WNT3A</i>	0,52	N/A
<i>GLUT3</i>	0,54	2,64	<i>TCF7L1</i>	0,14	N/A
<i>CREM</i>	-0,43	0,44	<i>MEF2B</i>	-1,57	N/A
<i>ARC</i>	-2,17	-0,06	<i>RHO</i>	-0,93	N/A
<i>CREB3</i>	-0,74	-0,67	<i>SMAD6</i>	N/A	-0,42
<i>ALS2</i>	-0,64	-1,44	<i>GLI4</i>	N/A	0,61
<i>NOTO</i>	-0,76	N/A	<i>NOTCH4</i>	N/A	7,16
<i>IRAK3</i>	-0,97	N/A	<i>SOX10</i>	N/A	5,83
<i>FRZB</i>	-0,18	N/A	<i>GLI4</i>	N/A	0,61
<i>HES7</i>	0,20	N/A	<i>FGF11</i>	N/A	-1,31
<i>SIX3</i>	0,41	N/A			

While the expression analysis of stemness genes in SH-SY5Y was parallel to the microarray data, diverse expression patterns for each gene were observed for other cell lines. This may be due to the complex control mechanism, dynamic regulation within different cell lines and combinatorial network between the genes of interest over the stemness genes (Table 5.9).



Table 5.9. The expression of pluripotency genes with (a) ELK-1 over-expression, (b) ELK-1 silencing

(a)					
ELK-1 Over-expression (fold change)					
Gene ID	SH-SY5Y	SKNBE(2)	T98G	A172	Microarray Data
<i>ELK1</i>	1,50	2,04	8,48	8,98	13,11
<i>SOX2</i>	1,54	0,41	0,37	-0,59	2,75
<i>NANOG</i>	1,96	-0,91	0,58	1,18	2,54
<i>POU5F1</i>	1,62	-1,20	0,56	0,32	3,68
(b)					
ELK-1 Silencing (fold change)					
Gene ID	SH-SY5Y	SKNBE(2)	T98G	A172	
<i>ELK1</i>	-0,54	-2,36	-0,60	-1,49	
<i>SOX2</i>	-0,84	-1,08	-0,56	-0,36	
<i>NANOG</i>	-0,99	4,85	-0,07	3,12	
<i>POU5F1</i>	-2,19	3,31	-0,67	1,06	

In SH-SY5Y cells; the expression of *SOX2*, *NANOG*, *POU5F1*, *GLUT3*, *TCF7L1*, *NODAL*, *IRAK3*, *FRZB*, *CREM* genes increased with Elk1-VP16 over-expression, whereas *NOTO*, *WNT3A*, *PAX6*, and *SIX3* genes were repressed in the presence of Elk1-VP16 and increased in siElk-1 silencing. Among these, *SOX2* showed an increase in the presence of Elk1-VP16 and its expression decreased with siElk-1 silencing in both SH-SY5Y and SKNBE(2) cells, while *NANOG* and *POU5F1* showed an opposite profile to SH-SY5Y in SKNBE(2) (these two genes have similarly increased in siElk-1 silencing in A172 cells, but repressed in T98G cells like in SH-SY5Y cells). *GLI4* and *ALS* genes increased in the presence of Elk1-VP16 in A172 cells and decreased with siElk-1 silencing (Table 5.7 and Table 5.8). The differences between the neuroblastoma and glioblastoma cell lines can be explained by the dynamics of the tumor formation, aggressiveness and relative proliferation pattern within those cells. The role of Elk-1 in each tumor type may be different, leading to the triggering of diverse genes. Even differences occur within same type of tumor cells.

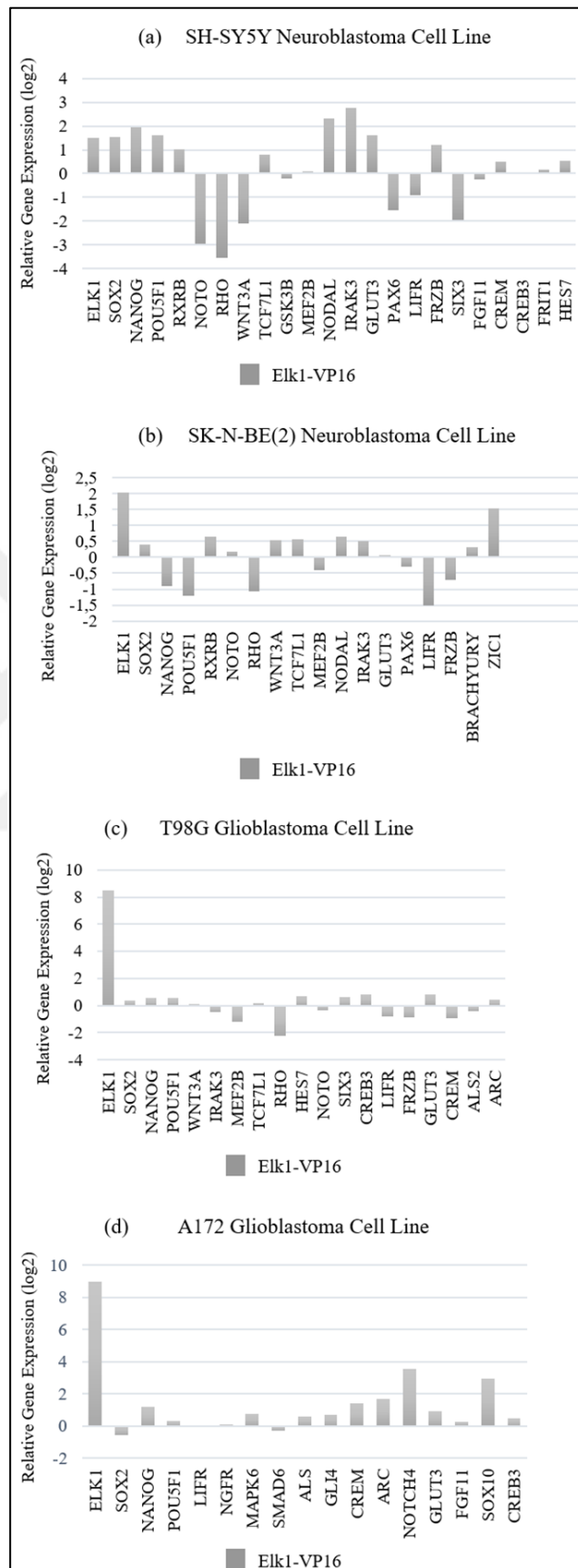


Figure 5.45. Expression profiles after over-expression with Elk1-VP16

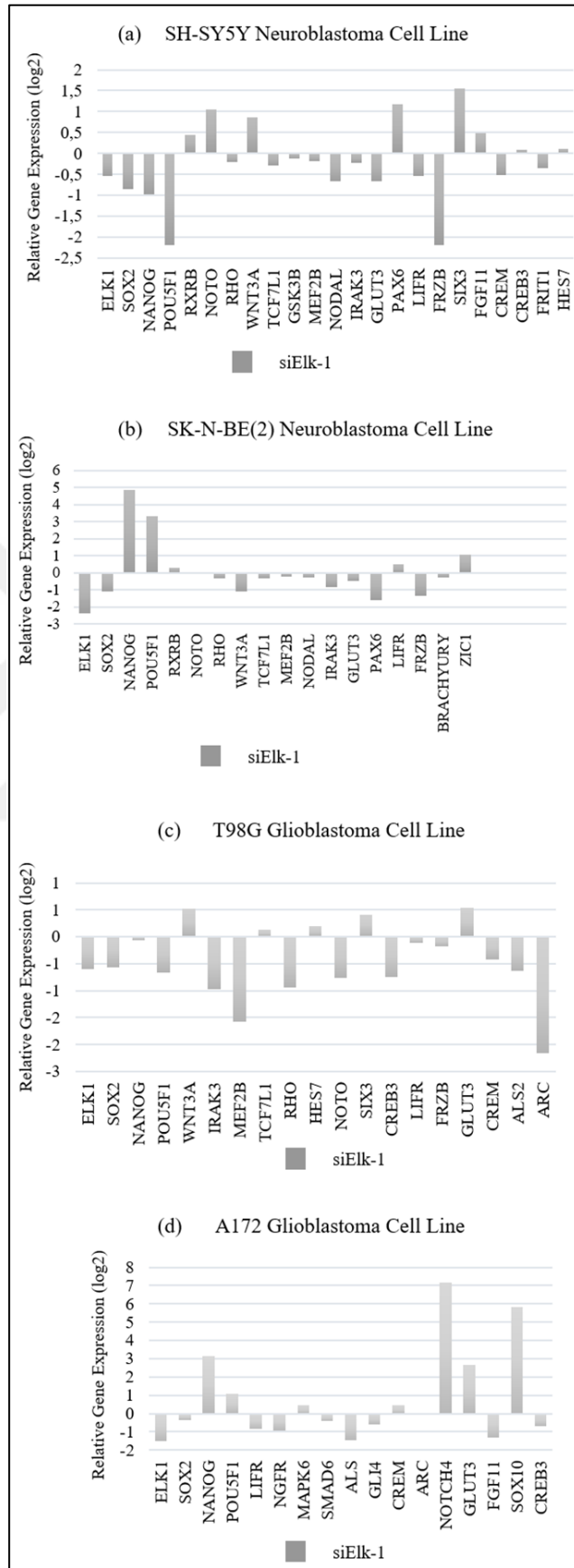


Figure 5.46. Expression profiles after silencing with siElk-1

## 5.6. CSC-RELATED SIGNALING PATHWAYS IN THE PRESENCE/ABSENCE OF ELK-1 IN CD133+ BTICS AND CD133- SPHEROIDS

The interplay between specific signal transduction pathways contributes to the behavior of CSCs. Determination of the CSC-associated pathways, the key members and the leading tumor phenotype can facilitate the detection of the effective therapeutic targets and the development of anti-cancer drugs.

The effect of Elk-1 over-expression and silencing on the expression of critical members of Wnt/  $\beta$ -catenin, Notch and Hedgehog pathways were evaluated. AXIN2, LGR5, GSK3 $\beta$ , and CTNNB1 ( $\beta$ -catenin) are the members of the Wnt/ $\beta$ -catenin pathway. When Elk-1 was over-expressed, AXIN2, LGR5, and CTNNB1 expressions increased with respect to control. However, the expression of CTNNB1 was significantly lower in CD133- Elk1-VP16 group than that of the CD133+ siElk-1 group.

When Wnt is absent, glycogen synthase kinase 3 (GSK3), Axin, casein kinase 1 (CK1) and adenomatous polyposis coli gene product (APC) forms a complex. Through the sequential phosphorylation of  $\beta$ -catenin by CK1 and GSK1,  $\beta$ -catenin is labeled for ubiquitinylation and eventually it is degraded [155]. That means, according to the results presented in Figure 5.47, the WNT signaling activity between the CD133- Elk1-VP16 and CD133+ siElk-1 groups are different. In CD133+ siElk-1 group of cells, the  $\beta$ -catenin was level significantly higher than that of the CD133- Elk1-VP16 group. When all three genes, namely AXIN2, GSK3 $\beta$  and CTNNB1 ( $\beta$ -catenin), are considered together, Wnt inactivation vs activation is seen, respectively.

LGR5 expression is important for the regulation of proliferation and/or survival of CSCs. While its knock-down leads to apoptotic cell-death, its over-expression supports oncogenesis. In neuroblastoma cells, LGR5 knock-down also leads to a reduction in phospho-MEK/ERK independent of  $\beta$ -catenin expression [156]. Also in Figure 5.47, the decrease in the LGR5 may be due to the silencing of Elk-1 in CD133+ siElk-1 group, independent of the increase in expression of  $\beta$ -catenin while with the over-expression of Elk-1 in the CD133- Elk1-VP16 group, its level increased with respect to the control group.

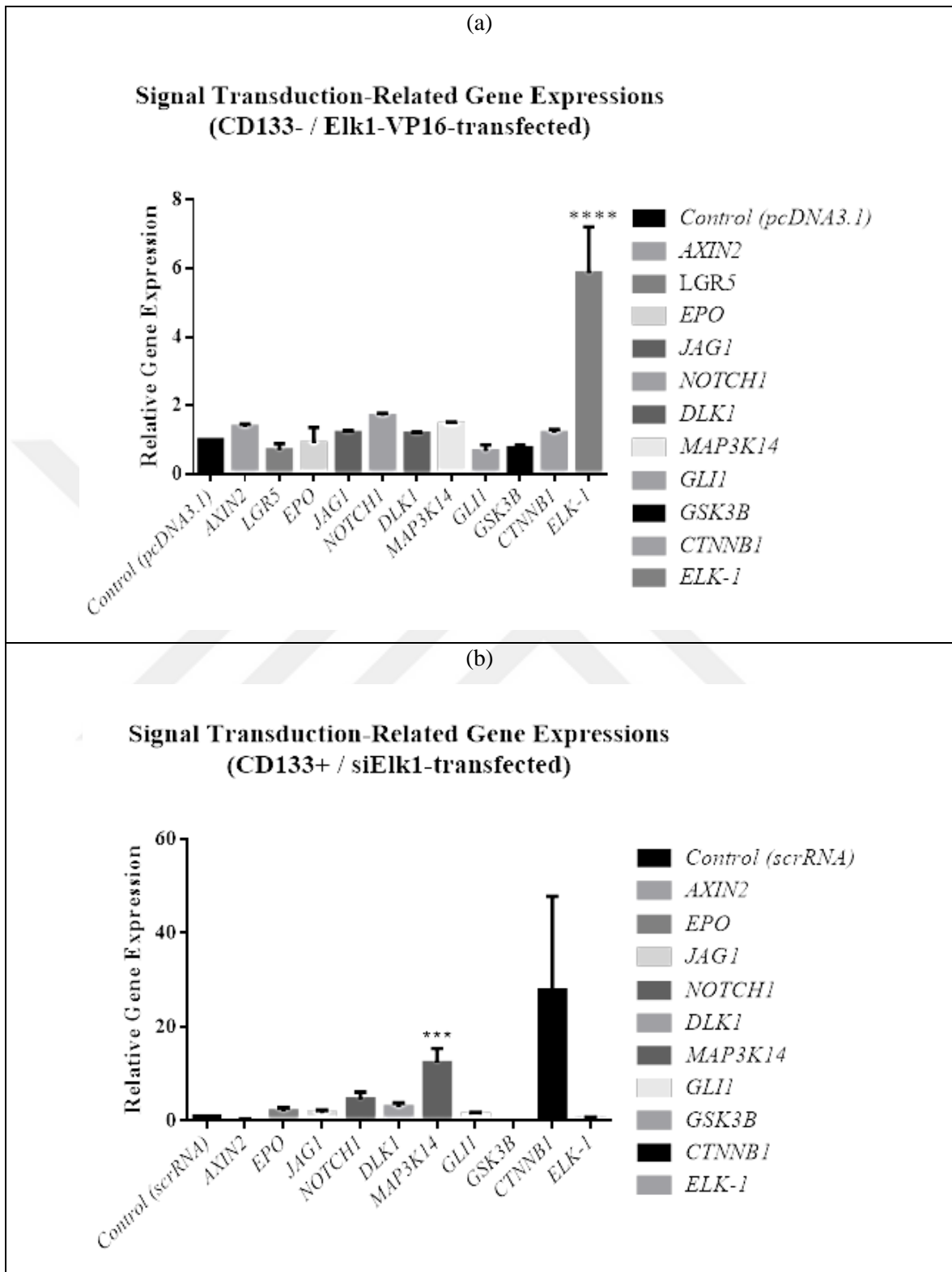


Figure 5.47. Gene expression of signaling pathway members. (One-way ANOVA, \*\*\* $p < 0.001$ , \*\*\*\* $p < 0.0001$ )

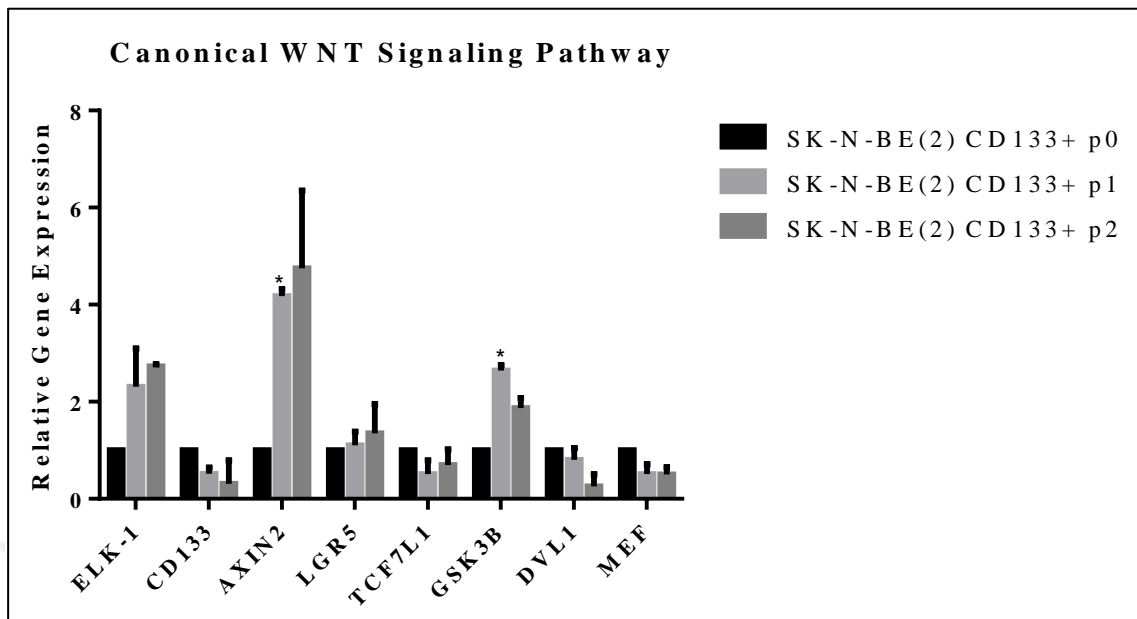


Figure 5.48. The change in the expression of canonical WNT signaling pathway members with respect to increasing passage number in SKNBE(2) CD133+ BTICs (One-way ANOVA, \* $p < 0.05$ )

In Figure 5.47, the decrease in Elk-1 expression led to an increase in the expression of Notch pathway members including *JAG1*, *NOTCH1*, and *DLK1*. The Hedgehog pathway member *GLII* and JAK/STAT pathway member *EPO* expressions changed in reverse pattern with Elk-1 expression in both CD133+ siElk-1 and CD133- Elk1-VP16 cells.

According to Figure 5.48, with increasing passage number, Elk-1 expression increased while CD133 expression decreased. This also supports the results obtained from Figure 5.47 in that, increasing Elk-1 expression also increases the expression of *LGR5*, *GSK3B*, and *AXIN2* genes.

## 6. CONCLUSION

It is clear that CSCs are crucial for the growth and maintenance of the tumors. It is still not possible to eliminate these cells even through cytotoxic or cytostatic treatments. CSCs play critical roles in the resistance and metastasis of the tumors. In theory, the evacuation of the CSC subpopulation can open the way for the control and cure of cancer. However, there are many challenges as the control of CSC biology has many parameters including the interaction between signaling pathways, microenvironmental effects, molecular markers, genetic and epigenetic factors, dimensions of self-renewal and heterogeneity within and between the spheroids. Unfortunately, all these parameters are also factual for healthy cells within the body, and this makes the problem more complicated. Stem cell formation and proliferation is also necessary for any organism starting from the early development to adulthood.

In recent years, contradictory findings have been identified in the biological function of Elk-1. A group of researchers – including AxanLab- reported that Elk-1 has a protective effect on many cells including neurons and it is over-expressed in brain tumors. On the other hand, Eberwine *et al.* showed that when Elk-1 mRNA was photo-transfected to dendrites, it caused neuronal apoptosis. They also demonstrated that the T417-phosphorylated form of Elk-1 was present in the inclusion bodies in neurodegenerative diseases and that Elk-1 was a pro-apoptotic protein [22, 38, 41, 157, 158]. Similarly, Elk-1 has been reported to interact with  $\alpha$ -synuclein bodies [41]. Although Eberwine and his team interpreted such results as Elk-1 leading to apoptosis in neurons, the other view is that Elk-1 plays a compensatory neuroprotective role in neurodegenerative diseases [33, 157]. In parallel, again the Eberwine group showed that the P-T417-Elk-1 phosphoprotein was found not only in neurodegeneration but also in colon adenocarcinomas. However, it has not been clarified how the same protein is associated with both neurodegeneration and tumorigenesis [159].

In order to clarify this issue, in previous projects that have been completed in our laboratory, full genome microarray studies were performed in Elk1-VP16-transfected SH-SY5Y neuroblastoma cells, and many Elk-1 target genes were determined. Some of them are related to survival/apoptosis/proliferation, stemness as well as hypoxic regulation in neurons.

Pluripotency genes contribute to the development of tumors, in particular to the renewal of the tumorspheres. According to the hypothesis, the silencing of Elk-1 in CD133+ BTICs would reduce proliferation, whereas in CD133- spheroids Elk-1 over-expression would bring cell proliferation to CD133+ BTICs level. With XTT analysis, the effect of Elk-1 over-expression and silencing on the proliferation of CD133+ BTICs or CD133- spheroids, respectively, were evaluated both in normoxia and hypoxia. The self-renewal potential of Elk-1-expressed cells was also assessed with soft agar assay. There was a subtle change in the colony numbers to support the idea that Elk-1 is effective. These were not enough to make inferences about the role of Elk-1 on CSCs.

To carry on, gene expressions and protein levels of the selected subset of genes were analyzed, their potential physical interactions on chromatin were checked, and promoter activities were determined. Elk-1 mRNA was detected at significantly higher levels in the CSC-enriched population of cancer cells, in other words, CD133+ BTICs and tumorspheres. In addition to detecting Elk-1 in the CSC population, a mutual relationship was found between the expression of Elk-1 and some key CSC markers and traits. Elk-1 over-expressed cells showed higher level of stemness genes (NANOG, SOX2, POU5F1), whereas RNA interference of Elk-1 led to a decrease in also the expression of these genes.

The results of luciferase were found to be more consistent with microarray findings compared to the qPCR results. The SOX2 promoter activity increased in all of the cells with Elk-1 over-expression, but no significant changes were observed with Elk-1 silencing in most cells. The NANOG promoter activity in SH-SY5Y, SKNBE(2), T98G and U87MG cells increased with Elk-1 overexpression and showed a decrease with Elk-1 silencing. There was no significant change in the Elk-1 silencing in A172 alone.

In the CSC model, it is stated that the tumors are not a homogeneous population and that cancer-initiating cells are only a sub-population [70]. The population obtained by CSC markers mentioned in this theory corresponds to the cells obtained by isolation of CD133+ cells from the total cells. Targeting of CSCs may lead to the differentiation or degeneration of tumor cells [160]. Therefore, CD133 + cells should be targeted in modern cancer therapy.

Cancer cells stabilize HIF-1 $\alpha$  similarly to hypoxia signals [161]. HIFs may be regulated through the RAS-MAPK signal pathway. It was demonstrated that RAS/ERK signal pathway could stimulate CD133 transcription [162]. Another study showed that in glioma



cells, phosphatidylinositol 3-kinase (PI3K-Akt) or ERK1/2 signaling pathways could decrease the increase in CD133 expression due to hypoxia [140]. HIF1 $\alpha$  promoter has MAPK binding domain and can bind to ERK2. In other words, the RAS/ERK signaling pathway can transcribe CD133 through HIF1 $\alpha$  and/or HIF1 $\beta$  independent of hypoxia [142]. This also supports our results in the regulation of hypoxia signaling pathways with Elk1-VP16-transfected cells found in microarray analysis. However, the potential Elk-1 potential target genes Notch, Wnt, and Hedgehog signaling pathway elements were not found to be Elk-1 targets as a result of our analysis.

Mouse fibroblast cells have been reprogrammed to activate the signaling pathways triggered by M9. The TFs role in the downstream of these pathways such as Elk-1 and GLI-2 bind and activate the endogenous neural genes to trigger neurogenesis. In addition to this, via SOX-2 triggering they are capable of forming NSCs [163]. The expression of *GLUT3* gene increases in all the analyzed cell lines within this thesis even in the normoxic state following Elk-1 over-expression. Glioblastoma and neuroblastoma cells provide energy by utilizing the selective aerobic glycolysis path known as the “Warburg effect,” as in other cancer cells. The reason why the tumor cells prefer to be found in hypoxic microenvironments with reduced energy production in this sense is not fully known. Glioblastoma stem cells; unlike the non-stem GBM cells and healthy cells, achieve their glucose uptake by the expression of specialized glucose transporter isoform type 3 (GLUT3). *GLUT3* expression is provided in a few different cell types, including ESCs [164]. When non-stem cell GBM cells are cultured in low glucose, by de-differentiation, they gain stem cell characteristics and embryonic stem cell factor NANOG is expressed. The correlation between NANOG and survival has been shown [165]. The positive correlation between POU5F1 and *GLUT3* in human ESCs has also been reported in the literature [166]. In our results, the relationship between *NANOG*, *POU5F1* and *GLUT3* expression levels related to Elk-1 level is consistent with the literature.

In BTICs, it has been demonstrated that the methylation status of SOX2 is correlated with both the expression of SOX2 and the aggressiveness of the GBM [167]. In another study, the fold level of increase of SOX2 in GMBs was correlated with CSC proliferation. They used CD133 $\pm$  fractions of DAOY human primary medulloblastoma cells and showed that high elevation (two-three folds increase) of SOX2 levels would lead the cells to exit from cell cycle and decrease in cell proliferation [168].

There have been reports indicating the conversion of CD133<sup>-</sup> cells to CD133<sup>+</sup> cells in culture conditions. CD133, being a multifaceted protein, reacts to changes within the culture rapidly, especially when conditions are not favorable. This may explain the conflicting results both within this thesis and the previously reported results.

There exists an interplay between autophagy and apoptosis within the cells. It is shown that the level of autophagy is regulated in the CD133<sup>+</sup> population of hepatocellular carcinoma CSCs with the upregulation of CD133 expression and the deprivation of oxygen as well as nutrient [169] The location of CD133 changes from the membrane to the cytoplasm. Similarly, in CD133<sup>+</sup> glioma cells, the CD133 co-localized with autophagy-related proteins while the levels of apoptosis decreased when the glucose level was lowered [170]. On the other hand, we have shown that Elk-1 transcription factor is associated with CD133 promoter *in vivo* through CHIP analysis. As being on the opposite site of the Eberwine group which assume Elk-1 as a pro-apoptotic gene, these data may ignite the question: May Elk-1 take the role as a supporter for the survival of BTICs in CD133<sup>+</sup> cells through the regulation of CD133 and balancing autophagy, not apoptosis?

CSCs should not be ignored in modern cancer research and applications. It will be a giant leap when the mechanism of the CSC maintenance is understood. With this thesis, the effects of Elk-1 transcription factor on brain tumor initiator cells and hypoxic microenvironment on pluripotency and neurogenesis were investigated in different cell lines. Elk-1 may have a potential role in the maintenance of the stemness properties of CSCs.

Further studies will be required in the future for more detailed analysis. Lineage tracing with high-throughput assays, comprehensive studies with single cells and organoids are state-of-the-art strategies. The fusion of basic science with these techniques can pave the way for the improvement of therapeutic approaches.

## REFERENCES

1. Singh SK, Hawkins C, Clarke ID, Squire JA, Bayani J, Hide T, et al. Identification of human brain tumour initiating cells. *Nature*. 2004;432(7015):396-401.
2. Findlay VJ, LaRue AC, Turner DP, Watson PM, Watson DK. Understanding the role of ets-mediated gene regulation in complex biological processes. *Advances in Cancer Research*. 2013;119(215):1-61.
3. Gutierrez-Hartmann A, Duval DL, Bradford AP. Ets transcription factors in endocrine systems. *Trends in Endocrinology and Metabolism*. 2007;18(4):150-8.
4. Hollenhorst PC, Jones DA, Graves BJ. Expression profiles frame the promoter specificity dilemma of the ets family of transcription factors. *Nucleic Acids Research*. 2004;32(18):5693-702.
5. Graves BJ, Petersen JM. Specificity within the ets family of transcription factors. *Advances in Cancer Research*. 1998;75(17):1-55.
6. Donaldson LW, Petersen JM, Graves BJ, McIntosh LP. Solution structure of the ets domain from murine ets-1: A winged helix-turn-helix DNA binding motif. *EMBO Journal*. 1996;15(1):125-34.
7. Szymczynska BR, Arrowsmith CH. DNA binding specificity studies of four ets proteins support an indirect read-out mechanism of protein-DNA recognition. *Journal of Biological Chemistry*. 2000;275(37):28363-70.
8. Brown LA, Amores A, Schilling TF, Jowett T, Baert JL, de Launoit Y, et al. Molecular characterization of the zebrafish *pea3* ets-domain transcription factor. *Oncogene*. 1998;17(1):93-104.
9. Maroulakou IG, Bowe DB. Expression and function of ets transcription factors in mammalian development: A regulatory network. *Oncogene*. 2000;19(55):6432-42.
10. Charlot C, Dubois-Pot H, Serchov T, Tournette Y, Wasylyk B. A review of post-translational modifications and subcellular localization of ets transcription factors:

- Possible connection with cancer and involvement in the hypoxic response. *Methods in Molecular Biology*. 2010;647(12):3-30.
11. Hipkind RA, Rao VN, Mueller CG, Reddy ES, Nordheim A. Ets-related protein elk-1 is homologous to the c-fos regulatory factor p62tcf. *Nature*. 1991;354(6354):531-4.
  12. Dalton S, Treisman R. Characterization of sap-1, a protein recruited by serum response factor to the c-fos serum response element. *Cell*. 1992;68(3):597-612.
  13. Giovane A, Pintzas A, Maira SM, Sobieszczuk P, Wasyluk B. Net, a new ets transcription factor that is activated by ras. *Genes and Development*. 1994;8(13):1502-13.
  14. Lopez M, Oettgen P, Akbarali Y, Dendorfer U, Libermann TA. Erp, a new member of the ets transcription factor/oncoprotein family: Cloning, characterization, and differential expression during b-lymphocyte development. *Molecular and Cellular Biology*. 1994;14(5):3292-309.
  15. Nozaki M, Onishi Y, Kanno N, Ono Y, Fujimura Y. Molecular cloning of elk-3, a new member of the ets family expressed during mouse embryogenesis and analysis of its transcriptional repression activity. *DNA and Cell Biology*. 1996;15(10):855-62.
  16. Stinson J, Inoue T, Yates P, Clancy A, Norton JD, Sharrocks AD. Regulation of tcf ets-domain transcription factors by helix-loop-helix motifs. *Nucleic Acids Research*. 2003;31(16):4717-28.
  17. Sharrocks AD. Complexities in ets-domain transcription factor function and regulation: Lessons from the tcf (ternary complex factor) subfamily. The colworth medal lecture. *Biochemical Society Transactions*. 2002;30(2):1-9.
  18. Janknecht R, Ernst WH, Pingoud V, Nordheim A. Activation of ternary complex factor elk-1 by map kinases. *EMBO Journal*. 1993;12(13):5097-104.
  19. Yang SH, Vickers E, Brehm A, Kouzarides T, Sharrocks AD. Temporal recruitment of the msin3a-histone deacetylase corepressor complex to the ets domain transcription factor elk-1. *Molecular and Cellular Biology*. 2001;21(8):2802-14.

20. Buchwalter G, Gross C, Wasylyk B. Ets ternary complex transcription factors. *Gene*. 2004;324(107):1-14.
21. Sgambato V, Vanhoutte P, Pages C, Rogard M, Hipskind R, Besson MJ, et al. In vivo expression and regulation of elk-1, a target of the extracellular-regulated kinase signaling pathway, in the adult rat brain. *Journal of Neuroscience*. 1998;18(1):214-26.
22. Barrett LE, Van Bockstaele EJ, Sul JY, Takano H, Haydon PG, Eberwine JH. Elk-1 associates with the mitochondrial permeability transition pore complex in neurons. *Proceedings of the National Academy of Sciences of the United States of America*. 2006;103(13):5155-60.
23. Besnard A, Galan-Rodriguez B, Vanhoutte P, Caboche J. Elk-1 a transcription factor with multiple facets in the brain. *Frontiers in Neuroscience*. 2011;5(12):35-42.
24. Yates PR, Atherton GT, Deed RW, Norton JD, Sharrocks AD. Id helix-loop-helix proteins inhibit nucleoprotein complex formation by the tcf ets-domain transcription factors. *EMBO Journal*. 1999;18(4):968-76.
25. Sharrocks AD. Erk2/p42 map kinase stimulates both autonomous and srf-dependent DNA binding by elk-1. *FEBS Letters*. 1995;368(1):77-80.
26. Barsyte-Lovejoy D, Galanis A, Sharrocks AD. Specificity determinants in mapk signaling to transcription factors. *Journal of Biological Chemistry*. 2002;277(12):9896-903.
27. Yang SH, Bumpass DC, Perkins ND, Sharrocks AD. The ets domain transcription factor elk-1 contains a novel class of repression domain. *Molecular and Cellular Biology*. 2002;22(14):5036-46.
28. Hollenhorst PC, McIntosh LP, Graves BJ. Genomic and biochemical insights into the specificity of ets transcription factors. *Annual Review of Biochemistry*. 2011;80(25):437-71.
29. Tootle TL, Rebay I. Post-translational modifications influence transcription factor activity: A view from the ets superfamily. *Bioessays*. 2005;27(3):285-98.

30. Salinas S, Briancon-Marjollet A, Bossis G, Lopez MA, Piechaczyk M, Jariel-Encontre I, et al. Sumoylation regulates nucleo-cytoplasmic shuttling of elk-1. *Journal of Cell Biology*. 2004;165(6):767-73.
31. Yang SH, Sharrocks AD. Convergence of the sumo and mapk pathways on the ets-domain transcription factor elk-1. *Biochemical Society Symposia*. 2006(73):121-9.
32. Lavaur J, Bernard F, Trifilieff P, Pascoli V, Kappes V, Pages C, et al. A tat-def-elk-1 peptide regulates the cytonuclear trafficking of elk-1 and controls cytoskeleton dynamics. *Journal of Neuroscience*. 2007;27(52):14448-58.
33. Demir O, Aysit N, Onder Z, Turkel N, Ozturk G, Sharrocks AD, et al. Ets-domain transcription factor elk-1 mediates neuronal survival: Smn as a potential target. *Biochimica et Biophysica Acta*. 2011;1812(6):652-62.
34. Demir O, Korulu S, Yildiz A, Karabay A, Kurnaz IA. Elk-1 interacts with neuronal microtubules and relocalizes to the nucleus upon phosphorylation. *Molecular and Cellular Neurosciences*. 2009;40(1):111-9.
35. Hunter DR, Haworth RA, Southard JH. Relationship between configuration, function, and permeability in calcium-treated mitochondria. *Journal of Biological Chemistry*. 1976;251(16):5069-77.
36. Halestrap AP, McStay GP, Clarke SJ. The permeability transition pore complex: Another view. *Biochimie*. 2002;84(2-3):153-66.
37. Vickers ER, Kasza A, Kurnaz IA, Seifert A, Zeef LA, O'Donnell A, et al. Ternary complex factor-serum response factor complex-regulated gene activity is required for cellular proliferation and inhibition of apoptotic cell death. *Molecular and Cellular Biology*. 2004;24(23):10340-51.
38. Demir O, Kurnaz IA. Wildtype elk-1, but not a sumoylation mutant, represses egr-1 expression in sh-sy5y neuroblastomas. *Neuroscience Letters*. 2008;437(1):20-4.
39. Tong L, Balazs R, Thornton PL, Cotman CW. Beta-amyloid peptide at sublethal concentrations downregulates brain-derived neurotrophic factor functions in cultured cortical neurons. *Journal of Neuroscience*. 2004;24(30):6799-809.

40. Roze E, Betuing S, Deyts C, Marcon E, Brami-Cherrier K, Pages C, et al. Mitogen- and stress-activated protein kinase-1 deficiency is involved in expanded-huntingtin-induced transcriptional dysregulation and striatal death. *FASEB Journal*. 2008;22(4):1083-93.
41. Iwata A, Miura S, Kanazawa I, Sawada M, Nukina N. Alpha-synuclein forms a complex with transcription factor elk-1. *Journal of Neurochemistry*. 2001;77(1):239-52.
42. Spradling A, Drummond-Barbosa D, Kai T. Stem cells find their niche. *Nature*. 2001;414(6859):98-104.
43. Lanza RP. *Essentials of stem cell biology*. San Diego: Elsevier Academic; 2006.
44. de Wert G, Mummery C. Human embryonic stem cells: Research, ethics and policy. *Human Reproduction*. 2003;18(4):672-82.
45. Biteau B, Hochmuth CE, Jasper H. Maintaining tissue homeostasis: Dynamic control of somatic stem cell activity. *Cell Stem Cell*. 2011;9(5):402-11.
46. Takahashi K, Yamanaka S. Induction of pluripotent stem cells from mouse embryonic and adult fibroblast cultures by defined factors. *Cell*. 2006;126(4):663-76.
47. Reardon S, Cyranoski D. Japan stem-cell trial stirs envy. *Nature*. 2014;513(7518):287-88.
48. Martin U. Therapeutic application of pluripotent stem cells: Challenges and risks. *Frontiers Medicine*. 2017;4(4):229-30.
49. Kempf H, Olmer R, Kropp C, Ruckert M, Jara-Avaca M, Robles-Diaz D, et al. Controlling expansion and cardiomyogenic differentiation of human pluripotent stem cells in scalable suspension culture. *Stem Cell Reports*. 2014;3(6):1132-46.
50. Kim K, Doi A, Wen B, Ng K, Zhao R, Cahan P, et al. Epigenetic memory in induced pluripotent stem cells. *Nature*. 2010;467(7313):285-90.

51. Altman J. Autoradiographic study of degenerative and regenerative proliferation of neuroglia cells with tritiated thymidine. *Experimental Neurology*. 1962;5(22):302-18.
52. Eriksson PS, Perfilieva E, Bjork-Eriksson T, Alborn AM, Nordborg C, Peterson DA, et al. Neurogenesis in the adult human hippocampus. *Nature Medicine*. 1998;4(11):1313-7.
53. Reynolds BA, Weiss S. Generation of neurons and astrocytes from isolated cells of the adult mammalian central nervous system. *Science*. 1992;255(5052):1707-10.
54. Morshead CM, Reynolds BA, Craig CG, McBurney MW, Staines WA, Morassutti D, et al. Neural stem cells in the adult mammalian forebrain: A relatively quiescent subpopulation of subependymal cells. *Neuron*. 1994;13(5):1071-82.
55. Gage FH. Mammalian neural stem cells. *Science*. 2000;287(5457):1433-8.
56. Menn B, Garcia-Verdugo JM, Yaschine C, Gonzalez-Perez O, Rowitch D, Alvarez-Buylla A. Origin of oligodendrocytes in the subventricular zone of the adult brain. *Journal of Neuroscience*. 2006;26(30):7907-18.
57. Riquelme PA, Drapeau E, Doetsch F. Brain micro-ecologies: Neural stem cell niches in the adult mammalian brain. *Philosophical Transactions of the Royal Society of London Series B: Biological Sciences*. 2008;363(1489):123-37.
58. Ge S, Goh EL, Sailor KA, Kitabatake Y, Ming GL, Song H. Gaba regulates synaptic integration of newly generated neurons in the adult brain. *Nature*. 2006;439(7076):589-93.
59. Ulloa-Montoya F, Kidder BL, Pauwelyn KA, Chase LG, Luttun A, Crabbe A, et al. Comparative transcriptome analysis of embryonic and adult stem cells with extended and limited differentiation capacity. *Genome Biology*. 2007;8(8):163-64.
60. Pesce M, Scholer HR. Oct-4: Gatekeeper in the beginnings of mammalian development. *Stem Cells*. 2001;19(4):271-8.



61. Masui S, Nakatake Y, Toyooka Y, Shimosato D, Yagi R, Takahashi K, et al. Pluripotency governed by *sox2* via regulation of *oct3/4* expression in mouse embryonic stem cells. *Nature Cell Biology*. 2007;9(6):625-35.
62. Loh YH, Wu Q, Chew JL, Vega VB, Zhang W, Chen X, et al. The *oct4* and *nanog* transcription network regulates pluripotency in mouse embryonic stem cells. *Nature Genetics*. 2006;38(4):431-40.
63. Wu T, Wang H, He J, Kang L, Jiang Y, Liu J, et al. Reprogramming of trophoblast stem cells into pluripotent stem cells by *oct4*. *Stem Cells*. 2011;29(5):755-63.
64. Niwa H, Miyazaki J, Smith AG. Quantitative expression of *oct-3/4* defines differentiation, dedifferentiation or self-renewal of es cells. *Nature Genetics*. 2000;24(4):372-6.
65. Stefanovic S, Puceat M. Oct-3/4: Not just a gatekeeper of pluripotency for embryonic stem cell, a cell fate instructor through a gene dosage effect. *Cell Cycle*. 2007;6(1):8-10.
66. Kopp JL, Ormsbee BD, Desler M, Rizzino A. Small increases in the level of *sox2* trigger the differentiation of mouse embryonic stem cells. *Stem Cells*. 2008;26(4):903-11.
67. Kim JB, Zaehres H, Wu G, Gentile L, Ko K, Sebastiano V, et al. Pluripotent stem cells induced from adult neural stem cells by reprogramming with two factors. *Nature*. 2008;454(7204):646-50.
68. Mitsui K, Tokuzawa Y, Itoh H, Segawa K, Murakami M, Takahashi K, et al. The homeoprotein *nanog* is required for maintenance of pluripotency in mouse epiblast and es cells. *Cell*. 2003;113(5):631-42.
69. Rosen JM, Jordan CT. The increasing complexity of the cancer stem cell paradigm. *Science*. 2009;324(5935):1670-3.
70. Reya T, Morrison SJ, Clarke MF, Weissman IL. Stem cells, cancer, and cancer stem cells. *Nature*. 2001;414(6859):105-11.

71. Pierce GB, Speers WC. Tumors as caricatures of the process of tissue renewal: Prospects for therapy by directing differentiation. *Cancer Research*. 1988;48(8):1996-2004.
72. Clarke MF, Fuller M. Stem cells and cancer: Two faces of eve. *Cell*. 2006;124(6):1111-5.
73. Nguyen LV, Vanner R, Dirks P, Eaves CJ. Cancer stem cells: An evolving concept. *Nature Reviews: Cancer*. 2012;12(2):133-43.
74. Takahashi S, Aiba K, Ito Y, Hatake K, Nakane M, Kobayashi T, et al. Pilot study of mdrl gene transfer into hematopoietic stem cells and chemoprotection in metastatic breast cancer patients. *Cancer Science*. 2007;98(10):1609-16.
75. Goldie JH, Coldman AJ. The genetic origin of drug resistance in neoplasms: Implications for systemic therapy. *Cancer Research*. 1984;44(9):3643-53.
76. Choi SA, Lee JY, Phi JH, Wang KC, Park CK, Park SH, et al. Identification of brain tumour initiating cells using the stem cell marker aldehyde dehydrogenase. *European Journal of Cancer*. 2014;50(1):137-49.
77. Vidal SJ, Rodriguez-Bravo V, Galsky M, Cordon-Cardo C, Domingo-Domenech J. Targeting cancer stem cells to suppress acquired chemotherapy resistance. *Oncogene*. 2014;33(36):4451-63.
78. Topcul M, Cetin I, Ozlem Kulusayin Ozar M. The effects of anastrozole on the proliferation of fm3a cells. *Journal of BUON*. 2013;18(4):874-8.
79. Bapat SA. Human ovarian cancer stem cells. *Reproduction*. 2010;140(1):33-41.
80. Otvos B, Silver DJ, Mulkearns-Hubert EE, Alvarado AG, Turaga SM, Sorensen MD, et al. Cancer stem cell-secreted macrophage migration inhibitory factor stimulates myeloid derived suppressor cell function and facilitates glioblastoma immune evasion. *Stem Cells*. 2016;34(8):2026-39.

81. Borah A, Raveendran S, Rochani A, Maekawa T, Kumar DS. Targeting self-renewal pathways in cancer stem cells: Clinical implications for cancer therapy. *Oncogenesis*. 2015;4(5):177-86.
82. Vermeulen L, De Sousa EMF, van der Heijden M, Cameron K, de Jong JH, Borovski T, et al. Wnt activity defines colon cancer stem cells and is regulated by the microenvironment. *Nature Cell Biology*. 2010;12(5):468-76.
83. Brabletz T, Jung A, Reu S, Porzner M, Hlubek F, Kunz-Schughart LA, et al. Variable beta-catenin expression in colorectal cancers indicates tumor progression driven by the tumor environment. *Proceedings of the National Academy of Sciences of the United States of America*. 2001;98(18):10356-61.
84. Beachy PA, Karhadkar SS, Berman DM. Tissue repair and stem cell renewal in carcinogenesis. *Nature*. 2004;432(7015):324-31.
85. Jiang J, Hui CC. Hedgehog signaling in development and cancer. *Developmental Cell*. 2008;15(6):801-12.
86. Yauch RL, Gould SE, Scales SJ, Tang T, Tian H, Ahn CP, et al. A paracrine requirement for hedgehog signalling in cancer. *Nature*. 2008;455(7211):406-10.
87. Venkatesh V, Nataraj R, Thangaraj GS, Karthikeyan M, Gnanasekaran A, Kaginelli SB, et al. Targeting notch signalling pathway of cancer stem cells. *Stem Cell Investigation* 2018;5(12):5-16.
88. Takam Kanga P, Dal Collo G, Midolo M, Adamo A, Delfino P, Mercuri A, et al. Inhibition of notch signaling enhances chemosensitivity in b-cell precursor acute lymphoblastic leukemia. *Cancer Research*. 2019;79(3):639-49.
89. Hu Y, Chen Y, Douglas L, Li S. Beta-catenin is essential for survival of leukemic stem cells insensitive to kinase inhibition in mice with bcr-abl-induced chronic myeloid leukemia. *Leukemia*. 2009;23(1):109-16.
90. Dierks C, Beigi R, Guo GR, Zirlik K, Stegert MR, Manley P, et al. Expansion of bcr-abl-positive leukemic stem cells is dependent on hedgehog pathway activation. *Cancer Cell*. 2008;14(3):238-49.

91. Pastrana E, Silva-Vargas V, Doetsch F. Eyes wide open: A critical review of sphere-formation as an assay for stem cells. *Cell Stem Cell*. 2011;8(5):486-98.
92. Bottenstein JE. *Neural stem cells: Development and transplantation*; New York: Springer; 2003.
93. Clark DW, Palle K. Aldehyde dehydrogenases in cancer stem cells: Potential as therapeutic targets. *Annals of Translational Medicine*. 2016;4(24):518.
94. Boesch M, Zeimet AG, Reimer D, Schmidt S, Gastl G, Parson W, et al. The side population of ovarian cancer cells defines a heterogeneous compartment exhibiting stem cell characteristics. *Oncotarget*. 2014;5(16):7027-39.
95. Singh SK, Clarke ID, Terasaki M, Bonn VE, Hawkins C, Squire J, et al. Identification of a cancer stem cell in human brain tumors. *Cancer Research*. 2003;63(18):5821-8.
96. Maric D, Barker JL. Neural stem cells redefined: A facts perspective. *Molecular Neurobiology*. 2004;30(1):49-76.
97. Shmelkov SV, St Clair R, Lyden D, Rafii S. Ac133/cd133/prominin-1. *International Journal of Biochemistry and Cell Biology*. 2005;37(4):715-9.
98. Corti S, Nizzardo M, Nardini M, Donadoni C, Locatelli F, Papadimitriou D, et al. Isolation and characterization of murine neural stem/progenitor cells based on prominin-1 expression. *Experimental Neurology*. 2007;205(2):547-62.
99. Irollo E, Pirozzi G. Cd133: To be or not to be, is this the real question? *American Journal of Translational Research*. 2013;5(6):563-81.
100. Pollard SM, Conti L, Sun Y, Goffredo D, Smith A. Adherent neural stem (ns) cells from fetal and adult forebrain. *Cerebral Cortex*. 2006;16(1):112-20.
101. Jensen JB, Parmar M. Strengths and limitations of the neurosphere culture system. *Molecular Neurobiology*. 2006;34(3):153-61.
102. Tsai RY, McKay RD. Cell contact regulates fate choice by cortical stem cells. *Journal of Neuroscience*. 2000;20(10):3725-35.

103. Jiang J, Yang W, Huang P, Bu X, Zhang N, Li J. Increased phosphorylation of ets-like transcription factor-1 in neurons of hypoxic preconditioned mice. *Neurochemical Research*. 2009;34(8):1443-50.
104. Muller JM, Krauss B, Kaltschmidt C, Baeuerle PA, Rupec RA. Hypoxia induces c-fos transcription via a mitogen-activated protein kinase-dependent pathway. *Journal of Biological Chemistry*. 1997;272(37):23435-9.
105. Forristal CE, Wright KL, Hanley NA, Oreffo RO, Houghton FD. Hypoxia inducible factors regulate pluripotency and proliferation in human embryonic stem cells cultured at reduced oxygen tensions. *Reproduction*. 2010;139(1):85-97.
106. Aprelikova O, Wood M, Tackett S, Chandramouli GV, Barrett JC. Role of ets transcription factors in the hypoxia-inducible factor-2 target gene selection. *Cancer Research*. 2006;66(11):5641-7.
107. Mannello F, Medda V, Tonti GA. Hypoxia and neural stem cells: From invertebrates to brain cancer stem cells. *International Journal of Developmental Biology*. 2011;55(6):569-81.
108. Neumann B, Walter T, Heriche JK, Bulkescher J, Erfle H, Conrad C, et al. Phenotypic profiling of the human genome by time-lapse microscopy reveals cell division genes. *Nature*. 2010;464(7289):721-7.
109. Goke J, Chan YS, Yan J, Vingron M, Ng HH. Genome-wide kinase-chromatin interactions reveal the regulatory network of erk signaling in human embryonic stem cells. *Molecular Cell*. 2013;50(6):844-55.
110. Kuroda Y, Wakao S, Kitada M, Murakami T, Nojima M, Dezawa M. Isolation, culture and evaluation of multilineage-differentiating stress-enduring (muse) cells. *Nature Protocols*. 2013;8(7):1391-415.
111. Walton DK, Gendel SM, Atherly AG. DNA sequence and shuttle vector construction of plasmid pgl3 from plectonema boryanum pcc 6306. *Nucleic Acids Research*. 1993;21(3):746.

112. Zobalova R, McDermott L, Stantic M, Prokopova K, Dong LF, Neuzil J. Cd133-positive cells are resistant to trail due to up-regulation of flip. *Biochemical and Biophysical Research Communications*. 2008;373(4):567-71.
113. He WY, Rao ZC, Zhou DH, Zheng SC, Xu WH, Feng QL. Analysis of expressed sequence tags and characterization of a novel gene, simg7, in the midgut of the common cutworm, *spodoptera litura*. *PloS One*. 2012;7(3):33621-34.
114. Bidlingmaier S, Zhu X, Liu B. The utility and limitations of glycosylated human cd133 epitopes in defining cancer stem cells. *Journal of Molecular Medicine*. 2008;86(9):1025-32.
115. Blazek ER, Foutch JL, Maki G. Daoy medulloblastoma cells that express cd133 are radioresistant relative to cd133- cells, and the cd133+ sector is enlarged by hypoxia. *International Journal of Radiation Oncology, Biology, Physics*. 2007;67(1):1-5.
116. Kelly SE, Di Benedetto A, Greco A, Howard CM, Sollars VE, Primerano DA, et al. Rapid selection and proliferation of cd133+ cells from cancer cell lines: Chemotherapeutic implications. *PloS One*. 2010;5(4):10035-42.
117. Mahller YY, Williams JP, Baird WH, Mitton B, Grossheim J, Saeki Y, et al. Neuroblastoma cell lines contain pluripotent tumor initiating cells that are susceptible to a targeted oncolytic virus. *PloS One*. 2009;4(1):4235-47.
118. Guo W, Patzlaff NE, Jobe EM, Zhao X. Isolation of multipotent neural stem or progenitor cells from both the dentate gyrus and subventricular zone of a single adult mouse. *Nature Protocols*. 2012;7(11):2005-12.
119. Todaro M, Alea MP, Di Stefano AB, Cammareri P, Vermeulen L, Iovino F, et al. Colon cancer stem cells dictate tumor growth and resist cell death by production of interleukin-4. *Cell Stem Cell*. 2007;1(4):389-402.
120. Lee J, Kotliarova S, Kotliarov Y, Li A, Su Q, Donin NM, et al. Tumor stem cells derived from glioblastomas cultured in bfgf and egf more closely mirror the phenotype and genotype of primary tumors than do serum-cultured cell lines. *Cancer Cell*. 2006;9(5):391-403.

121. Soeda A, Inagaki A, Oka N, Ikegame Y, Aoki H, Yoshimura S, et al. Epidermal growth factor plays a crucial role in mitogenic regulation of human brain tumor stem cells. *Journal of Biological Chemistry*. 2008;283(16):10958-66.
122. Valent P, Bonnet D, De Maria R, Lapidot T, Copland M, Melo JV, et al. Cancer stem cell definitions and terminology: The devil is in the details. *Nature Reviews: Cancer*. 2012;12(11):767-75.
123. Cieciura SJ, Marcus PI, Puck TT. Clonal growth in vitro of epithelial cells from normal human tissues. *Journal of Experimental Medicine*. 1956;104(4):615-28.
124. Bonnet D, Dick JE. Human acute myeloid leukemia is organized as a hierarchy that originates from a primitive hematopoietic cell. *Nature Medicine*. 1997;3(7):730-7.
125. Taddei ML, Giannoni E, Fiaschi T, Chiarugi P. Anoikis: An emerging hallmark in health and diseases. *Journal of Pathology*. 2012;226(2):380-93.
126. Lendahl U, Zimmerman LB, McKay RD. Cns stem cells express a new class of intermediate filament protein. *Cell*. 1990;60(4):585-95.
127. Zhang M, Song T, Yang L, Chen R, Wu L, Yang Z, et al. Nestin and cd133: Valuable stem cell-specific markers for determining clinical outcome of glioma patients. *Journal of Experimental and Clinical Cancer Research*. 2008;27(8):85-97.
128. Feng JM, Miao ZH, Jiang Y, Chen Y, Li JX, Tong LJ, et al. Characterization of the conversion between cd133+ and cd133- cells in colon cancer sw620 cell line. *Cancer Biology and Therapy*. 2012;13(14):1396-406.
129. Chaffer CL, Brueckmann I, Scheel C, Kaestli AJ, Wiggins PA, Rodrigues LO, et al. Normal and neoplastic nonstem cells can spontaneously convert to a stem-like state. *Proceedings of the National Academy of Sciences of the United States of America*. 2011;108(19):7950-5.
130. Gupta PB, Fillmore CM, Jiang G, Shapira SD, Tao K, Kuperwasser C, et al. Stochastic state transitions give rise to phenotypic equilibrium in populations of cancer cells. *Cell*. 2011;146(4):633-44.

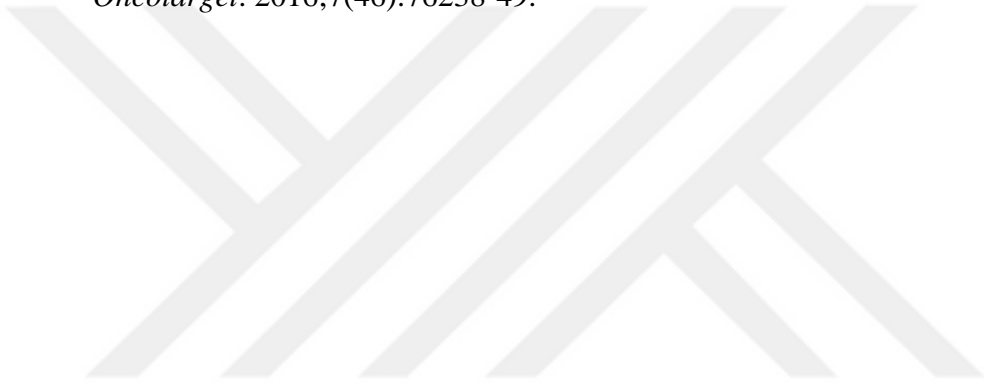
131. Dong L, Qi N, Ge RM, Cao CL, Lan F, Shen L. Overexpression of cd133 promotes the phosphorylation of erk in u87mg human glioblastoma cells. *Neuroscience Letters*. 2010;484(3):210-4.
132. Hayashi Y, Caboni L, Das D, Yumoto F, Clayton T, Deller MC, et al. Structure-based discovery of nanog variant with enhanced properties to promote self-renewal and reprogramming of pluripotent stem cells. *Proceedings of the National Academy of Sciences of the United States of America*. 2015;112(15):4666-71.
133. Ma X, Chen H, Chen L. A dual role of erk signaling in embryonic stem cells. *Experimental Hematology*. 2016;44(3):151-6.
134. Zhang K, Zhou Y, Zhao T, Wu L, Huang X, Wu K, et al. Reduced cerebral oxygen content in the dg and svz in situ promotes neurogenesis in the adult rat brain in vivo. *PloS One*. 2015;10(10):140035-54.
135. Jez M, Rozman P, Ivanovic Z, Bas T. Concise review: The role of oxygen in hematopoietic stem cell physiology. *Journal of Cellular Physiology*. 2015;230(9):1999-2005.
136. Jiang YZ, Liu YR, Xu XE, Jin X, Hu X, Yu KD, et al. Transcriptome analysis of triple-negative breast cancer reveals an integrated mrna-lncrna signature with predictive and prognostic value. *Cancer Research*. 2016;76(8):2105-14.
137. Krock BL, Skuli N, Simon MC. Hypoxia-induced angiogenesis: Good and evil. *Genes and Cancer*. 2011;2(12):1117-33.
138. Dews M, Homayouni A, Yu D, Murphy D, Sevignani C, Wentzel E, et al. Augmentation of tumor angiogenesis by a myc-activated microrna cluster. *Nature Genetics*. 2006;38(9):1060-5.
139. Chamorro-Jorganes A, Lee MY, Araldi E, Landskroner-Eiger S, Fernandez-Fuertes M, Sahraei M, et al. Vegf-induced expression of mir-17-92 cluster in endothelial cells is mediated by erk/elk1 activation and regulates angiogenesis. *Circulation Research*. 2016;118(1):38-47.



140. Soeda A, Park M, Lee D, Mintz A, Androutsellis-Theotokis A, McKay RD, et al. Hypoxia promotes expansion of the cd133-positive glioma stem cells through activation of hif-1alpha. *Oncogene*. 2009;28(45):3949-59.
141. Yoshida Y, Takahashi K, Okita K, Ichisaka T, Yamanaka S. Hypoxia enhances the generation of induced pluripotent stem cells. *Cell Stem Cell*. 2009;5(3):237-41.
142. Ohnishi S, Maehara O, Nakagawa K, Kameya A, Otaki K, Fujita H, et al. Hypoxia-inducible factors activate cd133 promoter through ets family transcription factors. *PloS One*. 2013;8(6):66255-78.
143. Matsumoto K, Arao T, Tanaka K, Kaneda H, Kudo K, Fujita Y, et al. Mtor signal and hypoxia-inducible factor-1 alpha regulate cd133 expression in cancer cells. *Cancer Research*. 2009;69(18):7160-4.
144. Wuebben EL, Rizzino A. The dark side of sox2: Cancer - a comprehensive overview. *Oncotarget*. 2017;8(27):44917-43.
145. Platet N, Liu SY, Atifi ME, Oliver L, Vallette FM, Berger F, et al. Influence of oxygen tension on cd133 phenotype in human glioma cell cultures. *Cancer Letters*. 2007;258(2):286-90.
146. Mut M, Lule S, Demir O, Kurnaz IA, Vural I. Both mitogen-activated protein kinase (mapk)/extracellular-signal-regulated kinases (erk) 1/2 and phosphatidylinositide-3-oh kinase (pi3k)/akt pathways regulate activation of e-twenty-six (ets)-like transcription factor 1 (elk-1) in u138 glioblastoma cells. *International Journal of Biochemistry and Cell Biology*. 2012;44(2):302-10.
147. Ma X, Wang B, Wang X, Luo Y, Fan W. Nanogp8 is the key regulator of stemness, emt, wnt pathway, chemoresistance, and other malignant phenotypes in gastric cancer cells. *PloS One*. 2018;13(4):192436-54.
148. Wasyluk C, Maira SM, Sobieszczuk P, Wasyluk B. Reversion of ras transformed cells by ets transdominant mutants. *Oncogene*. 1994;9(12):3665-73.
149. Semenza GL. Targeting hif-1 for cancer therapy. *Nature Reviews: Cancer*. 2003;3(10):721-32.

150. Kasza A, O'Donnell A, Gascoigne K, Zeef LA, Hayes A, Sharrocks AD. The ets domain transcription factor elk-1 regulates the expression of its partner protein, srf. *Journal of Biological Chemistry*. 2005;280(2):1149-55.
151. Hall J, Guo G, Wray J, Eyres I, Nichols J, Grotewold L, et al. Oct4 and lif/stat3 additively induce kruppel factors to sustain embryonic stem cell self-renewal. *Cell Stem Cell*. 2009;5(6):597-609.
152. Niwa H, Ogawa K, Shimosato D, Adachi K. A parallel circuit of lif signalling pathways maintains pluripotency of mouse es cells. *Nature*. 2009;460(7251):118-22.
153. Letourneau A, Cobellis G, Fort A, Santoni F, Garieri M, Falconnet E, et al. Hsa21 single-minded 2 (sim2) binding sites co-localize with super-enhancers and pioneer transcription factors in pluripotent mouse es cells. *PloS One*. 2015;10(5):126475-93.
154. Flavahan WA, Wu Q, Hitomi M, Rahim N, Kim Y, Sloan AE, et al. Brain tumor initiating cells adapt to restricted nutrition through preferential glucose uptake. *Nature Neuroscience*. 2013;16(10):1373-82.
155. He XC, Zhang J, Tong WG, Tawfik O, Ross J, Scoville DH, et al. Bmp signaling inhibits intestinal stem cell self-renewal through suppression of wnt-beta-catenin signaling. *Nature Genetics*. 2004;36(10):1117-21.
156. Vieira GC, Chockalingam S, Melegh Z, Greenhough A, Malik S, Szemes M, et al. Lgr5 regulates pro-survival mek/erk and proliferative wnt/beta-catenin signalling in neuroblastoma. *Oncotarget*. 2015;6(37):40053-67.
157. Anglada-Huguet M, Giralt A, Perez-Navarro E, Alberch J, Xifro X. Activation of elk-1 participates as a neuroprotective compensatory mechanism in models of huntington's disease. *Journal of Neurochemistry*. 2012;121(4):639-48.
158. Sharma A, Callahan LM, Sul JY, Kim TK, Barrett L, Kim M, et al. A neurotoxic phosphoform of elk-1 associates with inclusions from multiple neurodegenerative diseases. *PloS One*. 2010;5(2):9002-23.
159. Morris JF, Sul JY, Kim MS, Klein-Szanto AJ, Schochet T, Rustgi A, et al. Elk-1 phosphorylated at threonine-417 is present in diverse cancers and correlates with

- differentiation grade of colonic adenocarcinoma. *Human Pathology*. 2013;44(5):766-76.
160. Kamijo T. Role of stemness-related molecules in neuroblastoma. *Pediatric Research*. 2012;71(4):511-5.
161. Masson N, Ratcliffe PJ. Hypoxia signaling pathways in cancer metabolism: The importance of co-selecting interconnected physiological pathways. *Cancer Metabolism*. 2014;2(1):3-21.
162. Tabu K, Kimura T, Sasai K, Wang L, Bizen N, Nishihara H, et al. Analysis of an alternative human cd133 promoter reveals the implication of ras/erk pathway in tumor stem-like hallmarks. *Molecular Cancer*. 2010;9(12):39-52.
163. Zhang L, Gong Y, Zhao X, Zhou H. Comparative study between hypoxia and hypoxia mimetic agents on osteogenesis of bone marrow mesenchymal stem cells in mouse. *Chinese Journal of Reparative and Reconstructive Surgery*. 2016;30(7):903-8.
164. Hubert CG, Rivera M, Spangler LC, Wu Q, Mack SC, Prager BC, et al. A three-dimensional organoid culture system derived from human glioblastomas recapitulates the hypoxic gradients and cancer stem cell heterogeneity of tumors found in vivo. *Cancer Research*. 2016;76(8):2465-77.
165. Yamaguchi S, Kurimoto K, Yabuta Y, Sasaki H, Nakatsuji N, Saitou M, et al. Conditional knockdown of nanog induces apoptotic cell death in mouse migrating primordial germ cells. *Development*. 2009;136(23):4011-20.
166. Christensen DR, Calder PC, Houghton FD. Glut3 and pkm2 regulate oct4 expression and support the hypoxic culture of human embryonic stem cells. *Scientific Reports*. 2015;5(19):17500-24.
167. Alonso MM, Diez-Valle R, Manterola L, Rubio A, Liu D, Cortes-Santiago N, et al. Genetic and epigenetic modifications of sox2 contribute to the invasive phenotype of malignant gliomas. *PloS One*. 2011;6(11):26740-63.

168. Cox JL, Wilder PJ, Desler M, Rizzino A. Elevating sox2 levels deleteriously affects the growth of medulloblastoma and glioblastoma cells. *PLoS One*. 2012;7(8):44087-99.
  169. Chen H, Luo Z, Dong L, Tan Y, Yang J, Feng G, et al. Cd133/prominin-1-mediated autophagy and glucose uptake beneficial for hepatoma cell survival. *PLoS One*. 2013;8(2):56878-97.
  170. Sun H, Zhang M, Cheng K, Li P, Han S, Li R, et al. Resistance of glioma cells to nutrient-deprived microenvironment can be enhanced by cd133-mediated autophagy. *Oncotarget*. 2016;7(46):76238-49.
- 

## APPENDIX A: PROMOTER ANALYSIS

Human_Sox2-Colony_12_Reverse SOX2_promoter_from_TRED_[-70	ATAGGTACCGGGGAGTGATTATGGGAAGAAGGTTAGTAAGGAACAAAACA -----GGGGAGTGATTATGGGAAGAAGGTTAGTAAGGAACAAAACA *****
Human_Sox2-Colony_12_Reverse SOX2_promoter_from_TRED_[-70	ATGCACCGTTTTGTAAAGATAATAAATGGAACGTGGCTGGTAGATACTAT ATGCACCGTTTTGTAAAGATAATAAATGGAACGTGGCTGGTAGATACTAT *****
Human_Sox2-Colony_12_Reverse SOX2_promoter_from_TRED_[-70	TCAGTACATTTTCTTAGGGTGAGTAAGGGTAGACCAGGGGAGGAGGGGGC TCAGTACATTTTCTTAGGGTGAGTAAGGGTAGACCAGGGGAGGAGGGGGC *****
Human_Sox2-Colony_12_Reverse SOX2_promoter_from_TRED_[-70	GGAGAGAGTGTTACAGAAGAAAGAAAATAAGTAACCCTGATGGTTTAAGC GGAGAGAGTGTTACAGAAGAAAGAAAATAAGTAACCCTGATGGTTTAAGC *****
Human_Sox2-Colony_12_Reverse SOX2_promoter_from_TRED_[-70	CCTTTATAAAAAAGAAATGGCATCAGGTTTTTTTTCTTTATCCCCCCC CCTTTATAAAAAAGAAATGGCATCAGGTTTTTTTTCTTTATCCCCCCC *****
Human_Sox2-Colony_12_Reverse SOX2_promoter_from_TRED_[-70	ACCCACCCTTTGTAGTCAAGTGCATTTTAGCCACAAAGATCCCAACAAG ACCCACCCTTTGTAGTCAAGTGCATTTTAGCCACAAAGATCCCAACAAG *****
Human_Sox2-Colony_12_Reverse SOX2_promoter_from_TRED_[-70	AGAGTGGAAAGGAAACTTAGACGAGGCTTTGTTTGACTCCGTGTAGCGACA AGAGTGGAAAGGAAACTTAGACGAGGCTTTGTTTGACTCCGTGTAGCGACA *****
Human_Sox2-Colony_12_Reverse SOX2_promoter_from_TRED_[-70	ACAAGAGAAACAAAACCTACCTATTTGTAACGGACGTGCTGCCATTGCCCT ACAAGAGAAACAAAACCTACCTATTTGTAACGGACGTGCTGCCATTGCCCT *****
Human_Sox2-Colony_12_Reverse SOX2_promoter_from_TRED_[-70	CCGCATTGAGCGCCTACCTATTGAAATCTTTACGTCGGGACAATGGGAGA CCGCATTGAGCGCCTACCTATTGAAATCTTTACGTCGGGACAATGGGAGA *****
Human_Sox2-Colony_12_Reverse SOX2_promoter_from_TRED_[-70	GCGGCTAAAATTACCCTCTTGGGTCCTGGGC6GGCAAGATTCTGAGCCC GCGGCTAAAATTACCCTCTTGGGTCCTGGGC6GGCAAGATTCTGAGCCC *****

Figure A.1. Sequencing results for cloned *Homo sapiens* SOX2 promoter sequence

Human_Pou5f1-Colon_10_Revers POU5F1_promoter_from_TRED_[-	GAGTTTGGGGCAACTGGTTGGAGGGAAGGTGAAGTCAATGATGCTCTTG GAGTTTGGGGCAACTGGTTGGAGGGAAGGTGAAGTCAATGATGCTCTTG *****
Human_Pou5f1-Colon_10_Revers POU5F1_promoter_from_TRED_[-	ATTTAATCCCACATCATGTATCACTTTTCTTAAATAAAGAAGCCTGG ATTTAATCCCACATCATGTATCACTTTTCTTAAATAAAGAAGCTTGG *****
Human_Pou5f1-Colon_10_Revers POU5F1_promoter_from_TRED_[-	GACACAGTAGATAGACACACTTATCTTGGTTTGTCTTCAGTACTGAGG GACACAGTAGATAGACACACTTATCTTGGTTTGTCTTCAGTACTGAGG *****
Human_Pou5f1-Colon_10_Revers POU5F1_promoter_from_TRED_[-	TGGGGATGGGAATATCCAATGCTCATACCCAAGTGACCCTGAAACTAAGG TGGGGATGGGAATATCCAATGCTCATACCCAAGTGACCCTGAAACTAAGG *****
Human_Pou5f1-Colon_10_Revers POU5F1_promoter_from_TRED_[-	TGCCATTTACACTCCTTAAGGTCACACAACATCAGAGGGAGAGCTGGGAT TGCCATTTACACTCCTTAAGGTCACACAACATCAGAGGGAGAGCTGGGAT *****
Human_Pou5f1-Colon_10_Revers POU5F1_promoter_from_TRED_[-	TGCAGCCAAGTTTATTTGTACAGGGCCCTGTGATAGGCTAGTCCCAAAA TGCAGCCAAGTTTATTTGTACAGGGCCCTGTGATAGGCTAGTCCCAAAA *****
Human_Pou5f1-Colon_10_Revers POU5F1_promoter_from_TRED_[-	GCCTGTGATGCAAGAACTTTTGCCCATAGACTCAGTCACCATGTAGCTGT GCCTGTGATGCAAGAACTTTTGCCCATAGACTCAGTCACCATGTAGCTGT *****
Human_Pou5f1-Colon_10_Revers POU5F1_promoter_from_TRED_[-	TACCTGT-CAGAGCTGGCTTTTGTCTTCCCC-CCCACCC----- TACCTGTTCAGAGCTGGCTTTTGTCTTCCCCACCTACTCTGGAATTCTT *****

Figure A.2. Sequencing results for cloned *Homo sapiens* *POU5F1* promoter sequence

161021-044_K19_19ACBAB000-23 TRED_Human_Nanog_Promoter_Se	CCCCCTTTTTTTTTGAGACGTAGTCCCGCTCTGTTGCCAGGCTGGAG CCCCCTTTTTTTTTGAGACGTAGTCCCGCTCTGTTGCCAGGCTGGAG *****
161021-044_K19_19ACBAB000-23 TRED_Human_Nanog_Promoter_Se	TACAGTGGCGGATATCGGCTCACACAACCTCTGCCTCCAGGTTCAAG TACAGTGGCGGATATCGGCTCACACAACCTCTGCCTCCAGGTTCAAG *****
161021-044_K19_19ACBAB000-23 TRED_Human_Nanog_Promoter_Se	GGATTCTCCCGCTCAGCTTCCAGAGTAGCTGGGACTACAGACCCACC GGATTCTCCCGCTCAGCTTCCAGAGTAGCTGGGACTACAGACCCACC *****
161021-044_K19_19ACBAB000-23 TRED_Human_Nanog_Promoter_Se	TTTCTAATTTTTAAAAATATTAAAGTTTATCCCATTCCTGTTGAACCA TTTCTAATTTTTAAAAATATTAAAGTTTATCCCATTCCTGTTGAACCA *****
161021-044_K19_19ACBAB000-23 TRED_Human_Nanog_Promoter_Se	TATTCTGATTTAAAAGTTGAAAACGTGGTGAACCTAGAAGTATTTGTTG TATTCTGATTTAAAAGTTGAAAACGTGGTGAACCTAGAAGTATTTGTTG *****
161021-044_K19_19ACBAB000-23 TRED_Human_Nanog_Promoter_Se	CTGGGTTTGTCTCAGGTTCTGTTGCTCGGTTTCTAGTCCCCACCTAG CTGGGTTTGTCTCAGGTTCTGTTGCTCGGTTTCTAGTCCCCACCTAG *****
161021-044_K19_19ACBAB000-23 TRED_Human_Nanog_Promoter_Se	TCTGGGTTACTCTGCAGCTACTTTGCATTACAATGGCCTTGGTGAGACT TCTGGGTTACTCTGCAGCTACTTTGCATTACAATGGCCTTGGTGAGACT *****
161021-044_K19_19ACBAB000-23 TRED_Human_Nanog_Promoter_Se	GGTAGACGGGATTAACGTAGAATTACAAGGGTGGGTCAGTAGGGGGTGT GGTAGACGGGATTAACGTAGAATTACAAGGGTGGGTCAGTAGGGGGTGT *****

Figure A.3. Sequencing results for cloned *Homo sapiens* *NANOG* promoter sequence



161021-044_K19_19ACBAB000-23 TRED_Human_Nanog_Promoter_Se	TTTCTTAATTTTAAAAATATAAAGTTTTATCCCATTCCTGTTGAACCA TTTCTTAATTTTAAAAATATAAAGTTTTATCCCATTCCTGTTGAACCA *****
161021-044_K19_19ACBAB000-23 TRED_Human_Nanog_Promoter_Se	TATTCCTGATTAAAAAGTTGGAAACGTGGTGAACCTAGAAGTATTTGTTG TATTCCTGATTAAAAAGTTGGAAACGTGGTGAACCTAGAAGTATTTGTTG *****
161021-044_K19_19ACBAB000-23 TRED_Human_Nanog_Promoter_Se	CTGGGTTGTCTTCAGGTTCTGTGTCGGTTTTCTAGTTCGCCACCTAG CTGGGTTGTCTTCAGGTTCTGTGTCGGTTTTCTAGTTCGCCACCTAG *****
161021-044_K19_19ACBAB000-23 TRED_Human_Nanog_Promoter_Se	TCTGGGTTACTCTGCAGCTACTTTTGCAATACAATGGCCTTGGTGAGACT TCTGGGTTACTCTGCAGCTACTTTTGCAATACAATGGCCTTGGTGAGACT *****
161021-044_K19_19ACBAB000-23 TRED_Human_Nanog_Promoter_Se	GGTAGACGGGATTAAGTGAAGTACACAAGGGTGGGTGAGTGGGGGTG GGTAGACGGGATTAAGTGAAGTACACAAGGGTGGGTGAGTGGGGGTG *****
161021-044_K19_19ACBAB000-23 TRED_Human_Nanog_Promoter_Se	GCCCGCCAGGAGGGGTGGGTCTAAGGTGATAGAGCCTTCATTATAAATCT GCCCGCCAGGAGGGGTGGGTCTAAGGTGATAGAGCCTTCATTATAAATCT *****
161021-044_K19_19ACBAB000-23 TRED_Human_Nanog_Promoter_Se	AGAGACTCCAGGATTTAACGTTCTGCTGGACTGAGCTGGTGCCTCATG AGAGACTCCAGGATTTAACGTTCTGCTGGACTGAGCTGGTGCCTCATG *****
161021-044_K19_19ACBAB000-23 TRED_Human_Nanog_Promoter_Se	TTATTATGCAGGCAACTCACTTTATCCCAATTTCTTGATACTTTCTCTC TTATTATGCAGGCAACTCACTTTATCCCAATTTCTTGATACTTTCTCTC *****
161021-044_K19_19ACBAB000-23 TRED_Human_Nanog_Promoter_Se	TGGAGGTCCTATTTCTCAACATCTCCAGAAAAGCTTAAAGCTGCCTT TGGAGGTCCTATTTCTCAACATCTCCAGAAAAGCTTAAAGCTGCCTT *****
161021-044_K19_19ACBAB000-23 TRED_Human_Nanog_Promoter_Se	AACCTTTTTTCCAGTCCACCTCTTAAATTTTTTCCTCCT-----TA AACCTTTTTTCCAGTCCACCTCTTAAATTTTTTCCTCCTCTTCTCTATA

Figure A.4. Sequencing results for cloned *Homo sapiens* *NANOGE* promoter sequence

161021-044_M21_19ACBAB000-32 TRED_Human_Pou5f1_Promoter_S	A-----TAGGTACCCAGGCTATGGGAGCCCTCACTTCACTGCCTG GGCCCCATTTGGTACCCAGGCTATGGGAGCCCTCACTTCACTGCCTG * *****
161021-044_M21_19ACBAB000-32 TRED_Human_Pou5f1_Promoter_S	TACTCCTCGGTCCTTTCCCTG-----CCTTTCCCCCTGTCTCTGT TACTCCTCGGTCCTTTCCCTGAGGGGGAAGCCTTTCCCCCTGTCTCTGT *****
161021-044_M21_19ACBAB000-32 TRED_Human_Pou5f1_Promoter_S	CACCACTCTGGGCTCTCCCATGCATTCAAAGTGAAGTGCCTGCCCTTCTA CACCACTCTGGGCTCTCCCATGCATTCAAAGTGAAGTGCCTGCCCTTCTA *****
161021-044_M21_19ACBAB000-32 TRED_Human_Pou5f1_Promoter_S	GGAATGGGGGACAGGGGAGGGGAGGAGCTAGGGAAGAAAACCTGGAGT GGAATGGGGGACAGGGGAGGGGAGGAGCTAGGGAAGAAAACCTGGAGT *****
161021-044_M21_19ACBAB000-32 TRED_Human_Pou5f1_Promoter_S	TTGTGCCAGGGTTTTTGGGATTAAGTCTTCACTAAGGAAGGAATT TTGTGCCAGGGTTTTTGGGATTAAGTCTTCACTAAGGAAGGAATT *****
161021-044_M21_19ACBAB000-32 TRED_Human_Pou5f1_Promoter_S	GGGAACACAAGGGTGGGGCAGGGGAGTTTGGGGCAACTGGTTGGAGGG GGGAACACAAGGGTGGGGCAGGGGAGTTTGGGGCAACTGGTTGGAGGG *****
161021-044_M21_19ACBAB000-32 TRED_Human_Pou5f1_Promoter_S	AAGGTGAAGTCAATGATGCTCTTGATTTAATCCACATCATGATCAC AAGGTGAAGTCAATGATGCTCTTGATTTAATCCACATCATGATCAC *****

Figure A.5. Sequencing results for cloned *Homo sapiens* *POU5F1A1* promoter sequence

161021-044_C23_19ACBAB000-35 TRED_Human_Pou5f1_Promoter_S	CCTCACTTCACTGCACTGTACTCCTCGGTCCCTTCCCTGAGGGGAAGC CCTCACTTCACTGCACTGTACTCCTCGGTCCCTTCCCTGAGGGGAAGC *****
161021-044_C23_19ACBAB000-35 TRED_Human_Pou5f1_Promoter_S	CTTCCCCCTGTCTCTGTCACCACTCTGGGCTCTCCCATGCATTCAAAC CTTCCCCCTGTCTCTGTCACCACTCTGGGCTCTCCCATGCATTCAAAC *****
161021-044_C23_19ACBAB000-35 TRED_Human_Pou5f1_Promoter_S	GAGGTGCCTGCCTTCTAGGAATGGGGACAGGGGAGGGGAGGAGCTAG GAGGTGCCTGCCTTCTAGGAATGGGGACAGGGGAGGGGAGGAGCTAG *****
161021-044_C23_19ACBAB000-35 TRED_Human_Pou5f1_Promoter_S	GGAAAGAAAACCTGGAGTTTGTGCCAGGGTTTTGGGATTAAGTCTTCA GGAAAGAAAACCTGGAGTTTGTGCCAGGGTTTTGGGATTAAGTCTTCA *****
161021-044_C23_19ACBAB000-35 TRED_Human_Pou5f1_Promoter_S	TTCA-----GAATTGGGAACACAAGGGTGGGGCAGGGGAGTTTG TTCACTAAGGAAGGAATTGGGAACACAAGGGTGGGGCAGGGGAGTTTG *** *****
161021-044_C23_19ACBAB000-35 TRED_Human_Pou5f1_Promoter_S	GGGCAACTGGTTGGAGGAAGGTGAAGTTCAATGATGCTCTTGATTTTAA GGGCAACTGGTTGGAGGAAGGTGAAGTTCAATGATGCTCTTGATTTTAA *****
161021-044_C23_19ACBAB000-35 TRED_Human_Pou5f1_Promoter_S	TCCCACATCATGTATCACTTTTTTCTTAAATAAAGAAGCCTGGGACACAG TCCCACATCATGTATCACTTTTTTCTTAAATAAAGAAGCCTGGGACACAG ***** *****
161021-044_C23_19ACBAB000-35 TRED_Human_Pou5f1_Promoter_S	TAGATAGACACACTTATCTTGTTTGTCTTCAGTTACTGAGGTGGGGAT TAGATAGACACACTTATCTTGTTTGTCTTCAGTTACTGAGGTGGGGAT *****
161021-044_C23_19ACBAB000-35 TRED_Human_Pou5f1_Promoter_S	GGGAATATCCAATGCTCATACCCAAGTGACCCTGAAACTAAGGTGCCATT GGGAATATCCAATGCTCATACCCAAGTGACCCTGAAACTAAGGTGCCATT *****

Figure A.6. Sequencing results for cloned *Homo sapiens* *POU5F2Δ2* promoter sequence



```

161021-044_K02_19ACBAB000-47      GGGAGCCCTCACTTCACTGCACTGTACTCCTCGGTCCCTTTCCCTGAGGG
TRED_Human_Pou5f1_Promoter_S      GGGAGCCCTCACTTCACTGCACTGTACTCCTCGGTCCCTTTCCCTGAGGG
*****

161021-044_K02_19ACBAB000-47      GGAAGCCTTTCCCCTGTCTCTGTCACTCTGGGCTCTCCCATGCATT
TRED_Human_Pou5f1_Promoter_S      GGAAGCCTTTCCCCTGTCTCTGTCACTCTGGGCTCTCCCATGCATT
*****

161021-044_K02_19ACBAB000-47      CAAACTGAGGTGCCTGCCCTTCTAGGAATGGGGACAGGGGAGGGGAGG
TRED_Human_Pou5f1_Promoter_S      CAAACTGAGGTGCCTGCCCTTCTAGGAATGGGGACAGGGGAGGGGAGG
*****

161021-044_K02_19ACBAB000-47      AGCTAGGGAAGAAAACCTGGAGTTTGTGCCAGGGTTTTTGGGATTAAGT
TRED_Human_Pou5f1_Promoter_S      AGCTAGGGAAGAAAACCTGGAGTTTGTGCCAGGGTTTTTGGGATTAAGT
*****

161021-044_K02_19ACBAB000-47      TCTTCATTCACTAAGGAAGGAATTGGGAACACAAGGGTGGGGCAGGGG
TRED_Human_Pou5f1_Promoter_S      TCTTCATTCACTAAGGAAGGAATTGGGAACACAAGGGTGGGGCAGGGG
*****

161021-044_K02_19ACBAB000-47      AGTTTGGGGCAACTGGTTG-----TGAAGTTC AATGATGCTCTTGA
TRED_Human_Pou5f1_Promoter_S      AGTTTGGGGCAACTGGTTGAGGGAAGGTGAAGTTC AATGATGCTCTTGA
*****

161021-044_K02_19ACBAB000-47      TTTTAATCCACATCATGTATCACTTTTTCTTAAATAAAGAAGCTGGG
TRED_Human_Pou5f1_Promoter_S      TTTTAATCCACATCATGTATCACTTTTTCTTAAATAAAGAAGCTGGG
*****

161021-044_K02_19ACBAB000-47      ACACAGTAGATAGACACACTTATCTTGGTTTGTCTTCAGTTACTGAGGT
TRED_Human_Pou5f1_Promoter_S      ACACAGTAGATAGACACACTTATCTTGGTTTGTCTTCAGTTACTGAGGT
*****

161021-044_K02_19ACBAB000-47      GGGGATGGGAATATCCAATGCTCATACCCAAGTGACCTGAAACTAAGGT
TRED_Human_Pou5f1_Promoter_S      GGGGATGGGAATATCCAATGCTCATACCCAAGTGACCTGAAACTAAGGT
*****

161021-044_K02_19ACBAB000-47      GCCATTTACTCTCCTTAAGGTCACACAACATCAGAGGGAGAGCTGGGATT
TRED_Human_Pou5f1_Promoter_S      GCCATTTACTCTCCTTAAGGTCACACAACATCAGAGGGAGAGCTGGGATT
*****

161021-044_K02_19ACBAB000-47      GCAGCCAAGTTTATTTGTACAGGGCCCTGTGATAGGCTAGTTCCAAAAG
TRED_Human_Pou5f1_Promoter_S      GCAGCCAAGTTTATTTGTACAGGGCCCTGTGATAGGCTAGTTCCAAAAG
*****

```

Figure A.7. Sequencing results for cloned *Homo sapiens* *POU5F1Δ3*